Metal composition of zooplankton from the Western Indian Ocean

JD van Aswegen

 orcid.org 0000-0001-8482-6974

Dissertation accepted in fulfilment of the requirements for the degree *Master of Science in Environmental Sciences* at the North-West University

Supervisor: Prof H Bouwman

Graduation December 2020

23601892

Acknowledgements

- I would like to thank my supervision Prof. H Bouwman, for the mentorship he provided me with over these years. Thank you for taking a chance and believing in me.
- I would like to thank the POPT group for using their facilities.
- I would especially like to thank everyone from the IIOE II for fantastic adventures and forever memories.
- I would like to thank all my friends; without you, I would have surely lost my marbles long ago.
- To my family, these years were trying for us as a family. Thank you for your love and for supporting me fully in my endeavours no matter how ambitious.
- To God thank you for the talents and people you have gifted me with.

Abstract

The Indian Ocean is probably the least researched ocean of the world. It is the third largest ocean and has many unique topographic, geologic, oceanographic, biological, and socio-economic features. The current system is also complex and variable on small and large scales. Uniquely, there is a component of monsoon seasonality affecting currents.

In terms of zooplankton, little is known, and even less is published on metals, a major component of a class of pollutants that also occurs naturally. Due to development, trade, shipping (especially oil), an expanding human population, coupled with current and potential conflict, knowledge on the current state of pollution (or lack of) is needed to tract future impacts and development.

Plankton is one of the most important components of the ecology of any ocean. Pollutants can affect plankton, change the characteristics of pollutants, and can be assimilated and/or bioconcentrated. They also play major roles in the carbon and nitrogen cycles and the microbial loop. Disturbances of these major processes may affect ecosystem functions and affect human communities depending of the ocean. Metals, although all occurring naturally in seawater, may be elevated beyond natural background levels due to pollution, posing risk to biota.

Although some ecotoxicological work has been done on mammals, fish, birds, and coral, there is a great lack of knowledge regarding metal composition in zooplankton from the western Indian Ocean (WIO), the region where I conducted my research. In this region, I concentrated on the metal compositions of three currents. The South Equatorial Current (SEC) is the main current that carries warm water from the east towards the African continent. This current runs through the tropical region of the Indian Ocean where it branches into the Madagascar Current (MC) flowing south, and East African Coastal Current (EACC). Each of these currents have upwellings and eddies. The two latter currents also receive freshwater discharges (containing metals) from many rivers along the coast, while volcanic activity in the SEC might contribute metals as well.

I collected 94 zooplankton samples from the three currents, and analysed them with ICP-MS for 34 metallic elements. I analysed the data statistically but also looked at geographic interpolation.

Although I analysed 34 elements, I concentrated on 14 essential (V, Cr, Mn, Fe, Co, Cu, Zn, As, and Se) and five non-essential (Ni, Cd, Hg, Pb, and U) elements as set out by the ATSDR's substance priority list, and compared the elemental distributions and concentrations in zooplankton from the three currents. There were differences in concentrations of some elements between the three currents – each current therefore had distinguishable but subtle compositions of metals in their zooplankton. For many of the essential elements, it seemed as if physiological regulation by the zooplankton was adequate in maintaining a relatively homogenous distribution of concentrations, especially towards sites located distant from the African continent.

I found that V, Cr, As, Se, Hg, Ni, and U concentrations in zooplankton from some sites approached and exceeded the concentrations found in other studies. To the best of our knowledge, Ni had the second highest recorded concentration. With high concentrations from “hot spots”, a certain amount of concern is warranted. Geographically, a number of “hot spots” were found, mainly associated with harbours and river mouths of the MC and EACC, and some in shallow areas near the African mainland. However, there were differences in concentrations between these “hot spots”. There were also indications of volcanic contributions of metals in zooplankton collected from the SEC.

I cannot conclude definitively that increased concentrations of metals in zooplankton from the EACC, MC, and SEC “hot spots” were solely from terrestrial sources or linked with pollution. The “hot spots” do suggest localised impacts that were not natural, apart from volcanic activity. Factors such as currents, upwelling, atmospheric deposition and primary productivity can affect the concentrations of metals in zooplankton. Currents close to the coast, eddies, and seasonal effects can influence the stratification (mixing) of nutrients, zooplankton, and metals in the water column, and therefore concentrations in zooplankton.

I therefore recommend further research into phytoplankton and zooplankton from the WIO as well as research into water and sediment concentrations, especially near “hot spots”, as this will more closely identify different sources of metals and indicate areas to reduce metal pollution.

My research has established a baseline against which future studies can measure changes linked to pollution, and identified certain metals and locations that would warrant closer attention

Key words: Zooplankton, Western Indian Ocean, Metals, Mozambique Channel, East African Coastal Current, South Equatorial Current

Table of Content

Chapter 1: Introduction

1.1. General introduction

With a growing human population associated with increased urbanization and industrialization, a negative impact on a series of environments can be seen (Tu *et al.,* 2014). Environmental changes are happening at an unprecedented rate and occur at regional and global scales, influencing terrestrial and aquatic organisms (Hood *et al.,* 2015; Tu *et al.,* 2014). Today's environment is troubled by many problems, but the most threatening problem, arguably, remains combined stressors interacting with fresh- and marine waters.

The earth surface consists of 71% water, of which the marine environment makes up 96.5%. Approximately only 5% of marine species and effects of stress have been studied (Nunez, 2019). The marine and estuarine environments experience many forms and magnitudes of environmental stressors. These stressors push the boundaries of a normal environment due to the variation and differences caused by anthropogenic activities. The high frequency and intensity of these stressors tends to influence organisms, populations, and communities (Hood *et al.,* 2015).

Environmental stressors that have the biggest impact on the Indian Ocean includes rise in sea temperature, rise in sea-levels, ocean acidification (increased CO_2), eutrophication (increased N and P), deoxygenation, plastic, and metal pollution (Hood *et al.,* 2015; Obura *et al.,* 2019). These specific stressors have unforeseen circumstances on the coastal marine environment and are influencing the general biogeochemical cycles of oceans, including the Indian Ocean, the area of my study. In some cases, the intensity and impact of human activities is unprecedented and could eventually pose a threat to human food security. Current trends suggest if these activities are not managed and mitigated, they are likely to increase with a concomitant increase in threats to the environment. An additional concern is that these activities are continuously increasing, affecting the world's oceans, including the Indian Ocean (Hood *et al.,* 2015; Obura *et al.,* 2019).

Coastal ecosystems are of great interest where many complex physical, biological, chemical, and ecological processes occur. These processes all interact to determine the ecology found in and around coastlines (Leal *et al.,* 2009). Urbanization and industrialization are affecting coastal areas at an alarming rate, deteriorating the quality of oceans, as well as rivers, and canals. This is primarily due to industrial, agricultural, and domestic sources releasing large amounts of chemical and biological waste into the surrounding water sources (Obura *et al.,* 2019; Qin *et al.,* 2008; Tu *et al.,* 2014; van Aswegen *et al.,* 2019). The marine environment is not only influenced by land-based activities, but also through shipping, oil- and gas mining, and fallout from atmospheric particles, further decreasing water quality in marine and coastal environments (Llewellyn *et al.,* 2016; Meng *et al.,* 2008).

Ships, being one of many polluting sources, can release massive amounts of sulphur and nitrogen oxide from their engines, where these pollutants are deposited back into the ocean's biogeochemical cycle. This is evident due to increased eutrophication and atmospheric pollution acting as indicators, that the Indian Ocean is being polluted. These two pollution sources can be linked directly to population increases around the edge of the Indian Ocean (Hood *et al.,* 2015). The Food and Agriculture Organisation (FAO) as cited in Hood *et al.,* 2015 further strengthens

this statement since they reported that the concentrations of nitrogen (N) and phosphorous (P) have increased dramatically since the 1970s.

The N and P enrichment phenomenon coupled with other anthropogenic activities (wastewater, urbanization, industrial effluent, and agriculture) can cause an imbalance within natural water systems, resulting in algal blooms (Anderson *et al.,* 2002; Chen *et al.,* 2013; Teichberg *et al.,* 2010). This imbalance can cause the production of different species of phytoplankton and decrease the numbers of diatoms due to concomitant decreased silicate concentrations. When phytoplankton communities are phase-shifted, the food web can be altered, which could affect both human health and that of the aquatic organisms inhabiting the ecosystem (Dallas & Day, 2004).

Rivers and ground water are two additional sources responsible for carrying ever-increasing amounts of nutrients, carbon, and metallic elements into coastal areas (Pripp *et al.,* 2014). Eutrophication caused by riverine runoff is generally low within the north and southwestern areas of the Indian Ocean, whereas high nutrient levels can be detected in the north-eastern parts. The Bay of Bengal is a good example of high nutrient loads entering the coastal environment from rivers and urbanized areas such as wastewater treatment, industries, leaching, and direct disposal within the environment (Mukhopadhyay *et al.,* 2006; Paul *et al.,* 2008). Another major influence on the Indian Ocean's ecosystems is that of climate change. The complex interaction of biotic and abiotic systems within the Indian Ocean serves as an indication of how climate change can have both positive and negative implications concerning marine organisms (Hood *et al.,* 2015).

Aquatic organisms have long been used for monitoring pollution (He *et al.,* 1998). Over the past few decades, the concentration of pollutants such as metallic elements within marine biota has been increasing (Kaladharan *et al.,* 2005; Mubiana *et al.,* 2005). These metals occur naturally within the environment at low concentrations, but due to anthropogenic activities, these concentrations have steadily been increasing above natural background levels (Hipfner *et al.,* 2011) leading to potential health risks for aquatic organisms (García-Otero *et al.,* 2013; Velusamy *et al.,* 2014). Metallic elements have been extensively researched through chemical, toxicological, and ecological approaches (He *et al.,* 1998). Recent studies have indicated that these compounds are entering the environment at a higher rate than in previous years (Lagerström *et al.,* 2013; Srichandan *et al.,* 2016; Yasin *et al.,* 2010; Zhoa *et al.,* 2012;).

Srichandan *et al.,* (2016) stated that metal pollution is of concern due to the toxicity and persistence of these elements in the environment. Some elements have a tendency to assimilate or bioaccumulate in animals and eventually the food web (Achary *et al.,* 2017; Yang *et al.,* 2002). The magnitude of assimilation and/or bioaccumulation by animals in the marine environment is influenced by factors such as location, depth, distribution, trophic level, feeding habits, age, and size (Velusamy *et al.,* 2014). These factors remain poorly researched and further research is needed to be better understand the effects caused by an increase in pollutants, together with natural oceanic drivers and anthropogenic stressors (Everaert *et al.,* 2015).

In remote areas where human impacts are not proximate, metallic elements are introduced through atmospheric deposition (Qin *et al.,* 2008). Throughout the Indian Ocean, there are various natural dust regions contributing to atmospheric deposition. These regions include the seas near

the Arabian Peninsula, Somalia, Pakistan, and India (Figure 1.1) (Hood *et al.,* 2015). Anthropogenic releases from industrial pollution and waste burning can also be found in these regions, especially at the Bay of Bengal and the Arabian Sea (Hood *et al.,* 2015).

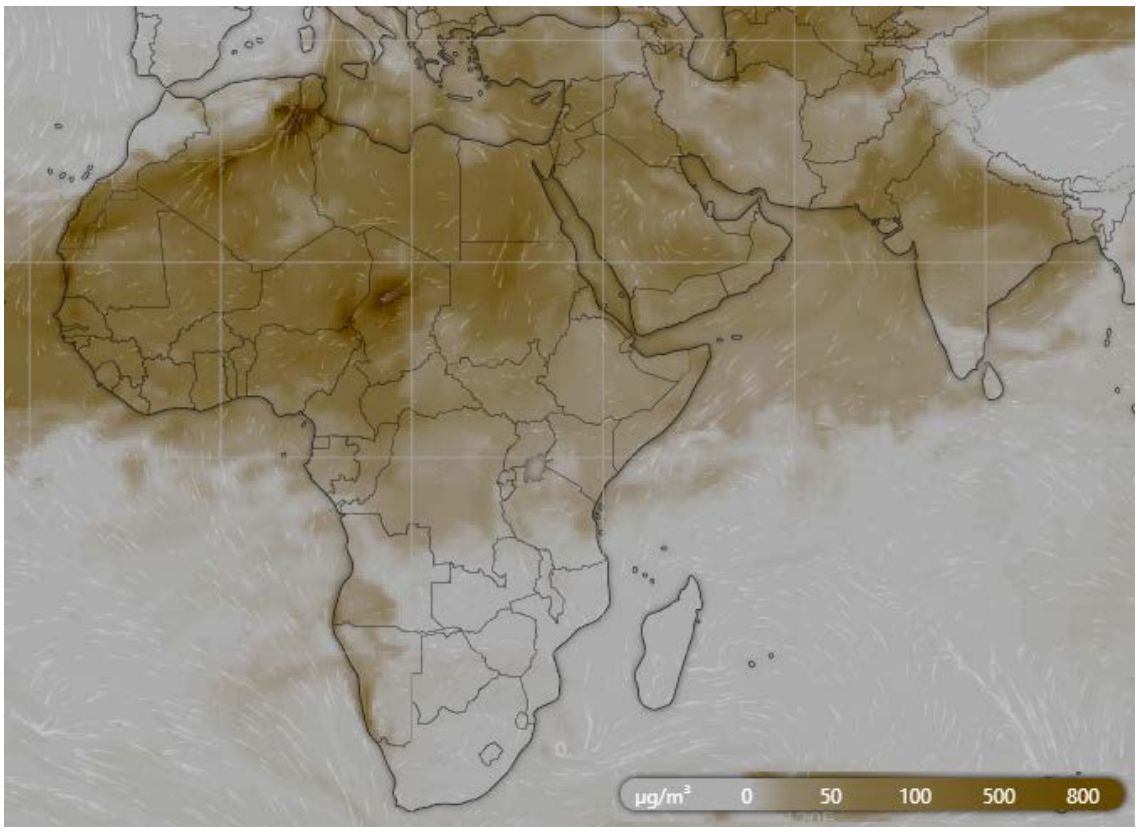

Figure 1.1: Map of Africa and India representing dust mass over the Arabian Peninsula, Somalia, Pakistan, and India with a concentration scale. White arrows are wind direction. The scale indicates dust deposition (µg/m^3 per day) (Windy.com).

When these atmospheric deposited metallic elements enter the environment through dust, they are redistributed through biogeochemical cycling and are frequently deposited into sediment. Sediment can thus be a target for the analysis of metallic elements. When these elements accumulate in sediment, they can later be reintroduced into the water column through upwelling events (Yang *et al.,* 2002). Furthermore, metallic elements in low concentrations in water, combined with organic matter, are incorporated in phytoplankton, eventually forming part of the food web and can ultimately start to bioaccumulate (García-Otero *et al.,* 2013).

Certain elements (copper (Cu), zinc (Zn), iron (Fe), chromium (Cr), and cobalt (Co)) are essential micronutrients needed for enzymatic reactions by producers, but they can also regulate primary productivity. By limiting primary productivity, the amount of CO_2 that is regulated limits the nutrient cycle within the given environment (García-Otero *et al.,* 2013; Lagerström *et al.,* 2013). Metal circulation in the ocean has complex interactions between biogeochemical processes in combination with physical characteristics. Biogeochemical data can therefore be used as an indication of what interactions are taking place in the water column (He *et al.,* 1998). These interactions can furthermore be used as mechanisms of tracing pollutant pathways into and throughout the ocean (Lagerström *et al.,* 2013).

Even though metallic elements can be used to trace pollution sources, a change in the ocean's chemistry, circulation, and temperature causes a transfer of organisms to new regions possibly changing the food web dynamic there (Hood *et al.,* 2015). These changes and unpredictability play a role in the structuring of many different biological communities that are found in coastal waters.

Two communities—phytoplankton and zooplankton—stand out when looking at the bottom of the food web. These two functional groups are responsible for several functions in the oceanic ecosystem (Leal *et al.,* 2009). The density and biomass of zooplankton in surface waters normally correlates with phytoplankton. And, since the abundance of zooplankton is determined through phytoplankton, the abundance can be traced back to predator-prey interactions. Zooplankton feeds on phytoplankton; in turn, planktivorous fish and larvae feed on zooplankton (Leal *et al.,* 2009). In this sense, zooplankton regulates the abundance of phytoplankton, and fish regulates the zooplankton biomass.

Other factors influencing the abundance of phytoplankton are light, temperature, nutrients, phosphates, nitrogen, and silica (Everaert *et al.,* 2015). Strong tidal currents and upwellings cause mixing of the water column, disturbing stratification. This effect causes phytoplankton and zooplankton in coastal areas to be distributed throughout the water column. In deeper water, the introduction of excess nutrients, phosphates, and nitrogen can cause phytoplankton blooms as well as affect the ecology (Leal *et al.,* 2009). The Indian Ocean may act as a model to indicate how climate change can influence the biogeochemistry and ecology of the world oceans through different factors, including that of zooplankton (Hood *et al.,* 2015).

1.2. The Indian Ocean

According to Hood *et al.* (2015), the Indian Ocean is a unique ecosystem in many ways. Kojadinovic (2016) stated that very little research has been done in the Indian Ocean, especially about metallic elements. Furthermore, he concluded that organisms at the top of the food web are usually exposed to high concentrations of metallic elements through the food they eat, combined with bioaccumulation from water (Kojadinovic *et al.,* 2007). Patterson *et al.* (2006) concluded similar stating that the eastern boundary of the Indian Ocean is less studied than the rest of the world's oceans in terms of microzooplankton. In general, the Indian Ocean remains one of the world's less-studied and under-sampled oceans when compared with the Atlantic and Pacific (Hood *et al.,* 2015).

The John Murry Expedition was one of the first major expeditions to the Indian Ocean. This expedition took place in 1933-34 and mainly focused on the Arabian Sea where the first oxygen deficiency in mesopelagic activities was recorded (Hood *et al.,* 2015). The overall general lack in research leads to many scientific questions arising and being unanswered, especially in terms of the zooplankton community and ecotoxicology of the Western Indian Ocean (WIO) (Hood *et al.,* 2015). This lack in research is a recurring theme in literature.

1.2.1. Indian Ocean topography

Aseismic ridges can be found throughout the world's oceans. In general, there are few seamounts in the Indian Ocean compared to the other oceans, with approximately 12%of all large seamounts being present within the Indian Ocean (Pitcher *et al.,* 2008). Seamount complexes in the Indian Ocean are associated with the Madagascar, Chagos-Laccadive, and Mascarene plateaus. These

ridges play an important role in depth, surface, and deep-sea circulation within the Indian Ocean (Hood *et al.,* 2015).

In the Indian Ocean, seven ridge-basins dominate the ocean floor topography. These include the Arabian, Agulhas, Crozet, Madagascar, Mascarene, and Mozambique ridges in the WIO and central Indian Ocean. Along the eastern side of the Indian Ocean there are two main ridges found namely Wharton and the South Australia basin (Hood *et al.,* 2015).

Three major rivers have broken through the ridges, discharging freshwater into the Indian Ocean. The Ganges River enters the Bay of Bengal, the Indus River enters the Arabian Sea, and the Zambezi River enters along the coast of Mozambique (Hood *et al.,* 2015).

Surface circulation in combination with landmasses tends to increase the biological productivity (Sigman & Hain, 2012) in the Indian Ocean. This can be due to the interaction of nutrient areas around Islands, as well as nutrient runoff from Island regions, which can lead to nutrients and pollutants such as metallic elements to enter the ecosystem (Hood *et al.,* 2015).

According to Hood *et al.* (2015), most of the suspended sediment that enters the Indian Ocean is from the Indian Subcontinent. This sediment load is of the highest when compared with the Indian, Pacific, and Atlantic Oceans. These sediment loads are generally deposited on continental shelves and associated slopes, and eventually into the abyss of the Indian Ocean. An example of this sediment deposit can be found along the coast of Somalia and Mozambique where the sediment deposition is more than a kilometre thick (Obura *et al.,* 2019).

Due to the specific topography and geometry found within the Indian Ocean, in combination with wind-driven monsoons, the circulation becomes unique and complex in the tropical regions of the Indian Ocean (Hood *et al.,* 2015). The seasonal complexity combined with centres where sediment enters the Indian Ocean plays an important role in the biogeochemical system of this ocean (Hood *et al.,* 2015).

1.2.2. Indian Ocean currents

I discuss the currents of the region where I conducted my studies as an important background and context of the findings of my study. Throughout the Indian Ocean, there are a number of complex major currents (Figure 1.2). The South Equatorial Current (SEC) is the main current that carries water from the east towards the African continent. This current runs through the tropical region of the Indian Ocean where, on the eastern side of Madagascar, it branches into two currents forming the South East Madagascar Current (SEMC) and Northeast Madagascar Current (NEMC) (Groeneveld & Koranteng, 2017; Obura *et al.,* 2019; Pripp *et al.,* 2014).

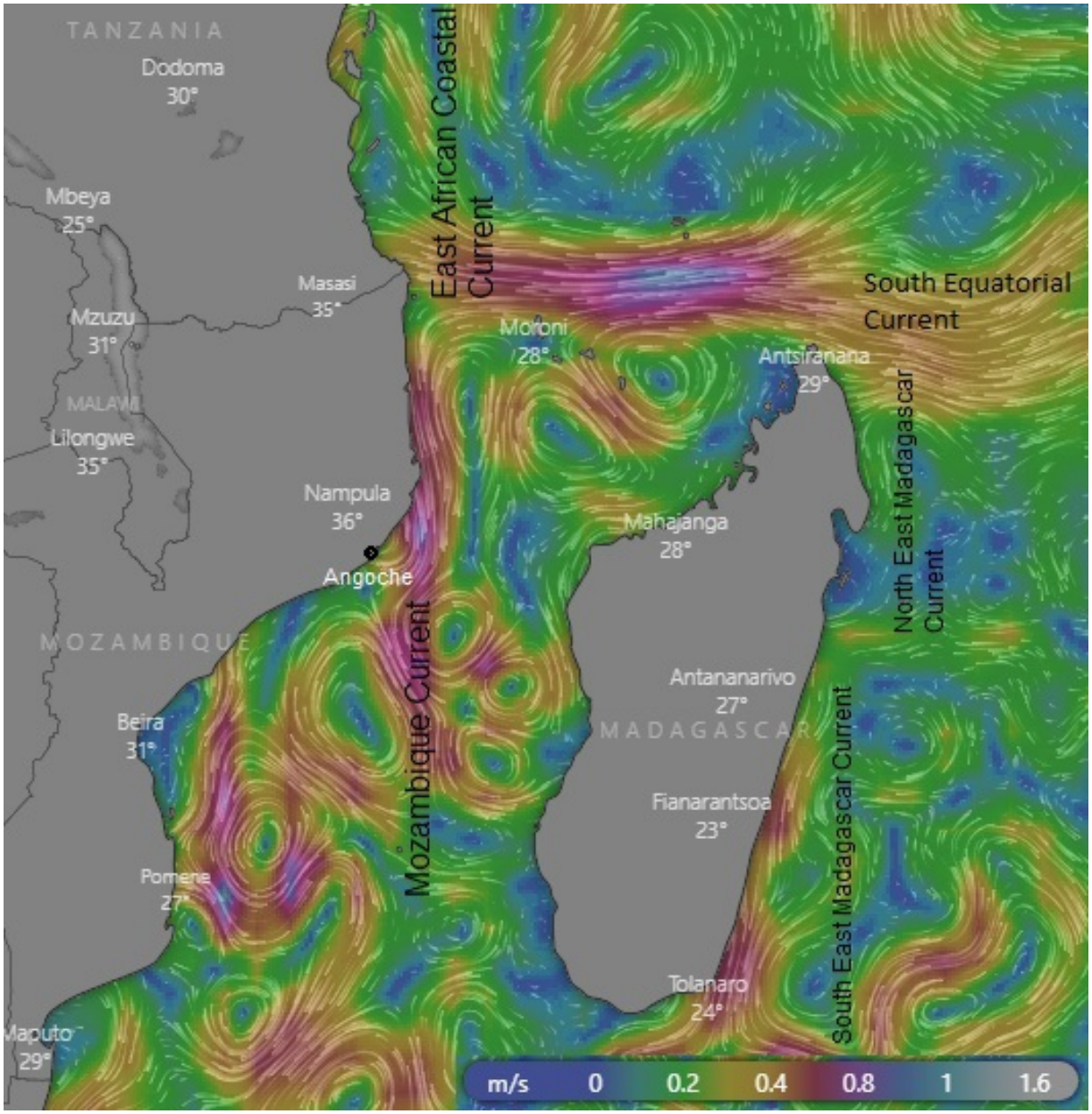

Figure 1.2: Map of main oceanic currents of the West Indian Ocean together with current speeds and eddies. Air temperature and cities are also included on the day the figure was created (15 November 2019) (Windy.com)

The SEMC and NEMC currents have an impact on the Mozambique Channel (MC) and Mozambique Current through shedding eddies into this channel. In the northern part of the MC, the NEMC breaks off south pushing eddies into the MC. The split tends to happen around the Comoros Islands. These eddies now travel through the MC along the coast of Mozambique and Madagascar (Figure 1.2) where it eventually breaks off back into the Indian Ocean, or join the greater Agulhas Current (AC) south along the east coast of South Africa (Barlow *et al.,* 2013; Groeneveld & Koranteng, 2017; Hood *et al.,* 2015; Obura *et al.,* 2019; Potier *et al.,* 2014). At the southernmost tip of Madagascar, the SEMC can either enter the MC or move back into the Indian Ocean as mentioned as eddies traveling along the western side of Madagascar (Hood *et al.,* 2015; Obura *et al.,* 2019).

Sections of the NEMC that do not enter the MC flows further west where it starts flowing northwards off the coast of Tanzania (Obura *et al.,* 2019). From June to September, the East

African Coastal Current (EACC) flows northwards forming part of the Somali Current (SC). [This information is relevant as it coincided with the time of sampling.] The SC then flows into the Arabian Sea where it influences the different monsoon seasons (Groeneveld & Koranteng, 2017; Hood *et al.,* 2015). This SC also breaks off to feed back into the South Equatorial Counter Current (SECC) leading back into the Indian Ocean (Groeneveld & Koranteng, 2017). Between the Atlantic, Pacific, and Indian Oceans, the latter is the least understood in terms of circulation; this may be because the Indian Ocean has unique geomorphology, seasonal influences, and unique surface and deep-water currents, in combination with upwelling and downwelling events (Hood *et al.,* 2015; Lamont *et al.,* 2014).

Water mixing also occurs within the MC. An example of this is the mixing of the Indonesian Throughflow (ITF) waters with waters of the SEC. This mixing of different water masses can be seen at different depths but is most prominent at the thermocline and other intermediate depths (Makarim *et al.,* 2019). Hood *et al.,* (2015) suggests that this mixing of water influences the physical and chemical properties of the Indian Ocean through the introduction of freshwater, and water from the Pacific Ocean. Furthermore, they suggest that the ITF can cause the exchange of physical and chemical properties as well as biological properties through the introduction of larvae, plankton, nutrients, and essentially the transfer of pollutants such as metallic elements.

Upwelling and downwelling zones greatly influence the biogeochemistry as well as planktonic ecosystems of coastal regions (Béhagle *et al.,* 2014; Pripp *et al.,* 2014). These influences can be traced back to boundary currents mixing coastal zones, impacting higher trophic levels and behaviour of organisms (Potier *et al.,* 2014). Even though most of the currents in the Indian Ocean are permanent, some are mainly influenced by seasonal changes. Currents such as the SC, West Indian Coastal Current (WICC), and East Indian Coastal Current (EICC) starts flowing slower and eventually dissipates following which the flow reverses depending on specific seasons. The SC is especially known for its strength and direction reversal properties (Hood *et al.,* 2015; Wang *et al.,* 2018).

The inclusion of warm water transport through the Indonesian Seas to the Indian Ocean plays a role in global thermoregulation. This water passes through the Indian Ocean and enters the Southern Atlantic Ocean through eddies breaking off from the greater AC at the tip of southern Africa (Lamont *et al.,* 2014). The exchange of water through the Indian Ocean mostly takes place within the tropical regions of the SEC, but heat transport through the MC into the AC is important for thermoregulation of the global oceans (Hood *et al.,* 2015).

The AC along the coast of South Africa is of importance due to the transfer of water from the Indian Ocean into the South Atlantic Ocean, carrying characteristics from the Indian Ocean into the South Atlantic Ocean through eddies and natural water transfer. Furthermore, strong associations can be found with upwelling events in the AC, MC, and Eastern Madagascar Current (EMC) (Lamont *et al.,* 2014; Lutjeharms & Bornman, 2010).

1.2.3. The Mozambique Channel (MC)

In the WIO, the MC can be found between Mozambique and Madagascar flowing southwards from the northern tip of Madagascar towards South Africa (Jose *et al.,* 2013; Potier *et al.,* 2014). This current connects with the Agulhas Current and eventually breaks of into smaller eddies returning into the Indian Ocean but can also cross into the Atlantic Ocean through the break off

of eddies at the southern tip of Africa (Halo *et al.,* 2014; Ternon *et al.,* 2014a; Ternon *et al.,* 2014b). In the northern part of the channel, the Comoros Islands can be found. Its geographical outline causes interesting flow patterns within the MC (Obura *et al.,* 2019; Ternon *et al.,* 2014a; Ternon *et al.,* 2014b).

From a biogeographical point of view, the MC has drawn a lot of attention due to the existence of a complex current system (Mattio *et al.,* 2016; Obura *et al.,* 2019). These complex flow patterns can be ascribed to eddies in the MC. Another factor influencing the complexity of the eddies and circulation is that of the topography in the MC and Indian Ocean (Barlow *et al.,* 2013; Obura *et al.,* 2019; Ternon *et al.,* 2014b).

As mentioned earlier, the SEC divides into different currents, eventually forming the northwards flowing SC and the southwards flowing MC (Kai & Marsac, 2010; Obura *et al.,* 2019). This leads to complex surface and bottom circulation, as also mentioned earlier. With this complex circulation and taking into consideration the shape of the Mozambique Channel, different processes occur due to the presence of upwelling and downwelling eddies (Béhagle *et al.,* 2014; Ternon *et al.,* 2014a; Ternon *et al.,* 2014b). Even though the MC traverses the Mozambique coastal area, the SC and MC both possess different oceanographic properties (Groeneveld & Koranteng, 2017). This combination has an impact on upwelling regions as well as the biodiversity (Kai & Marsac, 2010).

Whereas coastal water mainly consists of two types of surface water such as Tropical Surface Water (TSW) and Subtropical Surface Water (STSW), tropical water within the Indian Ocean is known to have lower salinity and higher temperatures in surface water, whereas water in the STSW has higher salinity (Groeneveld & Koranteng, 2017).

1.2.4. Eddies

I discuss eddies in detail, as this may affect the metal compositions of zooplankton, the subject of my study. Groeneveld & Koranteng (2017) found that anticyclonic eddies are more prone to downwelling. Heat and oxygen is pushed down to deeper water layers, whereas cyclonic eddies are connected to upwelling resulting in higher chlorophyll concentrations as well as cooler nutrient-rich water being drawn up from the deeper water layers changing the characteristics of the water (Marsac *et al.,* 2014; Pripp *et al.,* 2014). In contrast, Hood *et al.,* (2015) found that even though cyclonic eddies cause upwelling, they do sometimes have lower concentrations of chlorophyll and downwelling eddies sometimes have higher concentrations of chlorophyll. This leads to nutrients being transported between the African coasts and Madagascar in the MC (Groeneveld & Koranteng, 2017; Halo *et al.,* 2014; Obura *et al.,* 2019; Ternon *et al.,* 2014a).

It is well known that eddies play a role in the biological structuring of certain areas (Ternon *et al.,* 2014a). This can be seen by studying the lowest levels of the food web including that of chlorophyll, plankton, and zooplankton distributions in the Indian Ocean (Béhagle *et al.,* 2014; Halo *et al.,* 2014; Marsac *et al.,* 2014; Obura *et al.,* 2019).

According to Huggett (2014), the passage of mesoscale eddies through the Mozambique Channel also has a strong influence on the distribution of mesozooplankton, as biovolume in the cyclonic (cold-core) eddies were on average 55% greater than in the anti-cyclonic (warm-core) eddies sampled during four surveys (Béhagle *et al.,* 2014; Huggett, 2014; Marsac *et al.,* 2014). This is likely due to upwelling in the cores of the cyclonic eddies, resulting in enhanced nutrients, primary

production, and accompanying secondary production, which is supported by the higher abundance of copepod and euphausiid nauplii found in the cyclonic eddies when compared with the anticyclonic eddies. (Groeneveld & Koranteng, 2017; Halo *et al.,* 2014; Marsac *et al.,* 2014; Obura *et al.,* 2019)

Furthermore, primary production in the MC mostly increases due to increases of nutrients (and presumably metals as well) retrieved from coastal areas instead of eddies being the main source of nutrient input of deep-water nutrients to the euphotic zone (Barlow *et al.,* 2013; Hood *et al.,* 2015; Lamont *et al.,* 2014; Marsac *et al.,* 2014). The MC eddies play an important part within the ecosystem through shaping the behaviour of organisms as well as impacting the biodiversity and foraging of higher trophic levels (Hood *et al.,* 2015; Marsac *et al.,* 2014; Obura *et al.,* 2019). Eddies therefore, are likely to have an effect on metal concentrations in zooplankton.

The quantity and strength of eddies found within the MC can be strongly affected by the SEC which could, in turn, have a greater impact on higher trophic levels feeding in this area. This, in turn, would affect the transport of nutrients (and probably metals as well) between regions within the MC (Hood *et al.,* 2015; Lamont *et al.,* 2014; Obura *et al.,* 2019). Halo *et al.,* (2014), agreed with this statement as they found that anti-cyclonic eddies were predominantly found along the coast of Mozambique whereas cyclonic eddies predominantly travelled along the Madagascar coastline in an easterly direction within the Mozambique channel transporting nutrients and possible pollutants along the way.

1.2.5. Upwellings

In terms of energy, upwelling is a mode of energy transfer between the deep parts of the ocean, surface water, and the atmosphere. This energy transfer causes nutrients to be brought up from the sediment or deep ocean to be transferred into the food web (Sigman & Hain, 2012).

Malauene *et al.* (2014) stated that between the months of August and March every year, increased chlorophyll concentrations are found along the coastal region of Angoche (Figure 1.2) in Mozambique (Marsac *et al.,* 2014). This is primarily due to increased wind-driven upwellings during these periods. These wind-driven upwellings can also be seen at the southern tip of Tanzania near Mtwara. Specifically, the combination of wind, eddies colliding with coastal shelves, and the seafloor causing an upwelling region along Angoche; whereas wind-driven upwellings are also seen along the Comoros basin (Groeneveld & Koranteng *et al.,* 2017; Obura *et al.,* 2019).

Along the Mozambique coast, an inshore coastal current can be found flowing in a northerly direction. This specific current is known as the Delagoa Bight (DB) that mainly consists of eddies interacting with the area's topography to cause upwelling events on the Mozambican shelf (Groeneveld & Koranteng *et al.,* 2017; Lamont *et al.,* 2014; Potier *et al.,* 2014). Another input of excess nutrients can be traced back to the Zambesi River causing the Sofala Bank to be an area high in nutrients, resulting in the area being impacted by not only the river outflow but also that of passing eddies along the shelf. Since there is an increase in nutrients (and presumably metals as well), primary productivity increases, thus leading to enhanced productivity throughout the trophic levels (Groeneveld & Koranteng *et al.,* 2017; Pripp *et al.,* 2014). Groeneveld & Koranteng (2017) further highlights the biological importance of this area, noting that the Sofala Bank is an important distribution area for pelagic fish species.

It is well understood that the main source of increased primary production is that of nutrient availability and light intensity (Sigman & Hain, 2012). Mechanisms such as rivers tend to supply high concentrations of nutrients into the ocean that in return enhances primary production (Pripp *et al.,* 2014). In the WIO, there are mechanisms that affect the biomass, distribution, and abundance of organisms (Potier *et al.,* 2014). These mechanisms are, to name a few, oceanic upwellings, wind-driven upwellings, eddy circulation, and river inflow, which in turn causes mixing of water layers and therefore enhanced stratification (Groeneveld & Koranteng *et al.,* 2017; Obura *et al.,* 2019). Not only do eddies cause vertical stratification along the coast, but stratification can also be found within the open ocean where nutrients (and presumably metals) are transferred to different layers due to cyclonic eddies causing upwellings (Jose *et al.,* 2013; Lamont *et al.,* 2014; Lebourges-Dhaussy *et al.,* 2014).

Permanent upwelling zones can be found along the equator in the Atlantic and Pacific oceans. In contrast, the Indian Ocean has upwelling zones situated at higher and lower latitudes. This means that upwelling regions can be found for example along Somalia, Seychelles, and the northern tip of Mozambique (Hood *et al.,* 2015). Of the coast of Oman and Somalia, an extreme upwelling region can be found which is mainly produced by the Asian-African monsoon (Hood *et al.,* 2015).

The WIO is unique worldwide due to rich geophysical mechanisms that cause upwellings and this in turn results in the WIO differing vastly from the eastern side of the Indian Ocean (Hood *et al.,* 2015). This complexity may have an influence on metal concentrations and compositions in zooplankton of the WIO.

1.2.6. Ocean zonation

The northern part of the Indian Ocean has many freshwater influences especially in the Bay of Bengal, which may lead to increased stratification (Hood *et al.,* 2015). The northern Indian Ocean is also known for its oxygen-depleted water that influence benthic organisms as well as primary productivity (Marsac *et al.,* 2014). Dead zones are of major concern within coastal areas and the open ocean. These dead zones are formed by an increase in primary production leading to increased consumption of dissolved oxygen by primary producers and microbial communities (Hood *et al.,* 2015). The occurrences of dead zones in the Indian Ocean are on the rise, especially in the north (Hood *et al.,* 2015).

Deoxygenation has received increased attention during the last decade due to increased eutrophication. This, in combination with lower ventilation, increased stratification, and reduced upwelling places more stress on aquatic biota (Hood *et al.,* 2015). Furthermore, deoxygenation may lead to an expansion of intermediate water layers with conditions favouring increased loss of bioavailable nitrogen under anoxic conditions via denitrification and anaerobic ammonium oxidation reactions (Sigman & Hain, 2012). Moreover, deoxygenation will enhance production of climate-relevant trace gases such as N_2O, CH_4 and dimethylsulfide that are released to the atmosphere from upwelling regions in the northern Indian Ocean. Mesopelagic fish populations may therefore be threatened by a reduction in suitable habitat as respiratory stress increases (Hood *et al.,* 2015).

Global warming has been a major problem in the 21st century, causing a number of changes in the marine environment (increased water temperature, sea-level rise, and changes in ocean circulation). These changes affect the natural biogeochemical processes, which in return can

affect primary and secondary productivity (Sigman & Hain, 2012). Coastal areas are more susceptible to environmental changes due to total depth not being deep enough to maintain stability (Hood *et al.,* 2015).

Finally, the marine water column can be stratified in different layers according to nutrients, sunlight, temperature, and oxygen. Each layer houses different organisms that possess the ability to move between layers. In trophic networks, certain organisms remain important to ensure a healthy environment. Primary producers, secondary producers/consumers, and top predators are all-important within the epipelagic and mesopelagic layers (Béhagle *et al.,* 2014; Hood *et al.,* 2015; Lamont *et al.,* 2014; Sigman & Hain, 2012).

1.3. Biogeochemical cycles

There are three main biogeochemical cycles.

1.3.1. The carbon cycle

Carbon monoxide and carbon dioxide (CO_2) are the two most common forms of inorganic carbon found within the environment. Carbon dioxide fixation is the starting point of the carbon cycle and involves the alteration of CO_2 by changing it into organic matter. Plankton, bacteria, and protists play a fundamental part in the marine environment in terms of the ocean's carbon cycle. Phytoplankton are mainly found in surface water, and bacteria found beneath the euphotic layer, due to bacteria's ability to fix carbon under anoxic conditions in the absence of light (Sigman & Hain, 2012). These organisms are responsible for approximately half of the carbon fixing that takes place on earth. Apart from carbon fixing, phytoplankton is also a primary producer of dissolved organic matter (DOM) in marine ecosystems (García-Otero *et al.,* 2013; Willey *et al.,* 2011). With different stratification activities taking place in the world's oceans, there are certain areas with low stratification that can result in massive algal blooms under the right conditions (Patterson, 2006).

This constant rise in CO_2 in the atmosphere causes not only ocean acidification but also global ocean warming. With increased water temperature comes a decrease in stratification, causing a decrease in upwelling; this in turn leads to nutrients (and certain trace elements) from deep water and sediment not being able to reach the surface layers of the ocean. With a decrease in nutrient availability, decreased primary productivity and biogeochemistry may occur. This enormous change in the ocean's natural cycles can affect denitrification and eventually food webs and fisheries (Hood *et al.,* 2015).

1.3.2. The nitrogen cycle

One of three major oxygen-depleted zones can be found in the northern part of the Indian Ocean with oxygen almost reaching a concentration of zero in waters of the Arabian Sea. This may disrupt the biogeochemical processes in the Arabian Sea and Indian Ocean. Approximately 20% of the world's denitrification takes place in the Arabian Sea. The Arabian Sea has been identified as an area of global importance in terms of open-ocean denitrification, but the Bay of Bengal is also of concern due to decreasing oxygen concentrations. Although low oxygen concentrations are found, the Bay of Bengal's threshold is still just above the threshold where denitrification starts to occur (Hood *et al.,* 2015).

Algae, mainly cyanobacteria, convert atmospheric nitrogen into ammonia that can serve as another food source for phytoplankton (Sigman & Hain, 2012). Approximately 30-40% of nitrates

that are found within the Arabian Sea are produced from the fixation of atmospheric nitrogen, especially in euphotic zones. Nitrogen fixation is estimated to support up to 50% of new production in areas where low primary productivity is found (Hood *et al.,* 2015). Organic nitrogen fixation is mainly produced by two main groups of organisms; bacteria and archaea. These organisms are the main nitrogen fixers within the environment with lightning strikes, volcanic activity, and fertilizer manufacturing also contributing (Willey *et al.,* 2011). Even though being such an important event, there is still not enough data on nitrogen fixation to quantify with certainty what the total input of nitrogen is to the Indian Ocean (Sigman & Hain, 2012).

An increase in nutrients in the water will not only have dramatic effects on the biogeochemical cycle of the ocean but will also impact coastal food webs. As earlier stated, increased human population and coastal development have had and continuous to have severe negative effects on coastal environments. With increased nutrient effluent entering the marine environment, the chances of food webs and natural processes becoming perturbed greatly increase (Sigman & Hain, 2012). This leads to a further decrease in pH in the water column. Additionally, ammonia is transformed into ammonium that can influence biological interactions such as the microbial loop and phytoplankton interactions (Hood *et al.,* 2015).

1.3.3. The microbial loop

Over the decades, marine microbes have been able to adapt to continually changing physical and chemical parameters driven by anthropogenic activities. Changes in water temperature and chemistry will inevitably affect the Indian Oceans' microbial communities. There are few bacterial species in high abundance in these ecosystems. Changing any physical or chemical parameter can drastically influence the distribution and composition of the abundant bacteria, and in turn affect the important roles they play in various biological processes (Hood *et al.,* 2015). Bacteria involved with nitrogen fixation and denitrification can start to bloom, become toxic, and spread, eventually affecting the nitrogen cycle and the total chemistry of the water column (Hood *et al.,* 2015).

The microbial loop starts in the photonic layer, but mainly occurs underneath this layer, due to the bacteria's ability to function in low light. Processes such as remineralization take place through microbes, protists, flagellates, and microzooplankton that help to reintroduce nutrients into the photonic layer that in turn helps with the growth of phytoplankton. Since biological, chemical, and microbial activities are all linked, this redistribution process best describes the proper functioning within the environment (Patterson, 2006).

1.4. Trace metals in the Marine Environment

Just as the carbon, nitrogen, and microbial interactions interacts with each other, so does this affect how trace metals behave in water. With a worldwide increase in pollution, metallic elements have increased leading to growing concerns for human health. Metallic elements occur naturally or are present due to anthropogenic inputs to all ecosystems (Echeveste *et al.,* 2016; Qin *et al.,* 2008). It is therefore inevitable that these metallic elements ends up in the marine environment, where some of the elements are highly toxic and can start to bioaccumulate in marine organisms (Achary *et al.,* 2017).

Metallic elements have a fundamental role to play in how the ocean works. Certain metals such as Fe, Co, and molybdenum (Mo) can be used for biological processes and are elements that are

needed by various organisms. From a biological context, metallic elements can be classified as essential or non-essential (García-Otero *et al.,* 2013; Twining *et al.,* 2011). There are a number of ways for essential elements such as Fe to enter the marine environment; these include atmospheric dust, resuspension, and hydrothermal vents to name but a few (Nishioka *et al.,* 2013). Elements such as lead (Pb), and mercury (Hg) do not have a specific biological function (therefore non-essential), and as such can be toxic with increasing concentrations. With a change in climate and increased anthropogenic inputs, the concentration, distribution, and availability of metallic elements in the ocean are continuously changing, including interactions with carbon, nitrogen, and bacteria. The distribution and concentration of metallic elements are controlled by certain factors such as biological uptake, binding to organic or inorganic particles, and deposition into marine sediment (Aparicio-González *et al.,* 2012).

An example of this can be found along the coast of Vietnam were high metal concentrations have been found along the coast as well as in a variety of environmental samples. This raises concern due to the large human dependence on biota from contaminated environments (Tu *et al.,* 2014).

Water's composition is influenced by its specific physical-chemical properties. In terms of metals in water, the composition is also influenced by the availability of metals as well as the ability to be able to bind to biotic ligands. This means that certain metals can be toxic to organisms such as fish since they interfere with the physiological Ca and Na/K pump. This can in time lead to the swelling of fish gills and eventually death (Fisher & Hook, 2002). With an apparent shift in the global distribution of organisms, —especially poleward—might have effects on higher trophic levels, since food sources are shifting, eventually redistributing metallic elements from one region to another (Hood *et al.,* 2015).

The effect of pollutants occurring naturally has gained more attention in recent times, and remote areas such as the Arctic and Antarctic have become places of concern due to increased anthropogenic introduction of metals into food webs (Kojadinovic *et al.,* 2007; Nishioka *et al.,* 2013). This increased interest shows that the modern situation of pollution is a problem and up to date research is urgently needed (Echeveste *et al.,* 2016).

1.4.1. Metabolic and physiological influences of metals

Out of most of the pollutants that can be found in coastal and estuarine sediment, metallic elements are known to be the most persistently present (Meng *et al.,* 2008; Qin *et al.,* 2008; van Aswegen *et al.,* 2019). For this specific reason, they can be used as indicators of what is happening in the environment.

Physical, chemical, and biological dispersal plays an important part in what happens with these metallic elements once they enter the marine environment. Organic matter that enters the environment can be either consumed, sink to the seabed, or be demineralized. These factors help with the regulation of trace metals in the biogeochemical cycles (Srichandan *et al.,* 2016).

Metallic elements such as Mn, Fe, Co, Ni, Cu, and Zn play important roles in the marine environment, especially in biogeochemical processes. Ambient essential elements can be influenced by nutrients used for plankton growth since these elements can become exhausted in surface water and enriched at depths due to assimilation and accumulation, sinking, and subsequent remineralisation at deeper depths. Furthermore, there seem to be noticeable trends in the composition of metallic elements that are found within certain taxonomic groups, due to the

vertical distribution of metallic elements through biological and ecological processes in plankton. Even though this plays a major role in animals, the availability of these elements can be influenced, but availability and specific uptake mechanisms of organic compounds are not fully understood (Twining *et al.,* 2011).

The Arctic marine ecosystem is a good example of an ecosystem being impacted by metal pollution. This ecosystem has been receiving more attention ever since metallic elements have been found to be contaminating the ecosystem. Ritterhoff and Zauke (1997) stated that arsenic (As), Cd, Pb, Zn, vanadium (V) and antimony (Sb) in the Arctic accounts for approximately 6% of Eurasia's emissions. In the Arctic food web, zooplankton plays a crucial role since they are a food source for marine mammals, birds, and fish. Additionally, zooplankton can also contribute to bioaccumulation of these elements in higher trophic levels. Due to these dynamics, zooplankton is a good biomonitor to assess the presence and abundance of these elements in lower trophic levels in aquatic environments (Ritterhoff & Zauke, 1997).

Fisher and Hook (2002) found that gold (Au) and cadmium (Cd) can decrease the reproduction of zooplankton; but when these metallic elements were taken up from an aqueous solution, no reproductive effects were observed. Cadmium, Au, and Hg that have accumulated in organisms from aqueous solutions tend to accumulate on the exoskeleton of zooplankton, but metals ingested accumulated within the organism itself, thereby causing effects (Fisher & Hook, 2002).

Mercury is a well-known non-essential element and especially toxic at above background thresholds (ATSDR, 1999). Mercury can either occur naturally or enter the environment through anthropogenic inputs. Mercury's toxicity is determined by its chemical form and the concentrations in the environment. It occurs either in elemental, organic, or inorganic form. The most toxic of the three being organic mercury (methylmercury); for this reason, it is important to determine the specific type of Hg. Since Hg can be transported by air, the circulation time and the chemical transformation to methylmercury can cause organisms in remote areas of the world to be exposed to Hg, along with other pollutants (Pacheco *et al.,* 2010).

1.4.2. Oceanic nutrient transport

Mesoscale eddies change the biogeochemical process through physical, chemical, and biological interactions (Béhagle *et al.,* 2014). Eddies (cyclonic or anticyclonic) can influence the nutrient supply needed by organisms. Cyclonic eddies redistribute nutrient-rich water (deep water) into the eutrophic zone (Malauene *et al.,* 2014). In contrast, anticyclonic eddies displace water, nutrients, and chlorophyll to collect on the outskirts of the eddy (Béhagle *et al.,* 2014; Kolasinski *et al.,* 2012). Tropical parts of the ocean are usually limited in terms of nutrients. Organisms living in these areas are dependent on nutrient cycling and the vertical migration or redistribution of nutrients from nutrient-rich water (Kolasinski *et al.,* 2012). Nutrients from nutrient-rich sectors or layers can also be transported to areas or layers that are nutrient-poor, enhancing primary production and promoting biodiversity increases (Jose *et al.,* 2013; Malauene *et al.,* 2014).

An example of nutrient-limited waters is that of the MC. Although these waters aren't nutrient-rich and have low primary productivity, they support large numbers of top predators (Kolasinski *et al.,* 2012). The supply of nutrients within the MC can be ascribed to a number of factors, including upwelling (Section 1.2.5).

Huggett (2014) stated that during daytime, large gatherings of zooplankton occur at the surface of the MC, in combination with numerous Greater Frigate Birds (*Fregata minor*) which feed in this area especially with the association of zooplankton on the edges of eddies. Upwelling in the centre of cyclonic eddies, especially in oligotrophic systems, supply high nutrient levels leading to increased primary production, and increased zooplankton abundance and biomass (Huggett, 2014; Lebourges-Dhaussy *et al.,* 2014;Malauene *et al.,* 2014).

In the MC, general information of zooplankton is lacking. Knowledge on general biomass, community structures, and the distribution of zooplankton for eddies and between eddies are needed. Knowledge like this is needed to understand the fundamentals of normal functioning of mesoscale ecosystems. This knowledge, linked with feeding behaviour between trophic levels, will help with the understanding of how trophic transfer (of metals) occur (Huggett, 2014).

1.4.3. River runoff

Freshwater differs from ocean waters in many respects, mainly lower salinity. According to Groeneveld & Koranteng (2017), the WIO has been categorized in three parts namely North of 18 degrees south, central with increased riverine runoff, and south of 24 degrees with moderate influence of freshwater. The Zambezi River enters the ocean at approximately the central part along the coast of Mozambique. The Zambezi River has an extended influence on the salinity and nutrients in the ocean surface layer up to approximately 30 m and 50 m deep in stormy or rainy seasons stretching up to 50 km offshore (Nehama & Reason, 2014; Pitcher *et al.,* 2008).

River plumes in the oceans change the characteristics of the area they flow into due to the enhanced terrestrial nutrients causing possible eutrophication, an inflow of sediment, and river-borne pollutants (Pripp *et al.,* 2014). Seasonal influences of riverine flow change production in the Indian Ocean (Hood *et al.,* 2015). Increase in nutrients leads to increased primary productivity and eventually enhances local fish populations (Hung *et al.,* 2014). However, pollutants are also taken up by biota.

1.5. Role of plankton

Plankton is a general term that commonly refers to marine organisms that cannot escape currents but instead rely on currents for transport. Plankton includes phytoplankton, zooplankton, bacteria, and viruses (Willey *et al.,* 2011). Taking all of this into consideration, approximately 98% of the oceans living biomass is made up of plankton that produce about half of the world's oxygen. The other 2% is mainly comprised of organisms that are not reliant on currents for movement known as nekton; these include squid, crab, fish, and mammals (Groeneveld & Koranteng, 2017).

Phytoplankton are primary producers using sunlight and nutrients. Since they depend on sunlight, they are mostly found in the euphotic layer. Even though phytoplankton needs light and nutrients to thrive, they also depend on carbon dioxide, water depth, temperature, and grazers, resulting in differences in seasonal distribution (Groeneveld & Koranteng, 2017). Therefore, the increase in complexity of pollutants due to anthropogenic inputs can eventually have an effect on oceanic organisms leading to an impact on the global carbon and nitrogen cycles, bacterial activity and compositions, and ocean productivity (Echeveste *et al.,* 2016). On the other hand, exposure of phytoplankton to contaminants such as metallic elements increases their tolerance towards these pollutants (Echeveste *et al.,* 2016), leading to more complex dynamics.

Secondary producers/consumers in the marine environment mainly consist of zooplankton that feed on phytoplankton and small zooplankton (Marsac *et al.,* 2014). Zooplankton are mainly crustacean and gelatinous organisms that depend on currents to move long distances. These include some larval stages of fish and molluscs that later tend to move out of the currents and either become free-living or migrate to the benthic environment (Groeneveld & Koranteng, 2017).

Although being restricted to currents for migration and distribution, a mass vertical movement takes place on a diel basis. In the epipelagic and photic zones, zooplankton can strongly influence the vertical transfer of elements (Battuello *et al.,* 2016; Groeneveld & Koranteng, 2017; Marsac *et al.,* 2014; Potier *et al.,* 2014).This vertical migration towards surface waters takes place at night when predation risk is lower. One of the reasons for this daily migration is to feed on nutrients and food rich surface waters (Groeneveld & Koranteng, 2017).

Zooplankton can be categorised according to size; five size categories are generally recognised. These are nano-, micro-, meso-, macro-, and megaloplankton. Nanoplankton ranges between 2-20 µm, microplankton between 20-200 µm, mesozooplankton between 0.2-20 mm, macrozooplankton between 2-20 cm, and megaloplankton between 20-200 cm. Mesozooplankton consists mostly of crustacean zooplankton commonly sampled with bongo nets with 200-300 µm mesh (Groeneveld & Koranteng, 2017).

Four main ecological functions are ascribed to microzooplankton namely: grazing to regulate bacteria populations, nutrient regulation, transfer of organic matter and energy to higher trophic levels, and finally, assisting with primary productivity (Paterson, 2006). They may also cause to lure fish to areas where zooplankton are found in large numbers (Battuello *et al.,* 2016). Although these animals are crucial for the marine environment, the information about the interaction these animals have with pollutants is very scarce (Ziyaadini *et al.,* 2016).

Oligotrophic waters tend to have a lower zooplankton biomass than that of eutrophic waters (Marsac *et al.,* 2014; Patterson *et al.,* 2006; Pripp *et al.,* 2014). According to Ziyaadini *et al*. (2016), there are three main interactions with pollutants:

- Pollutants can have a toxic effect on zooplankton being either lethal or sub-lethal,
- Zooplankton can change the characteristics of the pollutants,
- Zooplankton can influence how pollutants are biomagnified throughout the trophic levels.

Due to these interactions, it is important to understand the way pollutants and zooplankton interact to determine fate and effects of both (Battuello *et al.,* 2016). Therefore, understanding zooplankton toxicology can lead to a better understanding of what impact pollutants may have on higher trophic levels and what processes in the biogeochemical cycles are influenced (Achary *et al.,* 2017; Battuello *et al.,* 2016; Marsac *et al.,* 2014).

1.5.1. History of zooplankton research in the Indian Ocean

The first recorded collection and study of zooplankton in the Indian Ocean was in 1857 to 1859. This collection was part of a circum-global scientific expedition, while other collections took place on the Danish RRS Dana and the British RRS Discovery II in the 1930s. After these expeditions, limited zooplankton sampling occurred between 1975 and 1993 along the coasts of Somalia, Mozambique, and Seychelles. The surveys were stopped and no new sampling in the WIO was conducted until the African Coelacanth Ecosystem Programme in 2002. This expedition took

place along the coast of southern Mozambique and along the eastern coast of South Africa. Zooplankton sampling only recurred during surveys taking place from 2007 onwards using bongo nets in combination with vertical multi-nets (Groeneveld & Koranteng, 2017).

Seven multidisciplinary expeditions were undertaken between 2007 and 2010 to better understand better the mesoscale eddies of the MC. These were important studies, because they helped with our understanding of the Indian Ocean's productivity, especially in the WIO (Groeneveld & Koranteng, 2017; Lamont *et al.,* 2014). Ternon *et al.,* (2014a) also remarked that information about the zooplankton from the Mozambique Channel is rare.

Even though these studies were conducted, the most important and thorough expedition for zooplankton collection was during the first International Indian Ocean Expedition (IIOE) in 1957. Zooplankton samples were collected for the IIOE in the upper 200 m using a standard oblique bongo net with a mesh size of 330 µm.

1.5.2. Trace metals in Zooplankton

One of the many reasons metallic elements have received attention is because they play a role in physiological functions (Section 1.4.1) (Pempkowiak *et al.,* 2006). High amounts of metals can enter the marine environment but the eventual concentrations can be relatively low due to dilution (Pempkowiak *et al.,* 2006). Both water and food contribute to the assimilation and/or accumulation of these elements by organisms. Trophic transfer plays an important role in metallic element accumulation (Zauke & Schmalenbach, 2006). Even though an increase in the concentration of certain metallic elements can be toxic such as in the case of nonessential metals, essential metal concentrations can have a positive effect at low concentrations. If any metal, nonessential or essential, exceeds certain concentrations it will become toxic (Battuello *et al.,* 2016).

In recent years, an increase in metallic element information can be seen, especially in regions such as the North Sea, Greenland Sea, and Weddell Sea (Zauke & Schmalenbach, 2006), as well as the North Atlantic and Pacific oceans, but little research has been conducted within the WIO (Lebourges-Dhaussy *et al.,* 2014). Worldwide, sampling of zooplankton have been used to determine where "hot spots" for zooplankton are, as well as to determine the amount of metallic element contamination in coastal areas (Pempkowiak *et al.,* 2006). These organisms especially close to coastal regions are exposed to elevated amounts of contaminants from inland sources (Battuello *et al.,* 2016). Essential and nonessential metals have been tested by Battuello *et al*. (2016), but no concentrations were found in zooplankton that were high enough to be of concern.

Metallic elements are redistributed into deeper water through zooplankton defecation. These elements can remineralise and dissolve. By assessing the environmental quality in terms of metallic elements in seawater, the availability of these elements is of importance since a high concentration can have toxic effects (Battuello *et al.,* 2016).

Within marine organisms, the accumulation patterns and accumulated concentration can vary between organisms of the same species. For example, different species of zooplankton from the same area have been found with different metallic elements concentrations (Zauke & Schmalenbach, 2006). Zooplankton can be used as biomonitors since they have a wide distribution, occupy different trophic positions, have high abundance, and have a high affinity for assimilating and/or bio-accumulating metals (Battuello *et al.,* 2016).

The role of zooplankton in the biogeochemical process is well known, particularly the redistribution of metallic elements through the water column. Due to this redistribution and high biomass and spatial distribution, numerous studies have used zooplankton as biomonitors (Zauke & Schmalenbach, 2006). Zauke & Schmalenbach (2006) found high concentrations of Cd in zooplankton from the Arctic region. Pempkowiak *et al*. (2006) found samples of zooplankton contained detectable concentrations of Al, Mn, and Hg. However, there may have been some contribution from inorganic matter analysed together with the zooplankton. Pempkowiak *et al*. (2006) found that even though the concentration of metals within the Baltic Sea was small, the sediment layers were enriched with cadmium, lead, zinc, copper, and mercury.

In the ocean's water column, zonal patterns can be seen. This physical zonation can be contributed to fluctuating salinity and temperature across continental shelves. Even though zonation occurs, it is not a definitive barrier separating communities of zooplankton but rather increases the diversity of zooplankton communities (Schultes *et al.,* 2013).

Since plankton can be used as good bioindicators of environmental change, more research and monitoring programs are recommended to determine the effects of pollutants on these ecosystems (Groeneveld & Koranteng, 2017). There have been many studies conducted on the distribution of metals and zooplankton along Indian coastal waters (Srichandan *et al.,* 2016) but none in the WIO. Therefore, studies that focus on metallic elements within this region, especially within zooplankton, are important.

1.6 Aim and objectives

- Characterise the metal content and relative compositions of zooplankton of the WIO
- Map and interpret the distribution of metals
- Identify zooplankton as “hot spot” indicator

Objectives

- Collect samples from various sites and depths along transects in the WIO
- Measure concentrations of metals and metalloids
- Assess metals in zooplankton as a spatial bioindicator
- Assess potential effects of zooplankton in the food web (literature based)

Chapter 2: Materials and methods

2.1. Ethical approval

Collection and analyses of samples was approved by the ethics committee of the North-West University (NWU) (NWU-01936-19-A9).

2.2. Study areas

Three study regions in the WIO were identified for sampling of zooplankton for metal analyses. Areas were classified according to the influence of three different oceanic currents. Samples were taken in the Mozambique Channel (MC) off the coast of Mozambique, in the East African Counter Current (EACC) of the coast of Tanzania, and in the South Equatorial Current (SEC) around the islands of Comoros, forming part of the WIO (Figures. 2.1, 2.2, 2.3, 2.4). The sampling was made possible due to participating in two Second International Indian Ocean II Expedition (IIOE 2) cruises. These cruises took place during October 2017 and June 2018 (Table 2.1; 2.2, 2.3). Very little research has been conducted on zooplankton in the WIO and even less has been conducted off the coasts of these regions.

The seas of the coasts of Mozambique and Tanzania are known for shipping, fishing, cities, agriculture, coastal mining, natural gas extraction, and oil drilling (Bosire *et al.,* 2016; Llewellyn *et al.,* 2016). According to the UNDESA (2019) database, approximately 110 million people live in the countries along the MC. Of the four bordering countries, Tanzania has 58 million people, followed by Mozambique with 30 million, Madagascar with a population of 27 million, and Comoros with approximately 850 000 people (Obura *et al.,* 2019).

Obura *et al.,* (2019) stated that the coastal development has been increasing at approximately double the predicted rate. This is mainly influenced by urbanization since these coastal areas have abundant natural resources. This is evident when looking at how many people are supported by fisheries alone. Approximately 56 000 people work in fisheries in Tanzania, with almost five times that number (280 000) in Mozambique (Obura *et al.,* 2018).

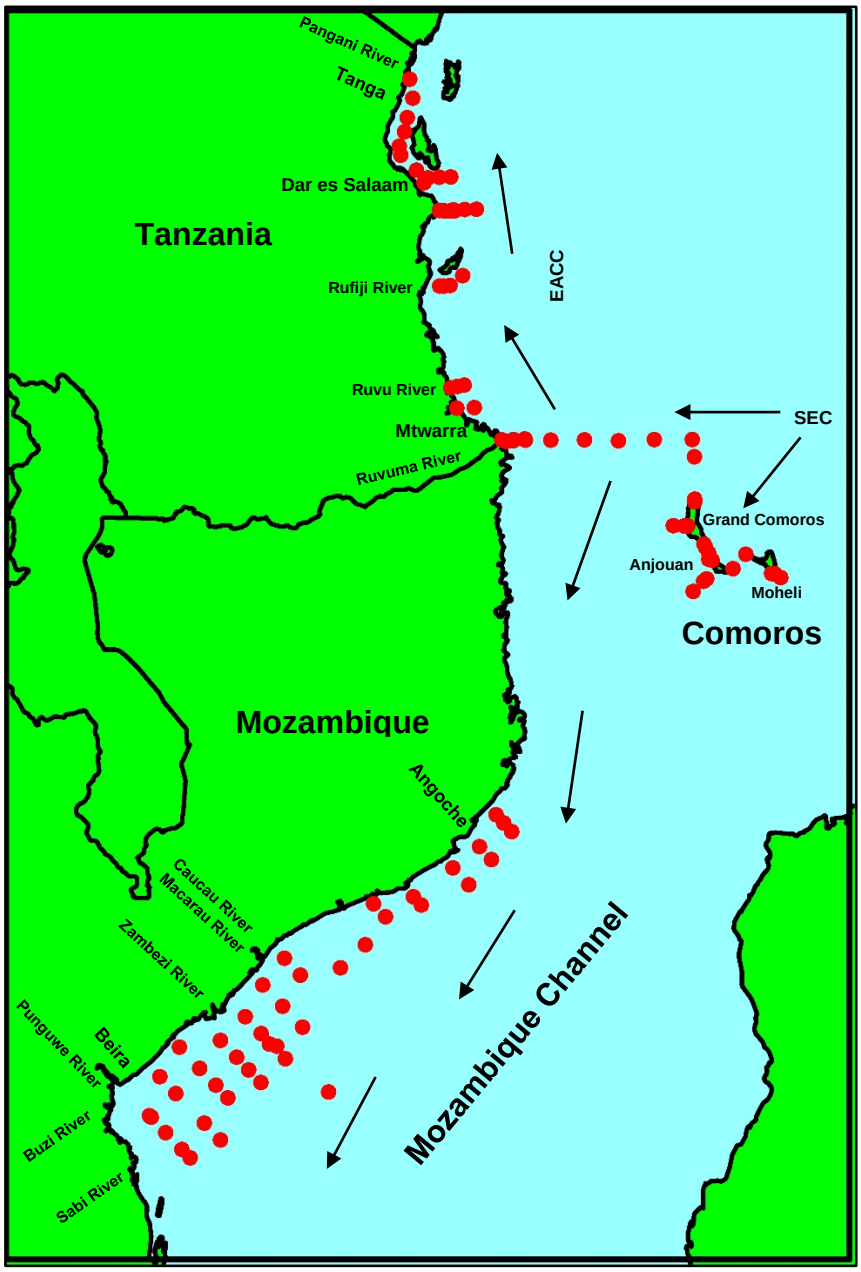

Figure 2.1: Locations of all hydrographic stations sampled during 2017 and 2018 within the MC, EACC, and SEC. Sampling began at Beira and ended just above Tanga. There were 29 transects running perpendicular to the coast and 94 stations were sampled for zooplankton.

2.2.1. Mozambique Channel: MC (Mozambique)

Mozambique has great and diverse mineral resource potential and is viewed an important exporter of raw materials, in particular coal, aluminium (Al) and gold (Au) (Marin *et al.,* 2016). According to the World Wildlife Foundation (WWF) (2018), 58 900 km^2 of Mozambique is under contract for oil and gas, with many of these located along the Mozambican coastline (Obura *et al.,* 2019). The study area falls in the greater area known as the Sofala Bank stretching from Beira 21°S in the southern parts of Mozambique up to Angoche 16°S in the northern part of Mozambique (Malauene *et al.,* 2018).

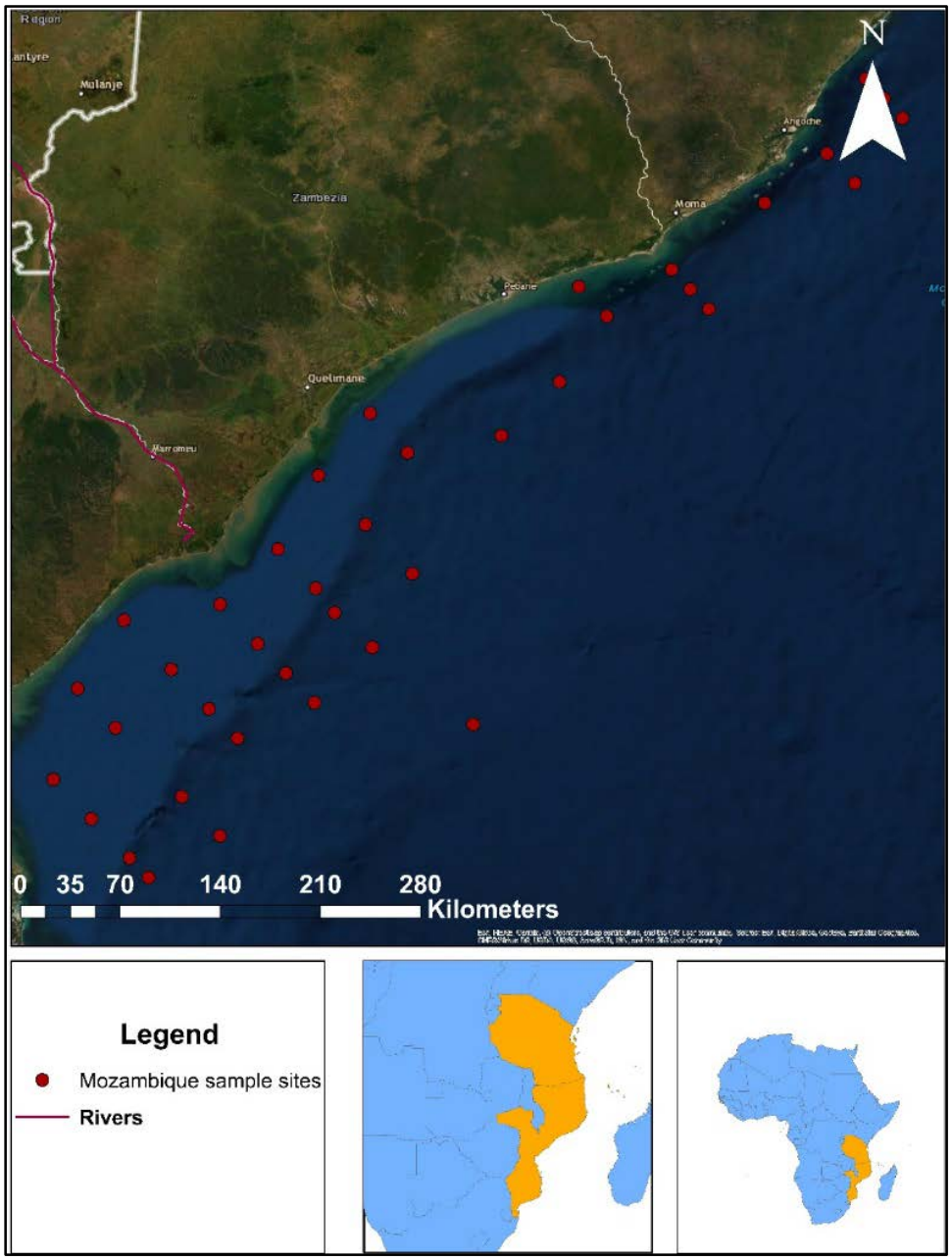

Figure 2.2: Locations of all hydrographic stations sampled during October-November 2017 in the Mozambique Channel. Sampling began at Beira and ended just north of Angoche. There were 14 transects running perpendicular to the coast and 39 stations. Zooplankton was sampled at every station along each transect.

Table 2.1: Station coordinates for every sample in the Mozambique Channel for 2017.

Grid	Latitude (degrees-south)	Longitude (degrees-east)	Year
M1-02	-20.31533333	35.3075	2017
M1-04	-20.56283333	35.54583333	2017
M1-06	-20.81533333	35.77816667	2017
M1-08	-20.93283333	35.90433333	2017
M2-01	-19.806	35.52316667	2017
M2-03	-19.993	35.6975	2017
M2-07	-20.42516667	36.11433333	2017
M2-10	-20.67983333	36.35466667	2017
M3-01	-19.31566667	35.75383333	2017
M3-03	-19.62766667	36.04916667	2017
M3-05	-19.87583333	36.28666667	2017
M3-07	-20.06333333	36.46866667	2017
M4-01	-19.091	36.23866667	2017
M4-02	-19.21566667	36.35416667	2017
M4-06	-19.6475	36.77183333	2017
M4-08	-19.83466667	36.94683333	2017
M5-04	-19.11633333	36.95966667	2017
M5-06	-19.23766667	37.08016667	2017
M6-01	-18.40483333	36.978	2017
M6-04	-18.716	37.27333333	2017
M6-09	-19.02383333	37.5665	2017
M7-01	-18.017	37.30116667	2017
M7-04	-18.26816667	37.53766667	2017
M8-05	-17.96916667	37.96916667	2017
M8-07	-18.15616667	38.15616667	2017
M9-05	-17.81716667	38.492	2017
M10-01	-17.25766667	38.64766667	2017
M10-03	-17.40383333	38.7935	2017
M11-01	-17.102	39.19033333	2017
M11-03	-17.236	39.31416667	2017
M11-04	-17.38916667	39.431	2017
M12-01	-16.66316667	39.75416667	2017
M13-02	-16.38366667	40.17316667	2017
M13-04	-16.57433333	40.3425	2017
M14-01	-15.91883333	40.42	2017
M14-03	-16.03733333	40.53	2017
M14-04	-16.1635	40.64633333	2017

2.2.2. East African Coastal Current: EACC (Tanzania)

Tanzania consists mainly of a large mainland sector and three major islands namely; Zanzibar, Mafia, and Pemba. Tanzania has a coastline that stretches from the northern border against Kenya towards the southern border of Mozambique. This stretch of coastline is approximately 800 km long and consists of a narrow section along the coast towards Kenya. The coastal section on the mainland consists mainly of thick sedimentary rock layers (Masalu, 2002).

In terms of mining and exporting of raw materials, Tanzania has become one of the most invested countries as well as one of Africa's top gold producing countries, next to South Africa (Bryceson *et al.,* 2012). Tanzania made a gross income of approximately US $1.4 billion in 2009 on gold exports alone, with Tanga, being one of the main mining regions. Mtwara is known for its variety of gemstone mines. Both mining regions are close to the (Bryceson *et al.,* 2012). Near Dar es Salaam, an increase in sand mining has been observed, especially in local streams (Masalu, 2002).

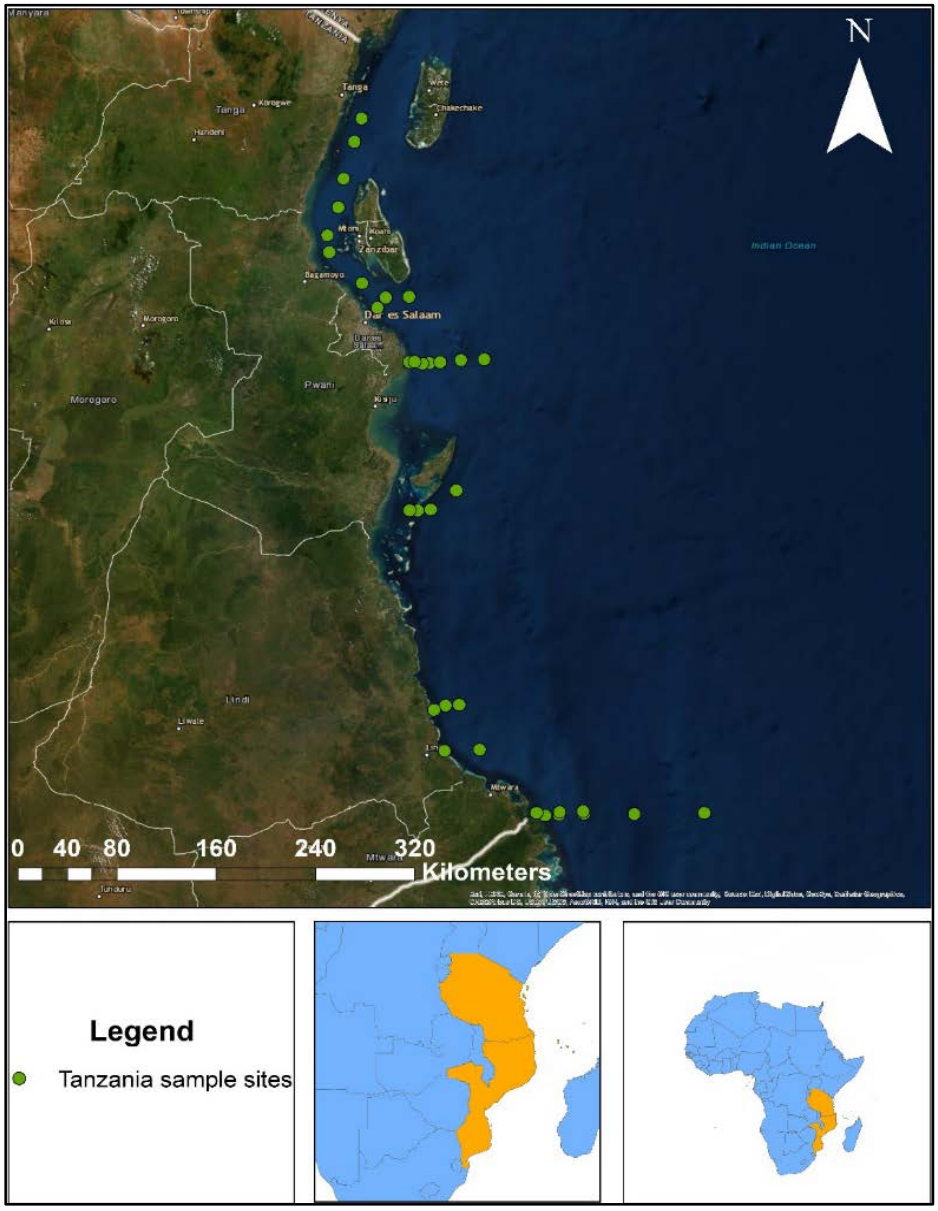

Figure 2.3: Locations of all hydrographic stations sampled during October-November 2017, and June-July 2018 in the East African Coastal Current. Sampling began at Mtwara and ended at

Tanga. There were 15 transects running perpendicular to the coast and 34 stations. Zooplankton was sampled at every station along each transect.

Table 2.2: Station coordinates for the East African Coastal Current for 2017-2018.

Grid	Latitude (degrees-south)	Longitude (degrees-north)	Year
T1-01	-10.43	40.50666667	2017
T1-03	-10.42	40.67533333	2017
T1-05	-10.42	40.84266667	2017
T2-01	-9.97	39.84133333	2017
T2-03	-9.96	40.09483333	2017
T6-02	-8.03	39.92716667	2017
T8-01	-7.08	39.62383333	2017
T8-05	-7.06	39.95916667	2017
T8-07	-7.05	40.12833333	2017
T9-02	-6.6	39.41416667	2017
T9-04	-6.59	39.58316667	2017
T-A2	-5.27	39.24066667	2018
T-A3	-5.44	39.187	2018
T-A4	-5.71	39.1095	2018
T-A5	-5.93	39.07033333	2018
T-A6	-6.14	38.99233333	2018
T-A7	-6.26	39.00583333	2018
T-A8	-6.49	39.24266667	2018
T-A9	-6.67	39.35466667	2018
T-B1	-7.08	39.58633333	2018
T-B2	-7.09	39.6795	2018
T-B3	-7.08	39.7305	2018
T-B4	-7.08	39.80916667	2018
T-C1	-8.17	39.74083333	2018
T-C2	-8.18	39.64683333	2018
T-C3	-8.18	39.58683333	2018
T-D1	-9.63	39.94633333	2018
T-D2	-9.63	39.848	2018
T-D3	-9.67	39.7635	2018
T-E1	-10.45	40.56933333	2018
T-E2	-10.44	40.67033333	2018
T-E3	-10.44	40.85116667	2018
T-E4	-10.44	41.21533333	2018
T-E5	-10.43	41.7215	2018

2.2.3. South Equatorial Current: SEC (Comoros)

The Comoros is a group of volcanic islands (Grand Comoros, Anjouan, and Moheli) located within the SEC in the northern part of the MC. These islands are approximately 5.4 million years old. There is a subsea mountain situated near Grand Comore, the summit of which reaches to about 15 m below sea level (Obura *et al.,* 2019). In general, the Comoros islands has a combined dry-land surface area of 2 235 km^2 (UNDESA, 2019).

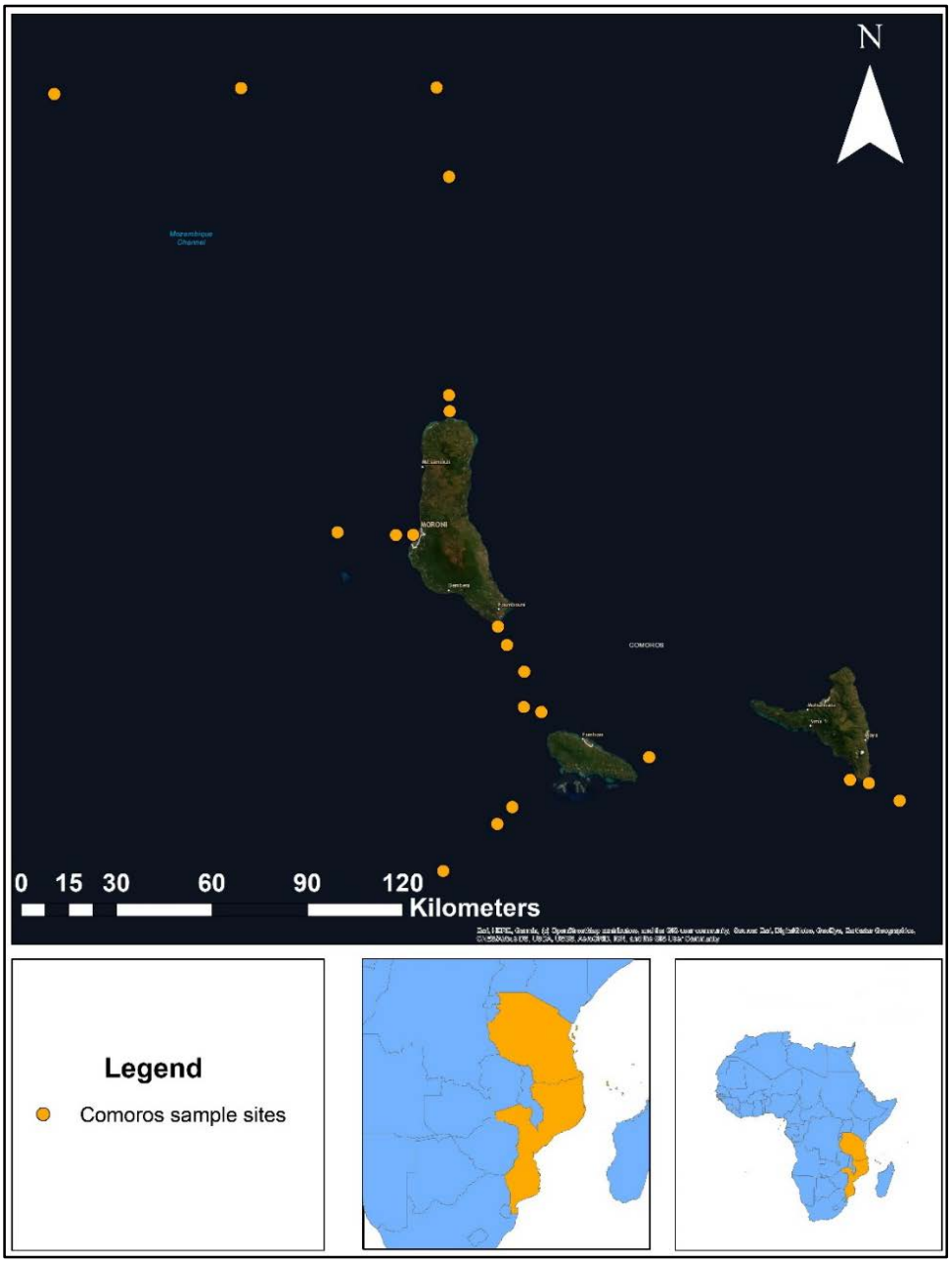

Figure 2.4: Graphical representation of sampling sites in the South Equatorial Current, sampled during, June-July 2018. Sampling began at Mtwara and ended at Moheli. There were eight transects running perpendicular to the coast and 21 stations. Zooplankton was sampled at every station along each transect.

Table 2.3: Station coordinates for every sampling station of the South Equatorial Current.

Grid	Latitude (degrees-south)	Longitude (degrees-north)	Year
C-E6	-10.445667	42.22733333	2018
C-E7	-10.429167	42.75533333	2018
C-E8	-10.427167	43.309	2018
C-F1	-10.68	43.34383333	2018
C-F3	-11.298	43.344	2018
C-F4	-11.343833	43.346	2018
C-F5	-11.6935	43.2425	2018
C-F6	-11.694167	43.19366667	2018
C-F7	-11.686333	43.02833333	2018
C-G1	-11.953	43.48183333	2018
C-G2	-12.005333	43.50766667	2018
C-G3	-12.080667	43.557	2018
C-G4	-12.195167	43.60466667	2018
C-G5	-12.463667	43.52266667	2018
C-G6	-12.511833	43.48016667	2018
C-G7	-12.645167	43.32766667	2018
C-H1	-12.323167	43.90966667	2018
C-H5	-12.3865	44.47816667	2018
C-H7	-12.4455	44.6185	2018
C-H8	-12.3965	44.53116667	2018

2.3. Sample collection and preparation

Samples were collected from the SA Agulhas II (Figure 2.5) during the IIOE 2 cruises in 2017 and 2018 (Tables 2.1, 2.2, 2.3). Zooplankton samples were collected using an oblique bongo net (2 x 200 µm mesh) (Figure 2.6 a, b, c), which was lowered down to 200 m in deep water, or 10 m above the seabed in regions shallower than 200 m (Pretorius *et al.,* 2016).

Figure 2.5: The SA Agulhas II docked in Cape Town Harbour (photo: Anne Treasure).

Figure 2.6: Oblique Bongo net being fitted with sampling bucket (a), rinsed for sample removal (b), and the entire net being taken out of the water (c).

Between the SEC, EACC, and MC, 98 day and night samples were collected (Figure 2.1, 2.2, 2.3) with an oblique bongo net (Figure 2.6 c) being dragged behind the vessel for 15 minutes at a constant speed of 2 knots (Al—marah *et al.,* 2018; Severini *et al.,* 2012; Thirunavukkarasu *et al.,* 2013). Samples were then split into two identical samples using a Folsom Plankton splitter (Figure 2.7) (Achary *et al.,* 2017). One half of the sample was given to students from UKZN for microplastic analyses and the other half was preserved in high-density polypropylene sample containers, in which 20% ethanol was added to make up 10% of the sample volume. Samples were then stored at 4°C aboard the vessel (Figure 2.5). The samples were transported on dry ice from Durban to the North-West University for further storage until analysis.

Figure 2.7: Folsom plankton splitter with collecting containers.

The conductivity, temperature, and depth rosette (CTD-rosette) system (Figure2.8) was used to collect additional physiochemical data (temperature, salinity, depth, fluorescence, and oxygen), for determination of relationships between environmental variables and metallic elements (Rejomon *et al.,* 2010). I used 507 data points.

Figure 2.8: Conductivity, Temperature, and Depth (CTD) sampler with 24 fitted 12 L collecting bottles.

2.4. Laboratory analysis

In the laboratory, stored samples were weighed (to determine the accurate mass of samples) and sub-samples were taken for further processing. Sub-samples were cleaned to remove any visible contamination from plastic or paint chips and placed in high-density polyethylene (HDPE) 50 mL centrifuge tubes (Achary *et al.,* 2017; Rejomon *et al.,* 2010; Salem & Ayadi, 2017). After each sample transfer, equipment was rinsed with acetone and hexane to remove any biological material. Cleaned samples were centrifuged at 4000 rpm for 15 minutes (Leal *et al.,* 2009; Tao *et al.,* 2012). Supernatant was decanted. Centrifuging was repeated until approximately 5 mL of sample pellet has formed at the bottom of the centrifuge tube. Sub-samples of approximately 5 mL were weighed to determine mass and stored at -80°C until completely frozen. Samples were desiccated using freeze drying at 8 kPa and -50°C, and transferred to the laboratory for analyses along with a standard reference material (SRM) (ERM-CE278K – mussel tissue) used as quality control (QC) with the same digestion protocol.

Compacted zooplankton pellets were analysed for 34 metallic elements, using the internationally standardized 3051A method (EPA, 2007) to determine the metal concentrations. The concentrations of metallic elements were determined using inductively coupled plasma mass spectrometry (ICP-MS) (Agilent 7500 series). Approximately 0.03 g (each accurately weighed) of the sample was placed into a Teflon tube and acid-digested by adding 9 mL of nitric acid and 3 mL of hydrochloric acid into the Teflon tube, capped, and placed in a high-performance microwave digestion system (Milestone, Ethos UP, Maxi 44). The sample was heated and allowed to run at 1800 MW for 15 minutes at 200 °C. After cooling, the digested sample was brought up to a final volume of 20 mL and analysed. Concentrations were expressed as mg/kg dry mass (dm). Analysis was conducted by the Eco Analytica Laboratory in Potchefstroom. I had 3 162 concentration data points.

2.5. Statistical analysis

I used two ways of analysing the data. I used univariate, bivariate, and multivariate statistics, comparing within and between the three currents. I also used geographic distributions and interpolation, using geographic analytical techniques.

The data were analysed using GraphPad Prism 8.02 (www.graphpad.com) to determine if the data points were normally distributed. One-way ANOVAs were used to determine the statistical significance with a Kruskal-Wallis, non-parametric test.

There was a large variation in concentrations. These might have been caused by small paint flecks, plastics, and/or micro mineral particles. Outliers were determined and removed from datasets. Hundred and fifty-one outliers (4.7% of the total) were removed from the data set of 34 metallic elements; however, these will be referred to in the discussion. I used the ROUT method in Prism to identify the outliers. This method finds a model that where the outliers have little impact, using a false discovery rate. Outliers far enough from the predicted model results are then considered outliers. The ROUT method was chosen as it is better than the normally used Grubbs' method, as it can detect two or more outliers better (Motulsky and Brown, 2006). Q was set at 1%. Confidence intervals of 95% were set for a statistical significance of ($p < 0.05$).

Linear regressions of elemental concentrations found for Mozambique, Tanzania, and Comoros were used to inspect if zooplankton can be used as a biological indicator for these regions. Each sampling site was used as an individual sample for statistical analysis since each site is exposed to possible different concentrations of metallic elements. Nonmetric multivariate statistics (NMS), with Sørensen as a distance measure, were used to determine and compare if any metallic elements from the different locations differ. Multivariate statistics were conducted using PC-ORD version 7 (MjM Software Design, www.pcord.com). Data concentrations were relativized for each individual element, to derive a relative profile of metallic elements. Two hundred and fifty runs of data were utilized for a starting configuration

Contour plots of zooplankton metallic element concentrations and certain environmental variables were plotted in Ocean Data View 4 (http://odv.awi.de) using variation intrapolation (DIVA). This allows an optimal interpolation of the data, compared to optimal interpolation. DIVA plotting is ideal since it takes into account the bathymetric features as well as coastlines for an exact division in the domain where the assessment is performed (Pretorius *et al.,* 2016). These graphs represent the geographical distribution of metallic elements along the coastlines of the designated areas.

Additional network analysis was conducted using R (version 3.6.0). The Spearman's rho values and p values were calculated using the rcorr function from the Himsc package (version 4.2-0). The network was visualized using the functions of the igraph package (version 1.2.4.1).

Chapter 3: Results

3.1. Analytical data

All 94 samples had quantifiable concentrations for all 34 metallic elements. Summarised statistics for the 3 196 concentrations are presented in Table 3.1.

Table 3.1. The minimum, median, mean, maximum concentrations (mg/kg dm), standard deviation (SD), and coefficient of variation (%CV) for 34 metallic elements in plankton from the EACC, MC, SEC combined, arranged from highest to lowest mean concentration. Concentrations are rounded to two significant numbers in all cases.

Element	Min	Median	Mean	Max	SD	%CV
Ca	7600	53000	55000	180000	31000	56
Mg	2800	12800	12300	25500	4600	38
Sr	125	9400	10000	38600	8500	85
Fe	880	4300	6040	25700	5300	88
Al	540	3030	4800	24900	4900	104
K	1050	3300	3300	6700	1300	40
P	890	2600	3200	14600	2400	75
Zn	120	570	710	2700	510	72
Cr	160	270	400	10000	1100	262
Ti	130	300	390	1300	250	65
Ni	47	68	150	5500	570	376
Ba	17	115	130	350	75	56
Cu	15	56	63	340	41	66
Mn	13	39	53	230	39	73
Mo	3.6	20	47	1600	170	360
B	11	42	42	97	19	46
Cd	1.2	28	27	779	15	57
Pb	3.8	10	21	800	82	388
V	3.4	16	17	50	8.7	51
Se	5.1	15	16	32	5.8	36
Rb	2	5.8	12	73	14	113
Pd	0.67	9.9	11	40	8.9	81
As	1.5	5.7	8.3	38	6.2	75
Co	2.1	3.7	4.5	15	2.5	55
U	1.3	3.7	3.8	10	1.3	34
Th	0.12	0.82	1.7	11	2	117
Hg	0.49	0.98	1.1	2.8	0.46	42
Sb	0.23	0.78	0.87	2.1	0.42	49
Ag	0.11	0.54	0.79	7.9	1	130
Bi	0.03	0.13	0.4	8.2	0.95	238
Au	0.0011	0.04	0.25	3.6	0.66	270
Be	0.01	0.08	0.17	1.1	0.2	119
Tl	0.016	0.16	0.15	0.4	0.08	55
Pt	0.072	0.1	0.15	3.3	0.34	220

High %CVs (> 200%) occurred for Pb (lead), Ni (nickel), Mo (molybdenum), Au (gold), Cr (chromium), Bi (bismuth), and Pt (platinum) (Table 3.1). A relatively low %CV was found for U (uranium) and Se (selenium).

One of the features of the dataset was the high variability between samples, as indicated by the %CVs in Table 3.1. Inspection of the data showed unusually high concentrations of certain elements inconsistent with the other elements in the same sample and when compared with other samples. This might be due to inorganic particles such as paint flecks, plastics, and suspended mineral particles (Bruland and Lohan, 2006). These outliers were identified in each individual dataset (EACC, MC, and SEC) using the iterative ROUT method in Prism that finds multiple outliers based on false discovery rate to identify which points falls outside the predicted distribution model. The identified outliers (n=151) were removed from further statistical analyses but are listed in Tables 3.2 to 3.4.

Table 3.2: Outliers (64) identified in the Mozambique Channel (MC) dataset that were removed from further statistics.

Stations	Element	Outlier (mg/kg dm)	Year
M4-02	Be	1.1	2017
M5-10, M10-03, M10-01	Al	18860, 25000, 17000	2017
M13-02, M14-04, M5-06	P	12000, 9700, 5100	2017
M1-02	Ca	180000	2017
M4-02, M10-01	Ti	1300, 1200	2017
M4-02	V	50	2017
M13-04, M11-01, M12-01, M10- 01	Mn	150, 150, 180, 230	2017
M4-02, M10-01	Fe	26000, 24000	2017
M4-02, M10-01	Co	15, 13	2017
M9-05	Ni	100	2017
M5-02, M1-08	Cu	200, 340	2017
M5-04, M3-05	Zn	1200, 2300	2017
M5-02	Se	31	2017
M4-02, M10-01	Rb	73, 57	2017
M13-02, M6-04, M2-01, M3- 03, M11-04	Sr	18000, 24000, 32000, 20000, 21000	2017
M1-04, M1-02	Mo	84, 280	2017
M13-02, M6-04, M2-01, M3- 03, M11-04	Pd	20, 27, 34, 22, 24	2017
M6-04, M12-01, M4-06, M7- 04	Ag	5.7, 2.4, 1.6, 2.7	2017
M9-05, M12-01, M1-02, M3- 05, M7-01	Pt	0.3, 0.1, 0.4, 0.1, 0.2	2017
M14-04, M12-01	Au	1.3, 1.8	2017
M6-04, M12-01	Hg	2.4, 2.3	2017
M5-02	Pb	800	2017
M9-05, M12-01, M4-06, M10-03, M8-05, M8-07, M6- 09, M10-01	Bi	1.9, 2.1, 0.9, 1.3, 1.8, 2.2, 1.5, 8.2	2017
M4-02, M10-01	Th	11, 8.9	2017
M14-03	U	10	2017

Outliers identified in the MC dataset are listed in Table 3.2. Bismuth had the most outliers (eight) in this specific data set with the highest concentration being 8.2 mg/kg dm.

Table 3.3: Outliers (65) identified in the East African Coastal Current (EACC) dataset that were removed from further statistics.

Station	Element	Outlier (mg/kg dm)	Year
T-A5, T-B2, T-B1, T- A8	Be	0.4, 0.8, 0.5, 0.4	2018
T-A5, T-B2, T-B1, T- A8	Al	19000, 24000, 13000, 16000	2018
T-A7, T9-02, T8- 01, T1-03, T8- 07	P	6900, 6800, 14000, 15000, 7900	2017, 2018
T-A5, T-B2, T-A8	Ti	650, 790,780	2018
T-A3, T-A8, T-A2, T6-02	Cr	870, 520, 10000, 1600	2017, 2018
T-A5, T-B2, T-B1	Mn	110, 160, 100	2018
T-A5, T-B2, T-A8, T- A2	Fe	16000, 16000, 14000, 25000	2018
T-B2, T-A2	Co	7.8, 15	2018
T-A2, T6-02, T1-01	Ni	630, 5500, 750	2017, 2018
T-A2	Cu	150	2018
T-A5, T-B2, T-B1, T- A8	Rb	24, 39, 28, 28	2018
T-A2, T6-02, T1- 01	Mo	110, 1600, 220	2017, 2018
T-B2, T-D1, T9-04	Ag	7.9, 3.3, 2	2018
T9-02, T8-05, T1- 01, T8-07	Ba	280, 340, 300, 290	2017
T-C3, T8-01, T1- 05, T6-02	Pt	0.2, 0.7, 3.3, 0.2	2017
T-A9, T-C1, T-B4, T- B1	Au	0.3, 2.5, 3.6, 0.7	2017, 2018
T-A9	Pb	30	2018
T8-01, T1-05, T2- 03, T2-01, T1- 03	Bi	0.9, 0.8, 1.5, 2.1, 0.4	2017
T-A5, T-B2, T-B1, T- A8	Th	2.9, 6.5, 4.7, 3.8	2018

Outliers identified in the EACC dataset are presented in Table 3.3. Bismuth and P were identified to have the most outliers (five each).

Table 3.4: Outliers (22) identified in the South Equatorial Current (SEC) dataset that were removed from further statistics.

Station	Element	Outlier (mg/kg dm)	Year
C-H8, C-H5, C-H2	Ti	760, 820, 940	2018
C-H2	Cr	470	2018
C-H2, C-E7	Ni	790, 200	2018
C-F1	Cu	140	2018
C-F7, C-E6	Zn	2700, 2300	2018
C-E6	Rb	7.5	2018
C-H2, C-E7	Mo	280, 60	2018
C-G6, C-H1, C-G7	Pt	0.2, 0.3, 0.3	2018
C-F3, C-F1	Au	0.1, 0.3	2018
C-H5, C-G2	Hg	0.8, 2.5	2018
C-F4	Pb	32	2018
C-F4	Bi	0.3	2018
C-H8	As	38	2018

Outliers identified from the SEC dataset are presented in Table 3.4. Titanium had the most outliers (three) at 940 mg/kg dm.

With the removal of the 151 identified outliers (4.7% of the original number of data points), the summary statistics of the combined dataset of the concentrations were re-calculated (Table 3.5).

Table 3.5: The minima, media, means, maxima concentrations (mg/kg dm), standard deviations (SD), and coefficient of variation (%CV) for 34 metallic elements in plankton from the Indian Ocean in the EACC, MC, and SEC combined, minus the outliers, arranged in the same order as Table 3.1.

Element	Min	Median	Mean	Max	SD	Original %CV	%CV
Ca	7600	52700	53700	119000	28000	56	52
Mg	2800	12800	12300	25500	4600	38	38
Sr	125	9200	9300	38600	8100	85	87
Fe	880	3800	5100	17300	3770	88	74
Al	540	2900	3900	16000	3300	104	85
K	1050	3300	3300	6700	1300	40	4
P	890	2500	2600	5100	920	75	36
Zn	120	560	650	2000	410	72	63
Ti	130	280	350	940	200	262	57
Cr	160	270	270	430	56	65	21
Ba	17	110	130	350	67	376	53
Ni	47	67	87	750	94	56	108
Cu	15	55	56	130	23	66	41
Mn	13	38	46	120	25	73	54
B	11	42	42	97	19	360	46
Cd	1.2	28	27	79	15	46	57
Mo	3.6	18	21	66	14	57	68
V	3.4	16	17	51	8	388	48
Se	5.1	15	16	32	5.8	51	36
Pb	3.8	10	12	35	7	36	57
Rb	2	5.5	10	45	11	113	105
Pd	0.67	9.8	10	40	8.4	81	82
As	1.5	5.4	7.9	22	5.5	75	69
Co	2.1	3.6	4.1	9.8	1.7	55	42
U	1.3	3.7	3.7	6.4	1.1	34	30
Th	0.12	0.77	1.4	6.9	1.6	117	110
Hg	0.49	0.97	1	2.4	0.38	42	37
Sb	0.23	0.77	0.87	2.1	0.42	49	49
Ag	0.11	0.53	0.56	1.3	0.23	130	41
Tl	0.016	0.16	0.15	0.4	0.08	238	55
Bi	0.03	0.12	0.15	0.45	0.095	270	65
Be	0.01	0.08	0.14	0.77	0.16	119	110
Pt	0.072	0.098	0.098	0.13	0.015	55	16
Au	0.0011	0.031	0.06	0.67	0.11	220	177

*MC = Mozambique Channel, EACC = East African Coastal Current, SEC = South Equatorial Current

The effect of the removal of the outliers are shown in the reduction in %CV for almost all elements when compared with Table 3.1. The mean %CV dropped from the original 117% to 61%. The difference was also statistically significant ($p = 0.0077$, Mann-Whitney). Therefore, the reduction in %CV probably removed the effects of contributions of non-planktonic materials to the overall

assessment, allowing differences and complementarities between the three datasets to be less hindered by spurious data.

The highest mean concentrations in decreasing order were Ca > Mg > Sr > Fe > Al > K > P (Table 3.5). The lowest mean concentrations were for Sb>Ag>Tl>Bi>Be>Pt>Au, with Au having the lowest mean concentration of 0.06 mg/kg dm. Gold also had the highest %CV of 177% and K the lowest at 4%. In decreasing order of %CV, the metals ranged as follows; Au > Th > Be > Ni > Rb had %CVs higher than 100, whereas, Sr > Al > Pd > Fe >As > Mo > Bi > Zn > Ti > Cd >Pb > Tl > Mn > Ba > Ca > Sb > V > B > Co > Cu > Ag > Mg > Hg > P > Se > U had relatively low %CV ranging from 87 between 30. The lowest %CVs was Cr > Pt > K.

Table 3.6: Summary statistics for (mg/kg dm) for five alkaline earth metal concentrations in zooplankton from the MC, EACC, and SEC, and one-way ANOVA p-values for each element.

		Alkaline earth metals					
Element	**Current**	**Min**	**Median**	**Mean**	**Max**	**SD**	**%CV**
Be (p < 0.0001)	MC	0.012	0.16	0.2	0.77	0.2	86
	EACC	0.015	0.08	0.09	0.23	0.06	67
	SEC	0.01	0.05	0.05	0.12	0.03	64
Mg (p = 0.0037)	MC	4019	12900	12500	25400	4800	38
	EACC	2800	11400	10400	21100	4700	45
	SEC	8300	14700	14600	19500	3040	21
Ca (p < 0.0001)	MC	7900	30600	37000	110000	26000	66
	EACC	8800	56000	63000	120000	29000	46
	SEC	7600	63000	63000	100500	18000	29
Sr (p < 0.0001)	MC	125	1260	2800	14700	4100	121
	EACC	134	10300	12000	38600	8600	69
	SEC	300	12500	13800	24300	6400	46
Ba (p = 0.0373)	MC	22	97	110	254	71	65
	EACC	17	115	125	249	49	39
	SEC	67	130	140	298	60	42

*MC = Mozambique Channel, EACC = East African Coastal Current, SEC = South Equatorial Current

Apart from Be, all alkaline metals had the highest concentration in zooplankton from the SEC (Table 3.6). The MC had the lowest concentrations of alkaline metals, apart from Be which had the highest concentration. Relatively low %CVs were calculated for all metals except for Sr from the MC with the highest %CV of 121%. The lowest %CV was for Mg from SEC at 21%. All alkaline metals were significantly different (ANOVA; p = 0.05) between the three currents.

Table 3.7: Summary statistics for concentrations (mg/kg dm) of nine transitional metals from Row 4 in zooplankton from the MC, EACC, and SEC, and one-way ANOVA p-values for each element.

Transitional metals: Row 4							
Element	**Current**	**Min**	**Median**	**Mean**	**Max**	**SD**	**%CV**
Ti (p = 0.0812)	MC	130	340	380	940	254	59
	EACC	150	250	280	570	99	36
	SEC	146	280	290	650	116	39
V (p = 0.9507)	MC	3.4	16	15	34	7.2	45
	EACC	4.4	17	18	37	8.6	51
	SEC	9.7	15	16	27	4.6	28
Cr (p < 0.0001)	MC	156	230	240	350	45	18
	EACC	170	298	300	430	57	19
	SEC	163	297	280	340	53	19
Mn (p = 0.3415)	MC	13	39	50	120	32	60
	EACC	18	37	43	100	19	45
	SEC	15	39	38	70	14	37
Fe (p = 0.0013)	MC	880	6000	6300	17300	7038	66
	EACC	1180	3200	3900	10100	3895	58
	SEC	950	2800	3300	6100	3328	50
Co (p = 0.0168)	MC	2.1	4.2	5.4	9.8	2.2	46
	EACC	2.3	3.5	3.9	7	1.2	30
	SEC	2.3	3.2	3.3	4.6	0.65	20
Ni (p < 0.0001)	MC	47	59	58	86	8.4	14
	EACC	50	84	120	160	26	32
	SEC	56	78	85	200	31	36
Cu (p = 0.0525)	MC	15	47	60	130	30	57
	EACC	25	58	57	100	17	31
	SEC	33	63	62	96	16	26
Zn (p < 0.0001)	MC	120	370	460	870	188	48
	EACC	170	810	840	2000	479	57
	SEC	350	760	800	1500	334	42

*MC = Mozambique Channel, EACC = East African Coastal Current, SEC = South Equatorial Current

Titanium, Mn, Fe, and Co had the highest mean concentrations in zooplankton from the MC for Row 4 transitional metals (Table 3.7). Vanadium, Cr, Ni, and Zn had the highest mean concentrations in plankton from the EACC. Only Cu had its highest mean concentration in plankton from the SEC. Of the nine Row 4 elements, only Cr, Fe, Co, Ni, and Zn were significantly different (ANOVA) between the currents, whereas Ti, V, and Mn were not. All the elements had relatively low %CVs with Mn the highest and Ni the lowest. Both these elements were from the MC. The element with the lowest overall %CVs was Cr, at 18%-19%.

Table 3.8: Summary statistics for concentrations (mg/kg dm) of four transitional metals from Row 5 in zooplankton from the MC, EACC, and SEC, and one-way ANOVA p-values for each element.

Transitional metals: Row 5							
Element	**Current**	**Min**	**Median**	**Mean**	**Max**	**SD**	**%CV**
Mo (p = 0.0142)	MC	3.6	8.2	20	55	14	87
	EACC	4.2	19	23	66	15	65
	SEC	12	22	24	52	9.7	40
Pd (p < 0.0001)	MC	0.71	1.9	3.7	17	4.5	104
	EACC	0.67	10	13	40	9.1	68
	SEC	0.8	13	15	28	6.6	46
Ag (p = 0.0496)	MC	0.11	0.48	0.5	1.2	0.26	52
	EACC	0.25	0.53	0.6	0.8	0.15	28
	SEC	0.3	0.63	0.7	1.3	0.24	37
Cd (p = 0.0001)	MC	1.2	15	22	51	15	78
	EACC	9.2	35	34	79	14	42
	SEC	2.3	33	32	52	12	36

*MC = Mozambique Channel, EACC = East African Coastal Current, SEC = South Equatorial Current

Except for Cd, all Row 5 transitional metals were found at the highest mean concentrations in the SEC, whereas the MC had the lowest mean concentration for all the elements (Table 3.8). All four elements were significantly (ANOVA) different between regions. All the elements had relatively low %CVs for each current with the highest %CV being Pd from the MC. The lowest reported %CV was for Ag from the EACC, at 28%-52%.

Table 3.9: Summary statistics for concentrations (mg/kg dm) of three transitional metals from Row 6 in zooplankton from the MC, EACC, and SEC, and one-way ANOVA p-values for each element.

Transitional metals: Row 6							
Element	**Current**	**Min**	**Median**	**Mean**	**Max**	**SD**	**%CV**
Pt (p < 0.0001)	MC	0.07	0.08	0.08	0.11	0.009	11
	EACC	0.08	0.1	0.1	0.13	0.013	13
	SEC	0.08	0.1	0.1	0.13	0.01	9.5
Au (p = 0.0917)	MC	0.0011	0.04	0.03	0.23	0.08	113
	EACC	0.007	0.04	0.1	0.67	0.16	193
	SEC	0.002	0.01	0.05	0.05	0.018	90
Hg (p = 0.3131)	MC	0.52	0.98	1	1.7	0.26	25
	EACC	0.49	0.99	1.1	2.4	0.49	45
	SEC	0.5	0.83	0.9	1.6	0.32	35

*MC = Mozambique Channel, EACC = East African Coastal Current, SEC = South Equatorial Current

Of all the Row 6 transitional metals, the highest mean concentrations in zooplankton were from the EACC, with the MC having the lowest mean concentrations for Pt and Au (Table 3.9). The EACC had the highest maximum concentration of Hg in zooplankton of all three currents combined, but only Pt was statistically significantly different (ANOVA; $p < 0.0001$). Platinum also had the lowest overall %CV, with the SEC having the lowest %CV for these elements. The highest

%CV was Au from the EACC. Of the 34 elements analysed, Row 6 (Au, Pt) had the lowest mean concentrations overall (Table 3.5).

Table 3.10: Summary statistics for concentrations (mg/kg dm) of four post-transitional metals in zooplankton from the MC, EACC, and SEC, and one-way ANOVA p-values for each element.

		Post transitional metals					
Element	**Current**	**Min**	**Median**	**Mean**	**Max**	**SD**	**%CV**
Al (p = 0.0054)	MC	540	4000	4300	13200	3825	75
	EACC	840	3000	3750	13000	2739	75
	SEC	560	1900	2100	4500	1209	58
Tl (p = 0.6093)	MC	0.016	0.13	0.2	0.4	0.09	61
	EACC	0.02	0.17	0.1	0.34	0.09	62
	SEC	0.04	0.17	0.2	0.23	0.05	31
Pb (p = 0.0783)	MC	5.3	11	14	35	7.9	55
	EACC	4.4	9.7	11	23	5.9	53
	SEC	3.8	8.4	10	27	6.4	61
Bi (p = 0.0025)	MC	0.04	0.16	0.2	0.45	0.12	63
	EACC	0.05	0.11	0.1	0.22	0.04	35
	SEC	0.03	0.08	0.1	0.23	0.05	55

*MC = Mozambique Channel, EACC = East African Coastal Current, SEC = South Equatorial Current

All post-transitional metals analysed had the highest mean concentrations in zooplankton from the MC, with the SEC having the lowest mean concentration except for Tl (Table 3.10). Aluminium and bismuth were significantly different (ANOVA) between currents. All the elements had relatively low %CVs. The highest %CV was 75% for Al from the MC and EACC. The lowest %CV was for Tl from the SEC at 31%.

Table 3.11: Summary statistics for concentrations (mg/kg dm) of three metalloids in zooplankton from the MC, EACC, and SEC, and one-way ANOVA p-values for each element.

		Metalloids					
Element	**Current**	**Min**	**Median**	**Mean**	**Max**	**SD**	**%CV**
B (p < 0.0001)	MC	12	33	33	82	14.5	44
	EACC	11	47	41	78	20	49
	SEC	39	60	87	97	13.3	23
As (p < 0.0001)	MC	1.5	3.7	4.5	8.3	1.77	42
	EACC	2.7	7.8	9.1	19	5.3	59
	SEC	4.2	14	13	22	5.18	38
Sb (p = 0.6382)	MC	0.23	0.79	0.9	2.1	0.5	56
	EACC	0.27	0.74	0.8	1.4	0.26	33
	SEC	0.43	0.81	1	2.1	0.47	50

*MC = Mozambique Channel, EACC = East African Coastal Current, SEC = South Equatorial Current

All metalloids had the highest mean concentrations in zooplankton from the SEC with the MC having the lowest mean concentration, apart from Sb (Table 3.11). All three of the metalloids had low %CV, with only B, and As being significantly different (ANOVA) between the currents. Arsenic had the highest %CV from the EACC, and SEC the lowest.

Table 3.12: Summary statistics for concentrations (mg/kg dm) of two alkali metal concentrations in zooplankton from the MC, EACC, and SEC, and one-way ANOVA p-values for each element.

Alkali metals							
Element	**Current**	**Min**	**Median**	**Mean**	**Max**	**SD**	**%CV**
K (p = 0.0659)	MC	1200	3000	3200	6600	1321	40
	EACC	1050	3100	2900	6700	1507	49
	SEC	2100	3700	3800	5600	942	25
Rb (p < 0.0001)	MC	2.3	13	14	45	12.9	77
	EACC	2	5.4	6.3	15	3.68	59
	SEC	2.1	2.9	3.1	5.5	1.07	34

*MC = Mozambique Channel, EACC = East African Coastal Current, SEC = South Equatorial Current

Potassium had the highest concentration in zooplankton from the SEC region, with Rb the highest from the EACC (table 3.12). Rubidium had the highest %CV from the MC and is the only element differing significantly between currents.

Table 3.13: Summary statistics for concentrations (mg/kg dm) of two non-metal concentrations in zooplankton from the MC, EACC, and SEC, and one-way ANOVA p-values for each element.

Non-metals							
Element	**Current**	**Min**	**Median**	**Mean**	**Max**	**SD**	**%CV**
P (p = 0.0003)	MC	890	1850	2100	4050	874	41
	EACC	1600	2800	2800	4900	781	27
	SEC	1800	2600	2900	5100	889	31
Se (p < 0.0001)	MC	5.1	12	13	31	4.6	35
	EACC	7.9	17	18	32	5.8	32
	SEC	7	18	18	30	5.7	32

*MC = Mozambique Channel, EACC = East African Coastal Current, SEC = South Equatorial Current

For both non-metals reported, the SEC had the highest mean concentration for P and Se in zooplankton, with the EACC having the same Se mean concentrations (Table 3.13). Both elements had low %CVs, with the highest (41%) and lowest (27%) for P from the MC and EACC. Both P and Se were significantly different (ANOVA) between currents.

Table 3.14: Summary statistics for concentrations (mg/kg dm) of two actinide concentrations in zooplankton from the MC, EACC, and SEC, and one-way ANOVA p-values for each element.

Actinides							
Element	**Current**	**Min**	**Median**	**Mean**	**Max**	**SD**	**%CV**
Th (p < 0.0001)	MC	0.14	1.9	2.1	6.9	1.9	79
	EACC	0.15	0.72	0.8	1.9	0.5	62
	SEC	0.12	0.46	0.5	1.1	0.3	63
U (p = 0.0060)	MC	1.3	3.5	3.7	6.2	1.1	33
	EACC	2.1	3.5	3.6	6.3	1.03	29
	SEC	2.4	4.5	6.1	6.4	1.04	24

*MC = Mozambique Channel, EACC = East African Coastal Current, SEC = South Equatorial Current

Uranium had the highest concentrations in zooplankton from all three currents, with the highest being 6.1 mg/kg dm from the SEC (Table 3.14) which also had the lowest reported %CV for this element (24%). The highest mean concentration for Th was in zooplankton from the MC along

with the highest %CV (79%). Both U and Th concentrations were significantly different (ANOVA) between currents.

Table 3.15: Number of statistically significant ANOVA differences between currents for each element, based on Tables 3.6 – 3.14.

	Mozambique Channel	**East African Coastal Current**	**South Equatorial Current**
Mozambique Channel		15	23
East African Coastal Current			5
South Equatorial Current			

Tables 3.6 to 3.14 shows the statistical summaries of all 34 metallic elements in zooplankton for the three currents. Each element was tested by ANOVA for differences between the three currents – the p-values are also presented in the same tables. Table 3.15 summarises the number of elements that differed in concentrations in zooplankton between the currents, using the Dunn's post-test. The MC and SEC had the greatest number of significant Dunn's post-test differences for elements (23), more than two-thirds of the elements analysed. Second were the differences between the MC and the EACC at 15 elements, with only five metals differing significantly between EACC and SEC.

3.2. Physical and chemical analysis

During sampling, the following physical and chemical parameters were measured: Conductivity, salinity, fluorescence, temperature, turbidity, oxygen, depth, and density. Summary statistics are presented in Tables 3.16 to 3.18.

Table 3.16: Minima, media, means, maxima, standard deviations, and %CVs for eight physical and chemical parameters for the MC samples.

Parameter	Min	Median	Mean	Max	SD	%CV
Conductivity (S/m)	4.2	4.5	4.8	5.5	0.48	10
Salinity (PSU)	34	35	35	36	0.24	0.7
Fluorescence (mg/m^3)	0.003	0.017	0.35	1.9	0.5	142
Temperature (°C)	14	17	20	36	4.8	24
Turbidity (NTU)	0.53	0.57	0.69	1.9	0.27	40
Oxygen (ml/L)	2.9	3.3	3.6	4.4	0.53	15
Depth (m)	12	200	128	200	87	68
Density (kg/m^3)	1023	1026	1026	1029	1.7	0.17

*MC = Mozambique Channel

Table 3.17: The minima, media, means, maxima concentrations (mg/kg dm), standard deviations (SD), and coefficients of variation (%CV) for eight physical and chemical parameters for the EACC samples.

Parameter	Min	Median	Mean	Max	SD	%CV
Conductivity (S/m)	3.8	4.5	4.7	5.6	0.5	11
Salinity (PSU)	35	35	35	35	0.13	0.37
Fluorescence (mg/m^3)	0.004	0.02	0.14	0.62	0.2	147
Temperature (°C)	9.8	16	19	27	5.3	28
Turbidity (NTU)	0.48	0.56	0.58	0.89	0.084	14
Oxygen (ml/L)	2.1	2.8	3	4.1	0.6	20
Depth (m)	26	200	156	200	70	45
Density (kg/m^3)	1022	1027	1026	1027	1.7	0.16

EACC = East African Coastal Current

Table 3.18: The minima, media, means, maxima concentrations (mg/kg dm), standard deviations (SD), and coefficients of variation (%CV) for eight physical and chemical parameters for the SEC samples.

Parameter	Min	Median	Mean	Max	SD	%CV
Conductivity (S/m)	3.7	4.7	4.7	5.5	0.4	8
Salinity (PSU)	35	35	35	35	0.2	0.6
Fluorescence (mg/m^3)	0.006	0.03	0.1	0.68	0.16	169
Temperature (°C)	14	19	19	27	3.4	17
Turbidity (NTU)	0.49	0.53	0.53	0.57	0.016	3
Oxygen (ml/L)	2	2.8	2.9	3.9	0.46	16
Depth (m)	64	200	177	200	47	26
Density (kg/m^3)	1023	1027	1026	1027	1.4	0.14

SEC = South Equatorial Current

Density and salinity were the most stable between the currents with low %CVs, while fluorescence had the highest variation, in excess of 140% (Tables 3.16 to 3.18).

Figure 3.1 are scatterplots of the physical and chemical parameters per current. Stations closer towards the coast were shallower than the open ocean. This led to two modals for conductivity, oxygen, and depth. All the parameters have an influence on the separation and distribution of one another indicating the complexity of the physical and chemical factors of the sampling areas. Due to the bimodal and even multimodal distributions of some of the datasets associated with depths, no statistical comparisons such as ANOVA will be valid.

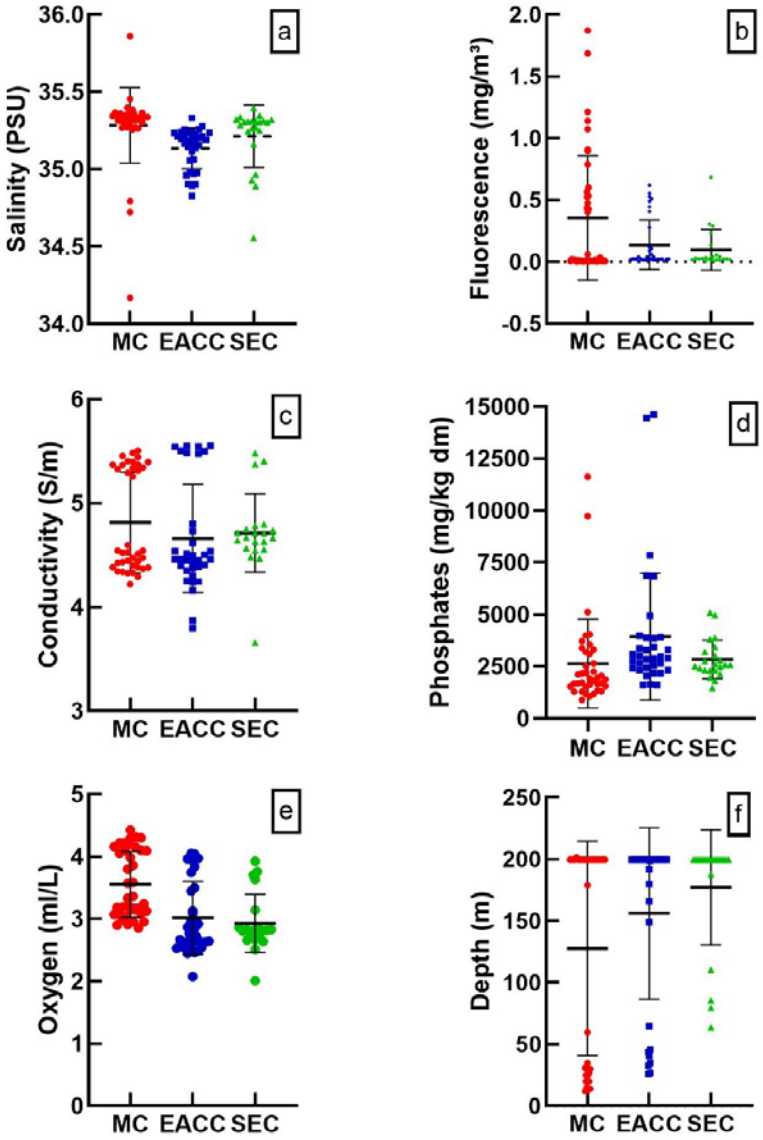

Figure 3.1: Scatterplots of physical and chemical parameters for current comparisons between salinity (a), fluorescence (b), conductivity (c), phosphate (d), oxygen (e), and depth (f) for the MC, EACC, and SEC. Mean and standard deviations are indicated.

Figures 3.2 (a-j) are linear regressions investigating the various physical and chemical parameters per current. Selected parameters were compared to determine if the relationship between any parameter is influenced by another. Significant associations can be seen between most of the parameters, although depth plays a major determining factor influencing others. Most

parameters split into areas close to the coast being shallower with warmer water, higher conductivity, fluorescence, and oxygen concentrations, representing the bi-modal distributions seen Figures 3.1 and 3.2. These interactions will complicate the interpretation of the data as many are inter-related, and not necessarily related with elemental compositions in zooplankton as planktonic diel vertical migrations that travel between water levels that differ in physical and chemical characteristics. All the interactions were statistically significant for one or more of the sampling currents for each comparison. The MC had the least number of significant interactions between physical and chemical parameters.

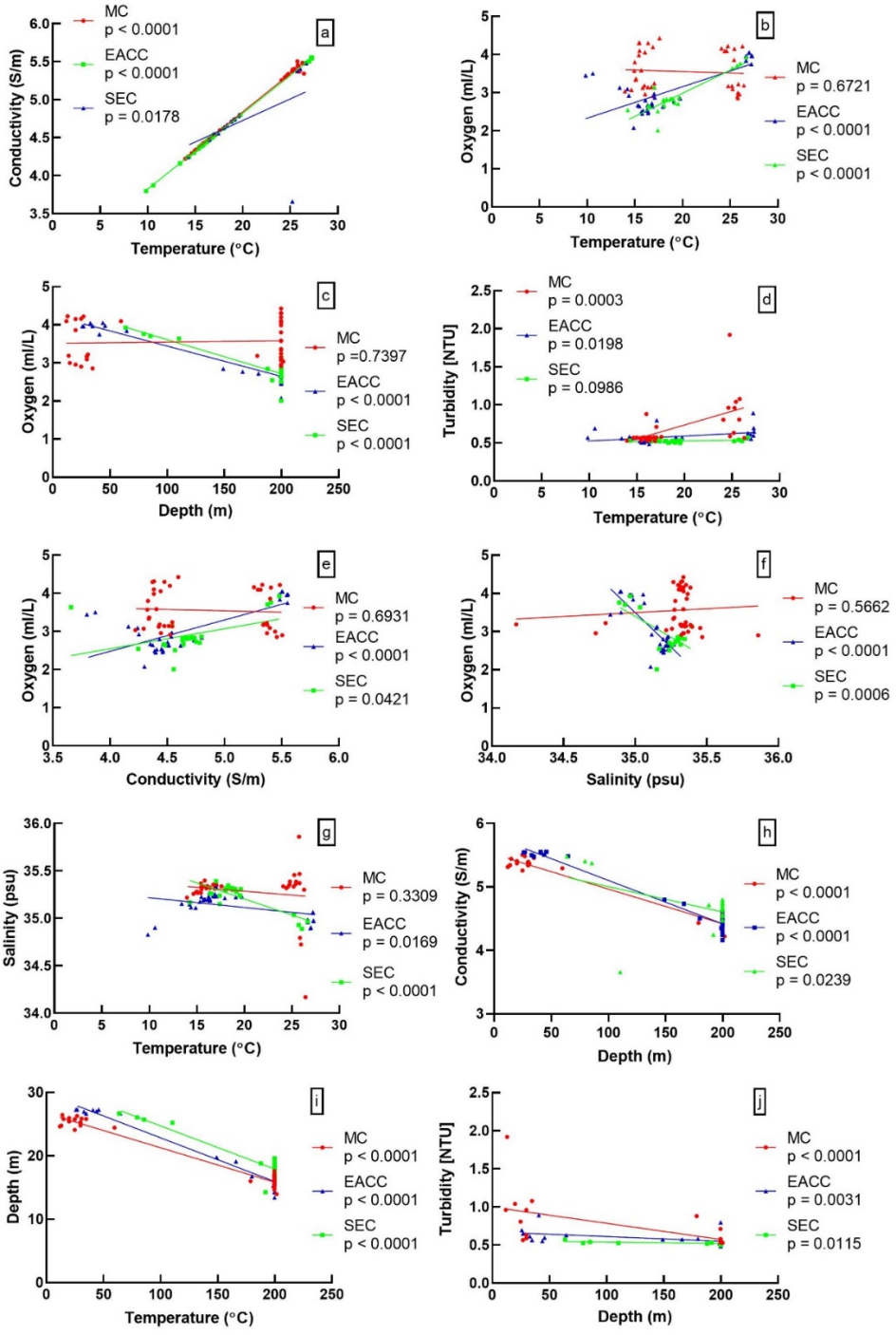

Figure 3.2: Linear regressions for different physical and chemical parameters run against each other to determine interactions, with (a) representing conductivity\temperature, (b)

temperature\oxygen, (c) depth\oxygen, (d) temperature\turbidity, (e) conductivity\oxygen, (f) salinity\oxygen, (g) temperature\salinity, (h) conductivity\depth, (i) temperature\depth, and (j) turbidity\depth. Associated p-values are presented. Currents are depicted by different colours, with the MC represented by red dots, EACC by blue triangles, and SEC by green squares.

Table 3.19: Significance (p-values) of linear regressions of physical and chemical parameters for 34 metallic elements for the MC, EACC, and SEC in a combined data set with sums of significant interactions across parameters and elements.

Element	Conductivity	Salinity	Fluorescence	Temperature	Turbidity	Oxygen	Density	Sum
Be	0.15	0.77	0.39	0.12	0.43	0.86	0.16	
B	0.76	0.06	0.11	0.6	0.15	0.37	0.71	
Mg	0.5	0.15	0.78	0.38	0.72	0.29	0.37	
Al	0.55	0.6	0.52	0.54	0.33	0.99	0.63	
P	0.12	0.27	0.18	0.14	0.86	0.078	0.14	
K	0.85	0.13	0.32	0.82	0.5	0.9	0.84	
Ca	0.8	0.45	0.67	0.85	0.31	0.61	0.79	
Ti	0.09	0.99	0.28	0.44	0.15	0.8	0.45	
V	0.41	0.69	0.13	0.44	0.21	0.085	0.38	
Cr	0.94	0.88	0.53	0.96	0.64	0.32	0.8	
Mn	0.11	0.62	0.25	0.097	0.13	0.43	0.1	
Fe	0.31	0.72	0.45	0.29	0.32	0.61	0.31	
Co	0.09	0.52	0.15	0.1	0.24	0.27	0.1	
Ni	0.45	0.99	0.52	0.73	0.9	0.46	0.66	
Cu	0.63	0.34	0.24	0.57	0.67	0.12	0.46	
*****Zn	0.83	0.97	0.33	0.97	0.31	*0.044	0.83	1
*****As	0.50	0.24	*0.017	0.99	*0.019	*0.017	0.71	3
Se	0.89	0.6	0.51	0.79	0.32	0.082	0.96	
Rb	0.14	0.63	0.43	0.09	0.57	0.97	0.13	
Sr	0.47	0.95	0.63	0.42	0.15	0.085	0.37	
Mo	0.4	0.99	0.5	0.74	0.92	0.53	0.7	
Pd	0.46	0.86	0.69	0.42	0.18	0.13	0.37	
Ag	0.25	0.81	0.66	0.23	0.4	0.1	0.24	
Cd	0.76	0.55	0.31	0.71	0.59	0.21	0.9	
*****Sb	0.08	0.056	0.29	*0.031	0.32	*0.006	*0.02	3
Ba	0.58	0.27	0.19	0.76	0.33	0.87	0.88	
Pt	0.84	0.56	0.6	0.77	0.65	0.71	0.7	
Au	0.48	0.28	0.18	0.56	0.97	0.36	0.64	
*****Hg	0.06	0.22	0.06	0.05	0.21	*0.006	0.041	1
*****Tl	0.06	0.99	*0.004	0.069	*0.048	*0.004	0.055	3
Pb	0.75	0.5	0.57	0.68	0.78	0.57	0.59	
Bi	0.58	0.54	0.18	0.59	0.93	0.98	0.68	
*****Th	0.08	0.58	0.35	*0.05	0.56	0.81	0.075	1
U	0.92	0.79	0.19	0.88	0.54	0.47	0.99	
Summary			2	2	2	5	1	

*Statistically significant elements and p-values. MC = Mozambique Channel, EACC = East African Coastal Current, SEC = South Equatorial Current

To assess the interactions between the 34 metallic elements with all physical parameters except depth (effectively, there were only two depths, Fig. 3.1F), linear regressions were conducted (Table 3.19). Only six elements (Zn, As, Sb, Hg, Tl, and Th) had significant associations with certain parameters. Zinc was found to be significant towards oxygen concentrations, whereas As and Tl concentrations in zooplankton were significantly associated with three different parameters, namely fluorescence, turbidity, and oxygen. Temperature, oxygen, and density were statistically significant for Sb. Mercury was found to be strongly associated with oxygen. In contrast, Th was significantly associated with temperature. Oxygen influences the most metals out of the 34 elements tested. Note should be taken that 238 regressions were done. Therefore, there is a chance of about 12 false positives at $p < 0.05$; exactly the number of significant interactions calculated here.

3.3. Calcium-based comparisons

Due to the difficulty relating the physical and chemical parameters with any metal concentration in Zooplankton (Section 3.2), I also chose to compare metal concentrations in zooplankton between regions based on Ca-normalised concentrations. Calcium is an important essential element and plays a very important role in ocean chemistry and biochemistry (Matthews *et al.,* 2008). Ratio-based comparisons based on Ca are used in situations like these, for instance, when metals in corals and zooplankton are compared to distinguish regional differences (Flegal *et al.,* 1986; Amiel *et al.,* 1973; Matthews *et al.,* 2008; Sletten *et al.,* 2017; Van der schyf *et al.,* 2020). The assumption here is that Ca is a near-enough stable physiological constant in the biological (zooplankton) matrix being analysed, relative to the variable surrounding marine medium from which other elements, especially the non-essential elements, could be assimilated or concentrated from.

Figures 3.3 to 3.11 represent calcium-based concentration regressions that were used to asses any possible sources of effect such as pollution or inherent chemical characteristics of the currents for specific groups of elements across the three different sampling areas. Thirty-three metal concentrations were regressed against Ca for each sampling area.

Figure 3.3 (a-d) represents the four alkaline earth metal ratios based on Ca, where Sr and Ba (c) show positive linear regressions. Sr (a) was statistically significant for all three currents, whereas only two regressions were statistically significant for Ba (c) in the MC and EACC. For both Mg (b) and Be (d), the EACC had statistically significant negative regressions. For the MC, only Be (d) had a statistically significant negative regression. Interestingly, the SEC did not show any significant regressions for alkali metals except for Sr.

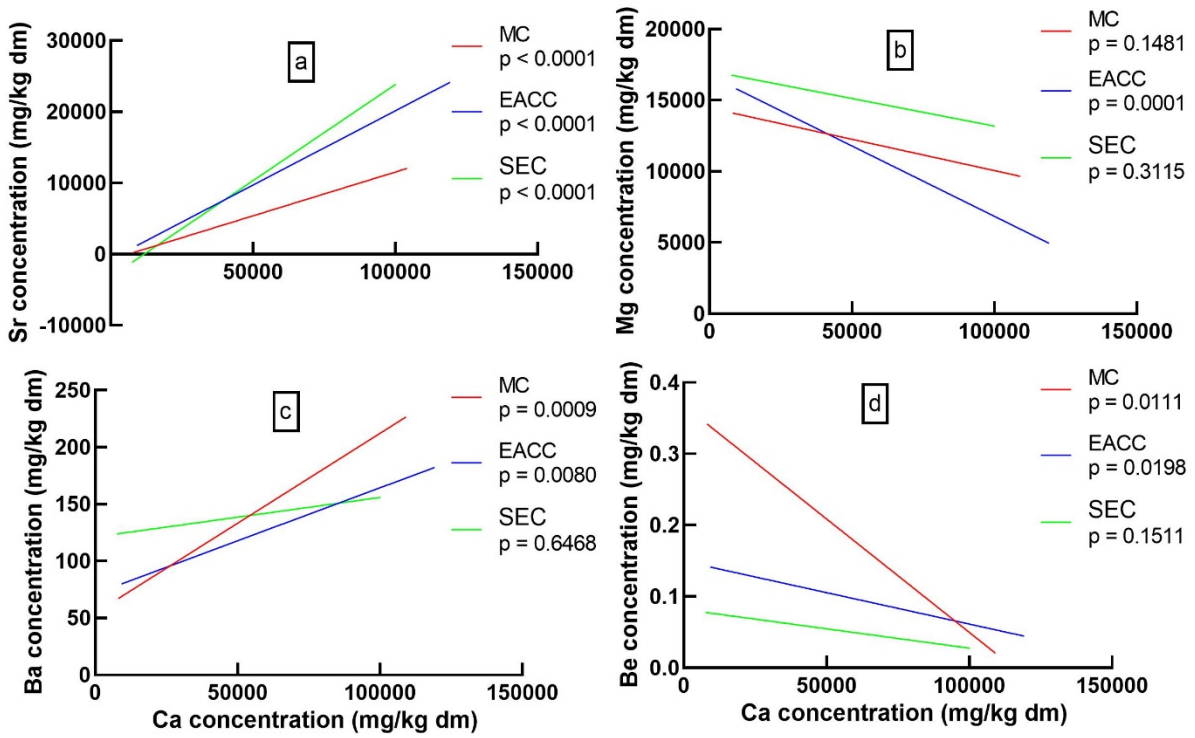

Figure 3.3: Linear regression comparison based on calcium for four alkaline earth metals; strontium (a), magnesium (b), barium (c), beryllium (d) (mg/kg dm). The Mozambique Channel (MC) is represented by red, East African Coastal Current (EACC) by blue, and South Equatorial Current (SEC) by green with associated p-values to indicate regressions statistically significant different from zero.

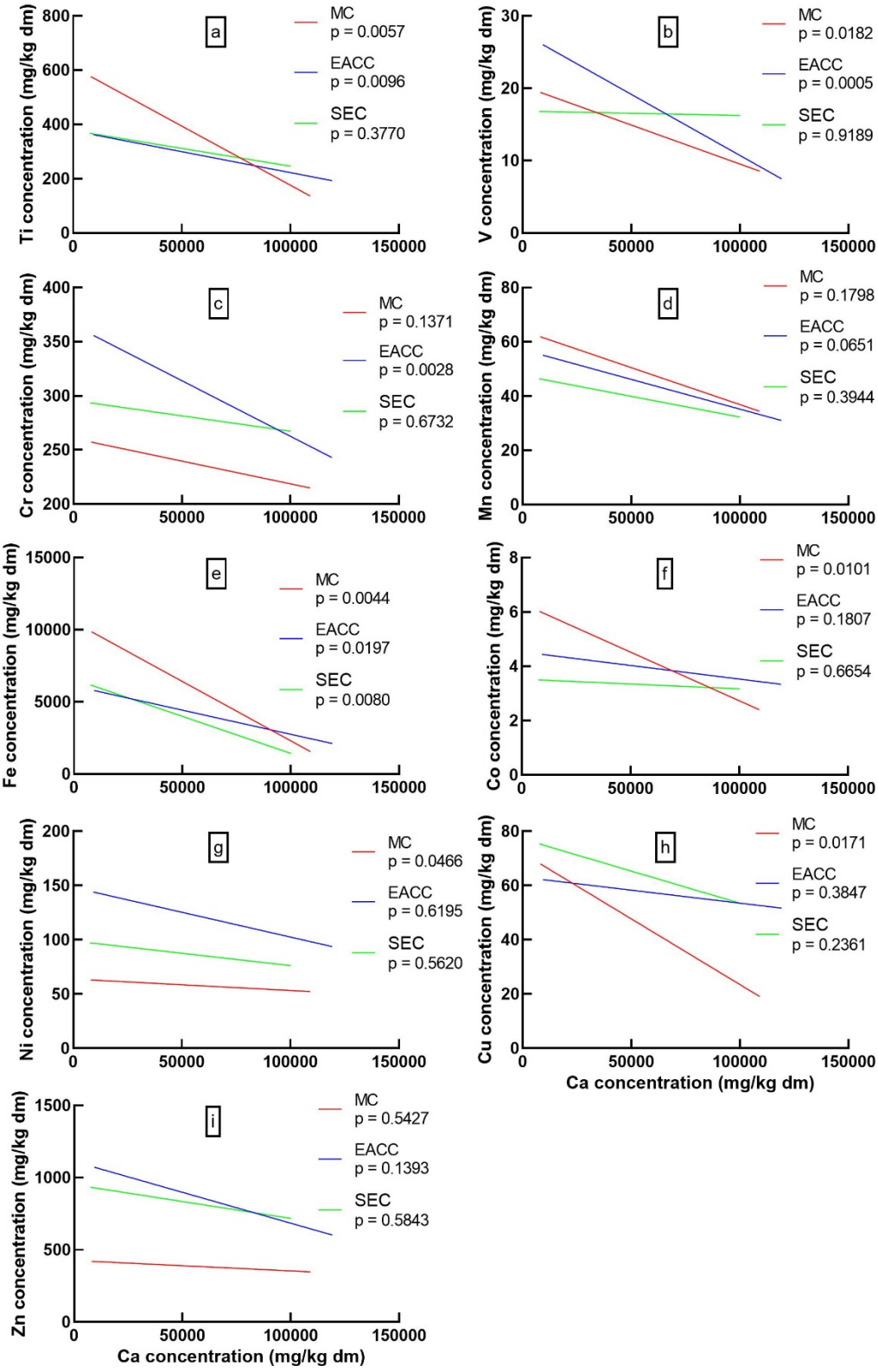

Figure 3.4: Linear regressions based on calcium for nine transitional metals; Row 4, titanium (a), vanadium (b), chromium (c), manganese (d), iron (e), cobalt (f), nickel (g), copper (h), and zinc (i) (mg/kg dm). The Mozambique Channel (MC) is represented by red, East African Coastal Current (EACC) by blue, and South Equatorial Current (SEC) by green with associated p values to indicate regressions statistically significant different from zero.

Figure 3.4 (a-i) shows no positive linear regressions for any Row 4 transitional metals in the MC, EACC, and SEC having different (y-axis) concentration ranges. For the MC, Ti (a), V (b), Fe (e), Co (f), Ni (g), and Cu (h) had statistically significant linear regressions. The EACC only had four significant regressions for Ti (a), V (b), Cr (c), and Fe (e), whereas the SEC only had one significant regression, namely Fe (e). No significant negative regressions were found for Mn (d) and Zn (i). The MC had the highest concentrations for Ti, Mn, Fe, and Co, as well as the lowest concentrations for Cr, Ni, and Zn (Table 3.7). The EACC had the highest concentrations for V, Cr, Ni, and Zn. The SEC had the highest concentration for Cu.

Of all four Row 5 transitional metals (Figure 3.5 a-d), only Ag (c) did not have two or more positive regressions. Only the EACC had a significant regression for Ag. Positive regressions were found for Mo (a), Pd (b), and Cd (d) with all three currents showing significant positive regressions for Pd. Molybdenum only had one significant negative regression from the EACC, whereas Cd did not have any negative regressions, but only two of the regressions were significant (Table 3.8), that being from the EACC and SEC.

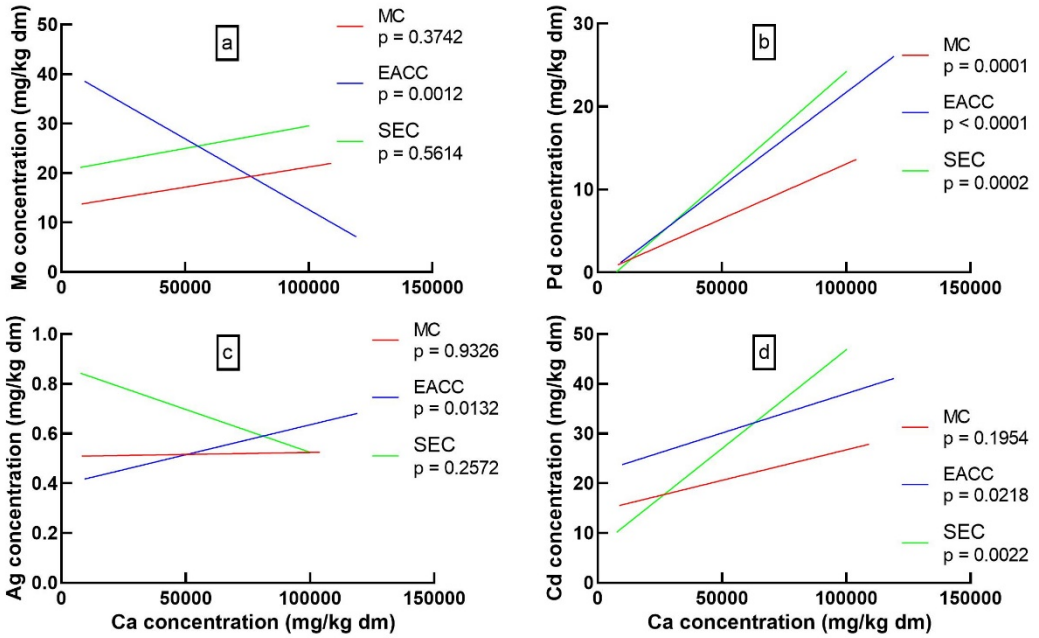

Figure 3.5: Linear regression comparison based on calcium for four transitional metals; Row 5, molybdenum (a), palladium (b), silver (c), and cadmium (d) (mg/kg dm). The Mozambique Channel (MC) is represented by red, East African Coastal Current (EACC) by blue, and South Equatorial Current (SEC) by green with associated p values to indicate regressions statistically significant different from zero.

Of all Row 6 transitional metals (Figure 3.6), only two Pt and Au had positive linear regressions, but no regressions in this group were significant. The lowest concentrations for Pt (a), Au (b), and Hg (c) was in the MC (Table 3.9). Concerning the EACC, the highest concentrations were found for all three metals from this group (Table 3.9). Lastly, the SEC did not have any significant regressions for any metal from these transitional metals but Hg showed significant negative regressions for all three currents.

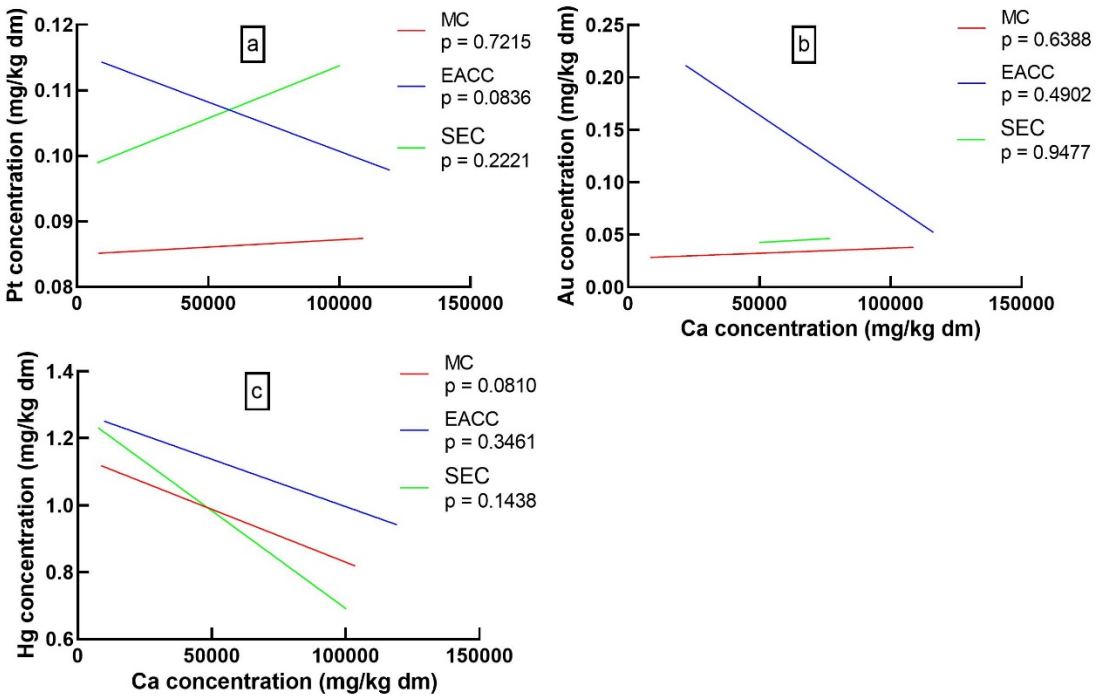

Figure 3.6: Linear regression comparison based on calcium for three transitional metals; Row 6, platinum (a), gold (b), and mercury (c) (mg/kg dm). The Mozambique Channel (MC) is represented by red, East African Coastal Current (EACC) by blue, and South Equatorial Current (SEC) by green with associated p values to indicate regressions statistically significant different from zero.

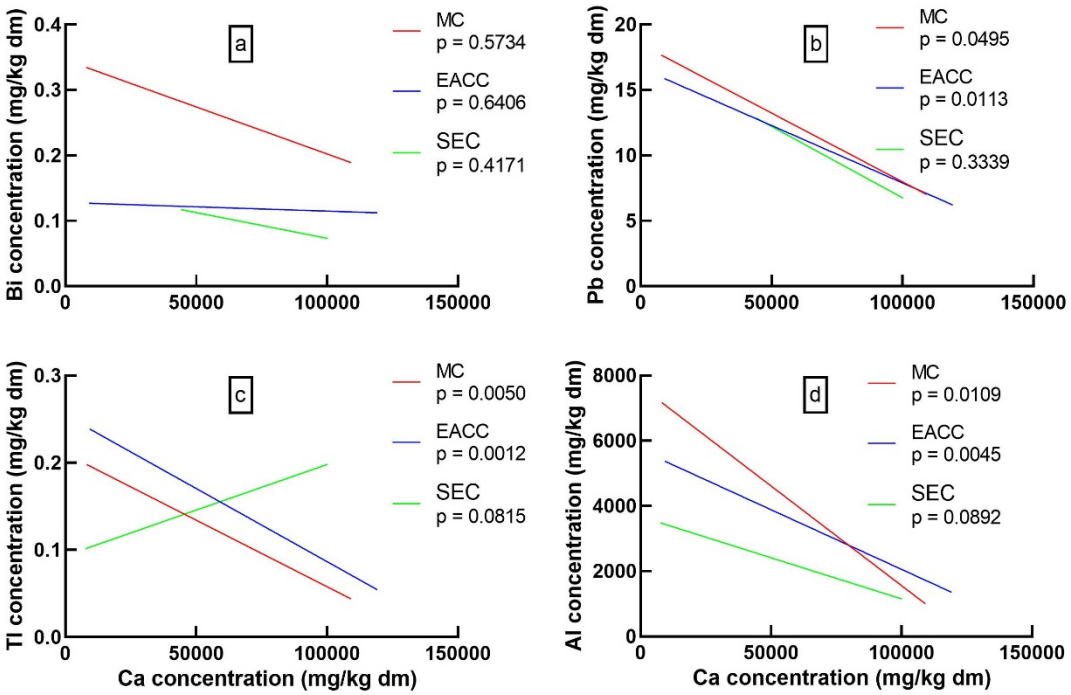

Figure 3.7: Linear regression comparison based on calcium for four post-transitional metals; bismuth (a), lead (b), thallium (c), and aluminium (d) (mg/kg dm). The Mozambique Channel (MC) is represented by red, East African Coastal Current (EACC) by blue, and South Equatorial Current

(SEC) by green with associated p values to indicate regressions statistically significant different from zero.

Figure 3.7 (a-d) shows only one positive linear regression, for Tl from the SEC, for all the post-transitional metals. Lead (b), Tl (c), and Al (d) had significant negative regressions. The SEC was the only current to have no statistically significant regressions for any element. For Bi (a), no significance (positive or negative) was found for all three currents. The MC had the highest concentration for Bi, Pb, and Al, whereas the SEC had the lowest concentration for all four elements (Table 3.10).

Of all the metalloids (Figure 3.8), only the EACC had statistically significant negative linear regressions for As (b) and B (c). Two positive regression can be seen at SEC for As and Sb (a) for the EACC, even though not being significant. The SEC had the highest concentrations for both Sb and B, with the MC having the lowest concentrations for As and B (Table 3.11).

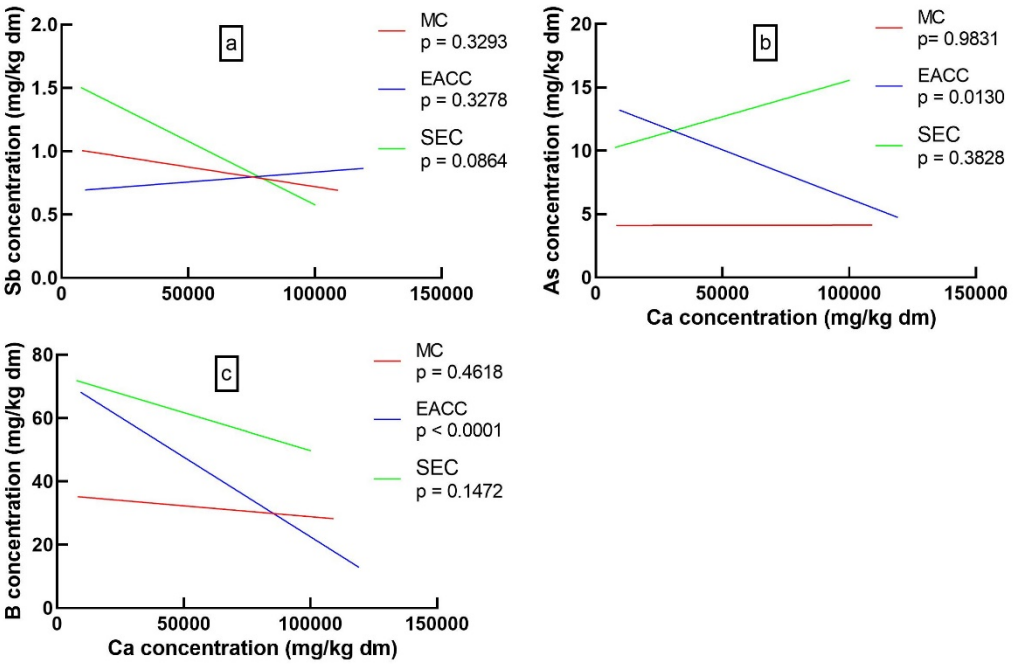

Figure 3.8: Linear regression representation based on calcium against three metalloids; antimony (a), arsenic (b), and boron (c) (mg/kg dm). The Mozambique Channel (MC) is represented by red, East African Coastal Current (EACC) by blue, and South Equatorial Current (SEC) by green with associated p values to indicate regressions statistically significant different from zero.

Both alkali metals (Figure 3.9) had significant negative regressions for the MC and EACC. The SEC was the only current not significant for both Rb (a) and K (b). The MC had the highest concentration for Rb and the lowest concentration for K, whereas the EACC had the highest concentration for K. For Rb the SEC had the lowest concentration (Table 3.12).

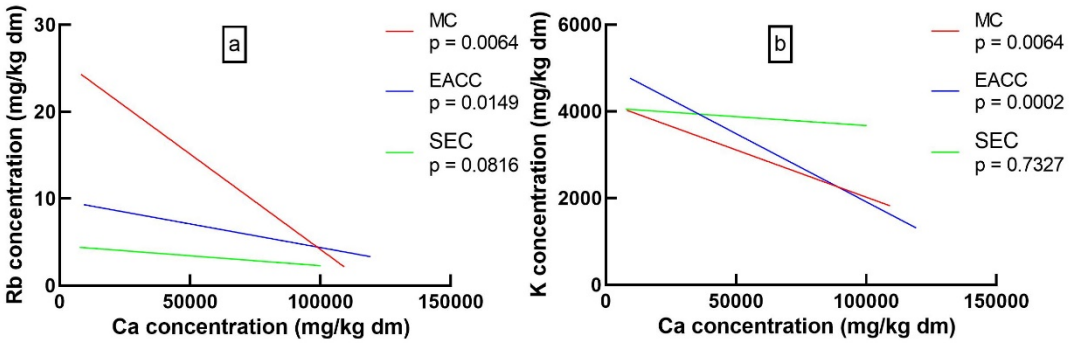

Figure 3.9: Linear regressions based on calcium versus two alkali metals; rubidium (a), and potassium (b) (mg/kg dm). The Mozambique Channel (MC) is represented by red, East African Coastal Current (EACC) by blue, and South Equatorial Current (SEC) by green with associated p values to indicate regressions statistically significant different from zero.

Selenium and P were the two identified non-metals (Figure 3.10) for this study. Both Se (a) and P (b) had positive linear regressions with only the MC being statistically significant (Table 3.13).

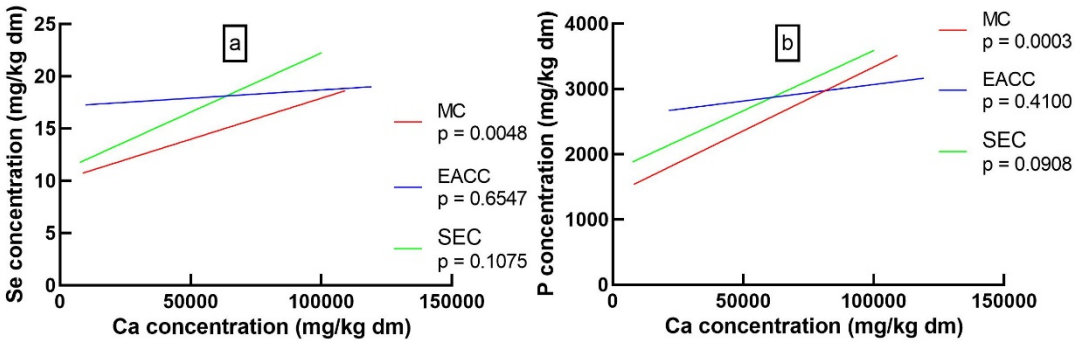

Figure 3.10: Linear regression comparison based on calcium against two non-metals; selenium (a), and phosphate (b), across the entire sampling area (mg/kg dm). The Mozambique Channel (MC) is represented by red, East African Coastal Current (EACC) by blue, and South Equatorial Current (SEC) by green with associated p values to indicate regressions statistically significant different from zero.

Actinides reported on (Figure 3.11) were U (a) and Th (b). Only the EACC had a statistically significant regression for U. Both the MC and EACC had significant negative regressions for Th, with the SEC being the only current not being statistically significant. The SEC had the highest U concentration and the lowest Th concentration. In contrast, the MC had the lowest U concentration and with the highest Th concentration (Table 3.14).

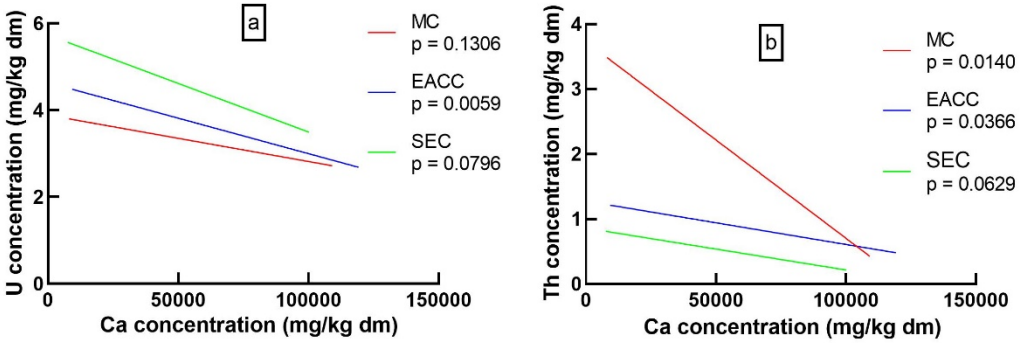

Figure 3.11: Linear regression representation based on calcium against two actinides; uranium (a), and thorium (b) (mg/kg dm). The Mozambique Channel (MC) is represented by red, East African Coastal Current (EACC) by blue, and South Equatorial Current (SEC) by green with associated p values to indicate regressions statistically significant different from zero .

Table 3.20: Summary of significant positive and negative regressions for each element from the MC, EACC, and SEC.

Mozambique Channel		East African Coastal Current		South Equatorial Current	
+	-	+	-	+	-
Sr	Be	Sr	Mg	Sr	Fe
Ba	Ti	Ba	Be	Pd	
Pd	V	Pd	Ti	Cd	
Se	Fe	Ag	V		
P	Co	Cd	Cr		
	Ni		Fe		
	Cu		Mo		
	Tl		Pb		
	Al		Tl		
	Rb		Al		
	K		As		
	Th		B		
			Rb		
			K		
			U		
			Th		
5	12	5	16	3	1

*MC = Mozambique Channel, EACC = East African Coastal Current, SEC = South Equatorial Current

In summary, it can be seen (Table 3.20) that the EACC had the most elements with significant negative regressions (16), the MC second with 12, and lastly the SEC with one. Both the MC and EACC had five positive significant regressions, whereas the SEC only had three significant positive regressions.

3.4. Multivariate analysis

Nonmetric Multidimensional Scaling (NMS) illustrated the relative compositional profiles of metallic elements in zooplankton (Figure 3.12) from the MC, EACC, and SEC (Table 3.5). Samples are more related to each other based on relative proportional composition (fingerprint)

the closer they are together. Elements that are grouped further away from each other are less similar based on their relative proportional composition. The final ordination needed three dimensions after 117 iterations to obtain a final stress of 12.77, with a final instability of 0.0000. This means that after 117 iterations the NMS will not be further improved. This shows the best-fit relationship between all the samples based on the available data. Final stress illustrates the total desired adjustment to show the ordination for three dimensions. For an excellent representation, a final stress should be between five and ten. McCune (2002) further states that if the final stress is below twenty the ordinations can be useful, but should not be used to investigate details patterns (McCune *et al.,* 2002).

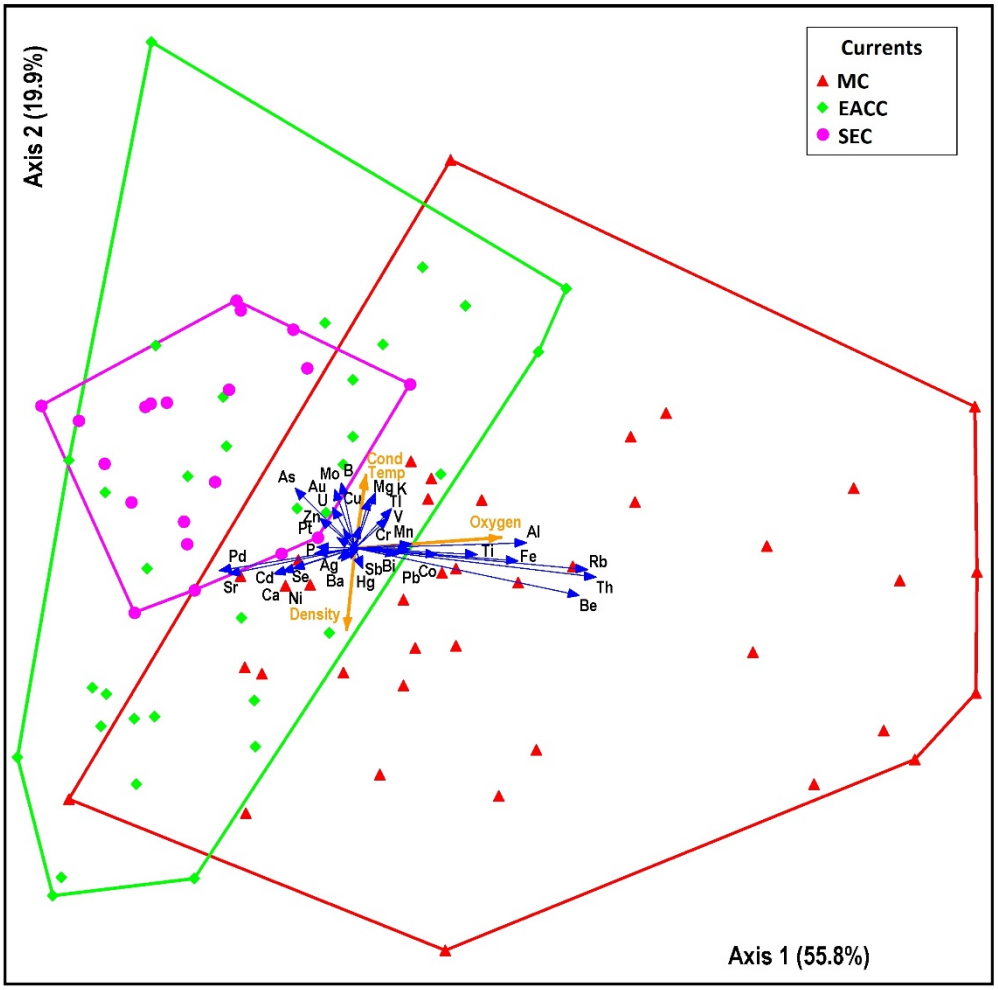

Figure 3.12: Nonmetric Multidimensional Scaling illustrating relative compositional profiles of metallic elements in zooplankton from the MC, EACC, and SEC with Sørenson as distance measure. The MC is represented in red, EACC in blue, and SEC in green with physical parameters in orange. Three dimensions were needed, with a final stress of 12.77 reached after 117 iterations to achieve a final instability of 0.0000. Axis 1 explained 55.8%% of the variation, and axis 2 explained 19.9%.

The three convex hulls illustrate the separation of metallic elements in association with zooplankton ('fingerprints'). The overlapping convex hulls indicate no clear difference between

the three areas. A relatively higher composition for the MC occurred for Al, Ti, Fe, Rb, Th, and Be, while Pd, Sr, Cd, and As had relatively higher relative compositions for the EACC and SEC.

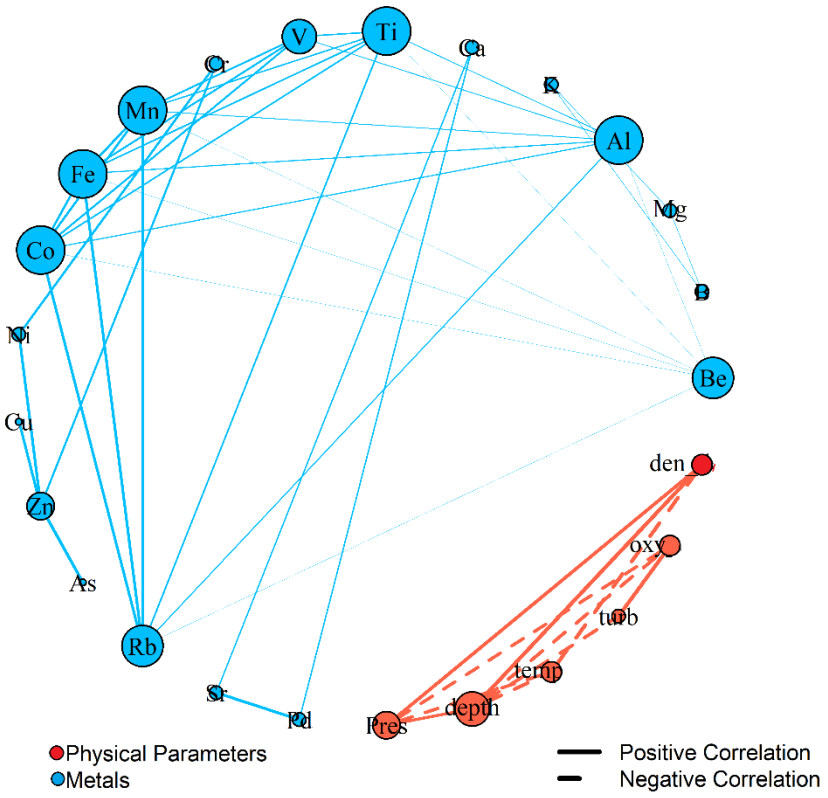

Figure 3.13: Network-analysis depicting the co-occurrences between metals (absolute values) and physical parameters measured in this study. Metals are represented by blue and physical parameters by red. The size of each node is directly related to the number of interactions. The size of each edge is directly related to the strength of the interaction. All interactions are significant ($p < 0.05$) and Spearman's rho-values of +/- 0.6 were used and regarded as sufficiently strong interactions.

The network analysis illustrated in Figure 3.13 indicates that there were no concurrent interactions between metallic elements and physical parameters (Table 3.19). Metals have different interactions and numbers of interactions with each other; this is the same for physical parameters. High interactions can be found between density, pressure, and depth, with an interaction between turbidity and oxygen. High interactions were found between Co, Fe, Mn, Ti, Al, Be, and Rb. Stronger interactions are indicated with thicker lines and larger circles.

3.5. Elemental comparative studies

Fourteen elements (Table 3.21) were chosen for comparisons with other studies, and further examination based on geographic patterns. These elements were selected based on their toxicities, being biologically essential, prior work, and of known interest. The concentrations of the 14 elements are compared to concentrations found throughout literature.

Table 3.21: Comparison of concentrations (mg/kg dm) gathered from literature and from our own data for 14 elements in copepods, mesozooplankton, and zooplankton.

Species	Country	Date	Unit	Mass	V	Cr	Mn	Fe	Co	Ni	Cu	Zn	As	Se	Cd	Hg	Pb	U	Reference
Copepods	Guanabara Bay (Brazil)	2005	mg/kg	dm							6.3				0.06		5.3		Kehrig et al. (2009)
Copepods	South Baltic Sea	1999	mg/kg	dm							20.5				2.5		12.9		Pempkowiak et al. (2006)
Copepods	Australia and New Zealand Coasts	1999	mg/kg	dm							46				5.1		0.94		Barwick & Maher (2003)
Meso	Bahía Blanca estuary	2005-2006	mg/kg	dm							37.34				3.7		13.4		Severini *et al.,* 2013
Meso	Bahía Blanca estuary	2005	mg/kg	dm							41.3				0.3				Severini *et al.,* 2009
mixed copepod	Iberian deep sea	2002	mg/kg	dm							11	234			6.3		0.8		Zauke *et al.,* 2006
Zooplankton	Lochnagar	1997-1998	mg/kg	dm						2.24	45.9	223			2.41	0.23	12.3		Yang *et al.,* 2002
Zooplankton	Caoqiao River	2010	mg/kg	dm		22.58				28.95	191.4	948.01			1.91		52.82		Tao *et al.,* 2012
Zooplankton	Bay of Bengal	nr	mg/kg	dm			95	4011	11	21	33	1701					158		George & Kureishy, 1979
Zooplankton	Izmir Bay	1996	mg/kg	dm			333	62593		207	293	2534							Kontas, 2008
Zooplankton	Kalpakkam, southeast coast of India	2011-2013	mg/kg	dm		70.9	171.3	9227	3.9	34.1	42.8	262.3			4.4		27.9		Achary *et al.,* 2017
Zooplankton	Bay of Bengal, India (Rushikulya estuary)	2010-2011	mg/kg	dm	1.96	4.55	49.72	6388	0.65	3.1	14.38	1408	5.73	1.9	1.5		4.16		Srichandan *et al.,* 2016
Zooplankton	Indian Ocean	nr	mg/kg	nr			7	94	4	3	5	31							Sen Gupta & Singbal., 1988
Zooplankton	eastern Arabian Sea	2002-2003	mg/kg	nr				1786.1	14.2	18.6	21.5	374.1			16.5		4		Rejomon *et al.,* 2008
Zooplankton	western Bay of Bengal	2002-2003	mg/kg	nr				14073.1	24.2	29.5	46.2	2000.1			18.7		6.55		Rejomon *et al.,* 2008
Zooplankton	Buenos Aires, Argentina	nr	mg/kg	wm			291.75	37287			1348	896.89			1348		2013.5		Scarlato *et al.,* 1997
Zooplankton	western Bay of Bengal, coastal	2003	mg/kg	nr				15272.1	27.1	36.2	48.4	2515.6			23.4		7.7		Rejomon *et al.,* 2008
Zooplankton	Bay of Bengal, coast	2003	mg/kg	nr				44894.1	46.2	62.8	84.9	7546.8			46.2		19.2		Rejomon *et al.,* 2009
Zooplankton	Bay of Bengal, offshore	2004	mg/kg	nr				3423.4	19.5	25.3	29.4	502.3			14.3		3.2		Rejomon *et al.,* 2009
Zooplankton	east Arabian Sea inter monsoon fall	2003	mg/kg	nr				3467	14.2	20.7	21	443			16		5		Rejomon, 2005
Zooplankton	western Bay of Bengal winter monsoon	2002	mg/kg	nr				14073	24	30	46	2001			19		6.5		Rejomon, 2005
Zooplankton	northeastern Arabian Sea spring intermonsoon	2004	mg/kg	nr				4622	14.7	18.2	25.2	1177			21.7		6.6		Rejomon, 2005
Zooplankton	Conception Bay, Newfoundland	1996	mg/kg	dm							410	920			40		67		Morneau., 1997
Zooplankton	Southwest Coast of India	2006	mg/kg	dm			1.91				1.31	2.77			0.04	0.02	2.57		Balasubaramanian *et al.,* 2012
Zooplankton	west coast of India	2009-2010	mg/kg	dm		25.85									4.875		27.63		Kadam & Tiwari., 2012
Zooplankton	Mozambique Channel	2017	mg/kg	dm	15	240	50	6300	5.4	58	60	460	4.5	13	22	1	14	3.7	This study
Zooplankton	East African Coastal Current	2017-2018	mg/kg	dm	18	300	43	3900	3.9	120	57	840	9.1	18	34	1.1	11	3.6	This study
Zooplankton	South Equatorial Current	2018	mg/kg	dm	16	280	38	3300	3.3	85	62	800	13	18	32	0.9	10	6.1	This study

*Meso = Mesozooplankton, nr = Not reported

3.6. Geographical distributions

Statistical analyses based purely on data does not always reveal geographical patterns. Below, I present interpolated maps of concentrations in zooplankton, irrespective of depth, to investigate spatial patterns.

Distribution patterns can be seen with certain 'hot spots' clearly indicated in the following figures. The left column of each set of figures has the maps with interpolated concentration distributions according to highest concentration for that specific current (a, b, and c). The right-hand column displays the same concentrations, but now on the same scale for all three currents combined (d, e, and f) enabling comparisons between the three currents. Samples collected in the MC and EACC are not spatially connected as indicated by longitude (°S). Context is provided in text as to possible sources that may explain 'hot spots', such as harbours and river mouths, as these could not be displayed on the maps. The descriptions should be read in conjunction with Figure 2.1. I frequently used the terms 'relatively, 'high', 'low', elevated' or similar, indicating internal comparisons to minimise overly belaboured the text.

3.6.1. Vanadium

Zooplankton in the EACC (a) in general had higher concentrations (Figure 3.14). Sites situated deeper and further away had lower concentrations, with the highest concentration at Tanga in the northern part of the EACC (a). High concentrations occurred at the northern most region in MC (b), as well as at the harbour situated at 20°S and 35°E. The higher concentration at these sites may be attributed towards pollution sources from the harbour itself but may also be influenced through the Pungwe and Buzi River (b) entering the Indian Ocean. Lower concentrations occurred where the Zambezi River (19°S, 36°E) enters the Indian Ocean (b). Lower concentrations occur in the upwelling zone moving towards Angoché. Higher V concentrations occurred at almost every site furthest away from the coastline of Mozambique (b).

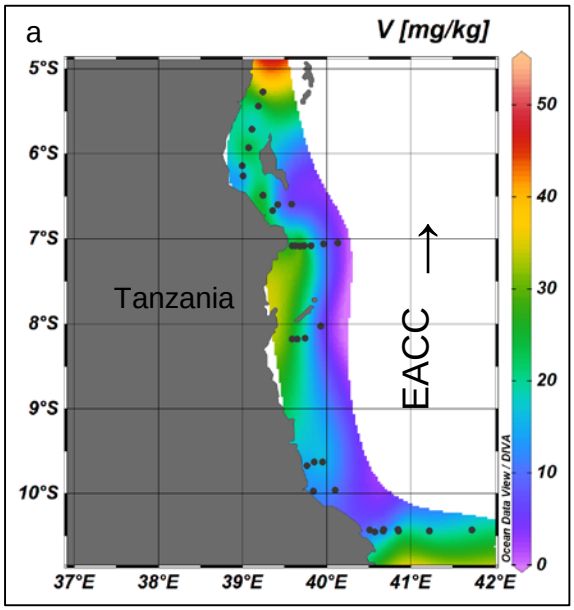

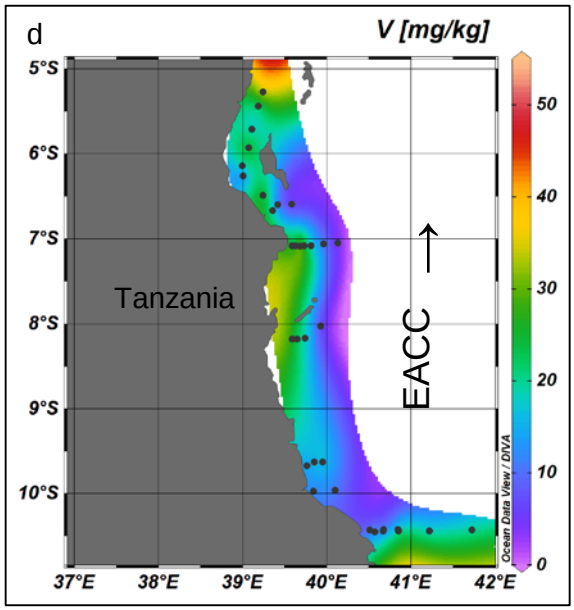

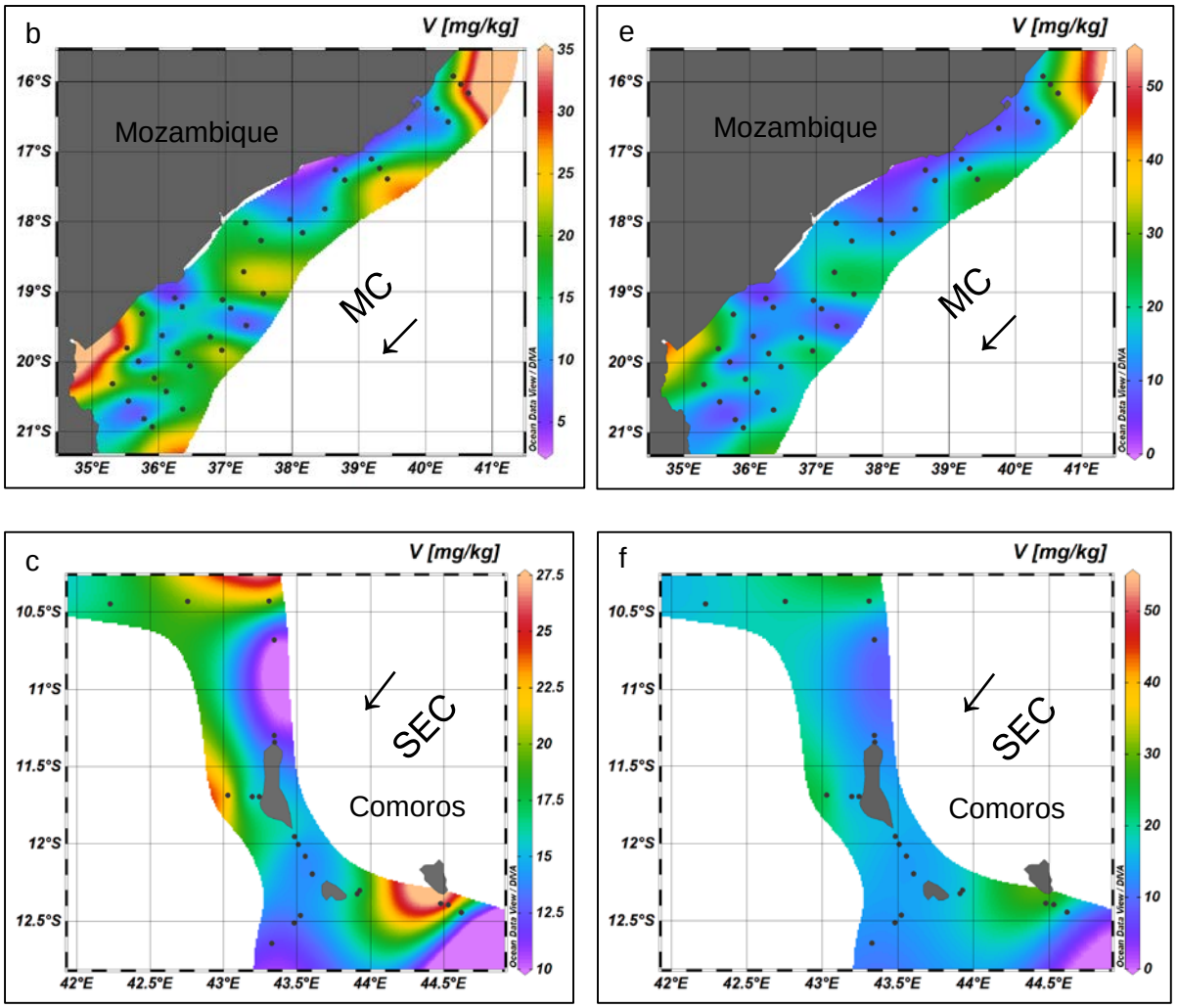

Figure 3.14: Distribution of vanadium concentrations in zooplankton of the EACC (a), MC (b), and SEC (c) in mg/kg dm. Note difference in concentration scales (z-axes) between the two columns. The left-hand column is scaled for the maximum of each current, while the right-hand column (d, e, and f) has the same scale across each map. Concentrations are colour coded, with the highest concentrations in red, and the lowest in purple. The main current direction is represented by an arrow.

In comparison with the MC and EACC, the SEC (c) had a more homogenous V concentration distribution. The three islands of Comoros (c) showed different distribution patterns for vanadium. The highest V concentration was found around 44.5°E (c), with concentrations decreasing westwards as the SEC moves further towards the MC. The lowest V concentration was found between 10.5°S and 11.5°S (c).

As with Figure 3.14 a, b, and c, Figure 3.14 d, e, and f show a clear distribution of V compared between the three currents. 'Hot spots' can be seen in the MC and the EACC. At the most southern part of the EACC, relatively low concentrations were found, with concentrations increasing northwards in the EACC. The highest concentration as indicated in (Figure 3.14 d) was found at the most northern point of the study area (5°S, 39.3°E). The MC (Figure 3.14 e) had two 'hot spots' with one at the beginning of the MC and the other at the southern sites (e). As the concentrations became less from North to

South, clear intervals of concentrations can be seen shifting between 20 mg/kg dm and 5 mg/kg dm.

3.6.2. Chromium

Chromium concentrations in zooplankton (Figure 3.15) were evenly distributed in the EACC (a), with higher concentrations closer to the coast (a). Relatively high concentrations occurred between 40.7°E and 41.5°E. The highest concentration was at the most eastern sample of the study area (a).

In the MC (b), high Cr concentrations were distributed throughout, with the highest concentrations between 300 and 350 mg/kg dm (b), respectively. The lowest Cr concentration (b) was 150 mg/kg dm. Four distinct 'hot spots' (b) can be seen in the MC (16°S, 18°S, 20°S, and 21°S). Samples between 20°S and 21°S (Figure 3.15 b, e) may possibly be influenced by rivers (Pungwe River, Buzi River, and Sabi River) entering the Indian Ocean (Figure 2.1).

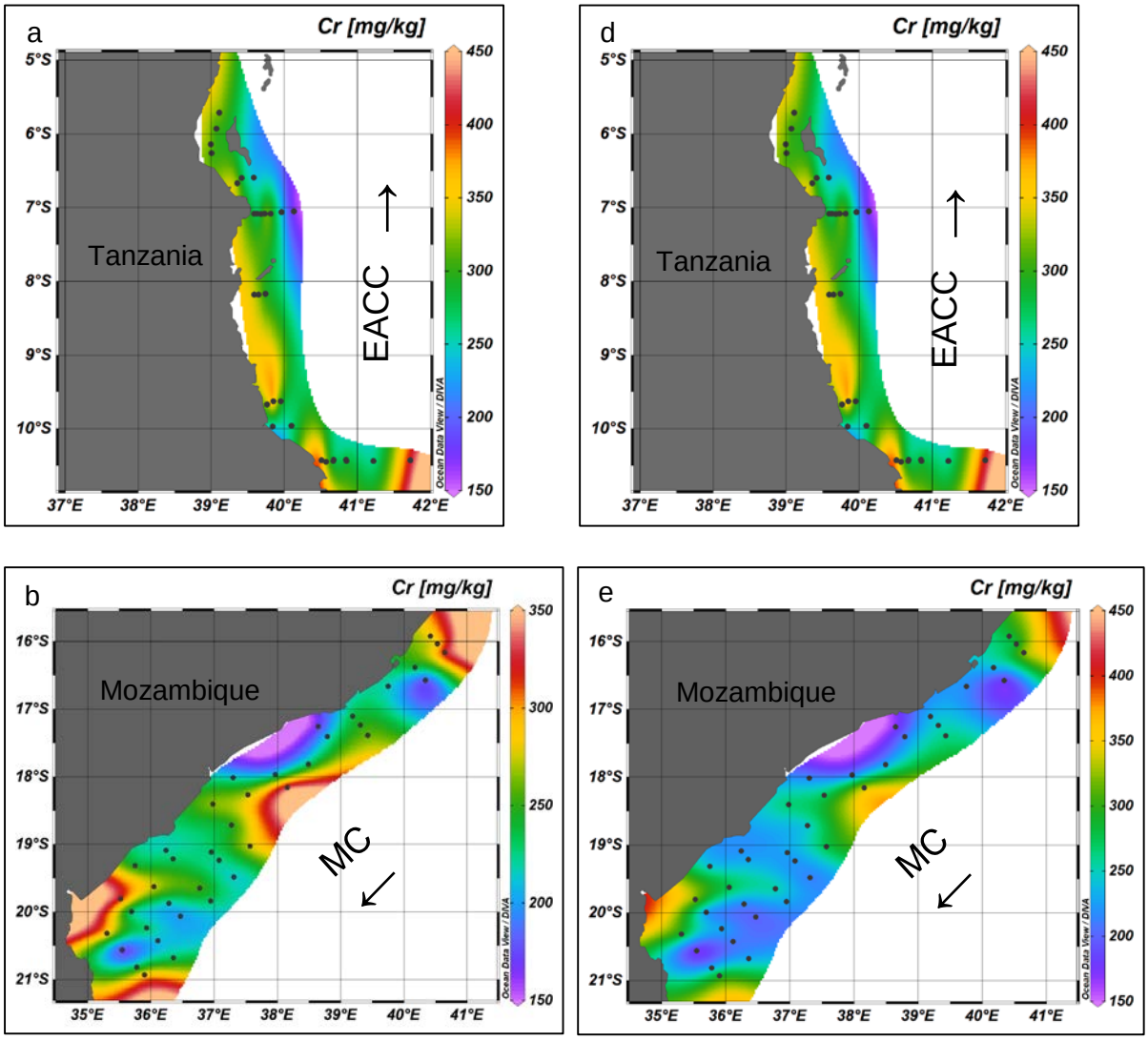

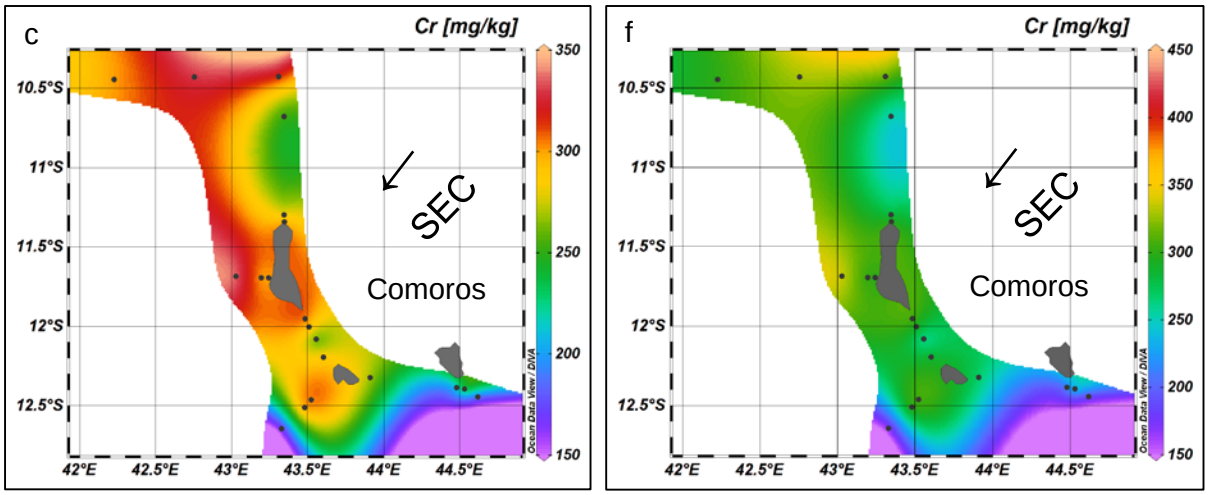

Figure 3.15: Distribution of chromium concentrations in zooplankton of the EACC (a), MC (b), and SEC (c) in mg/kg dm. Note difference in concentration scales (z-axes) between the two columns. The left-hand column is scaled for the maximum of each current, while the right-hand column (d, e, and f) has the same scale across each map. Concentrations are colour coded, with the highest concentrations in red, and the lowest in purple. The main current direction is represented by an arrow.

Chromium concentrations in zooplankton in the SEC (c) showed a wide range of concentrations around the Islands of Comoros. The highest Cr concentrations in the SEC occurred at 10.5°S and 11.7°S (c), with the lowest of 150 mg/kg dm at 12.7°S. Relatively high concentrations (275 mg/kg dm to 300 mg/kg dm) were found between 12°S and 12.7°S (c). Figure 3.15 (a), (b), and (c) all have the same scale. A clear difference in concentrations as well as 'hot spots' can be seen. No notable difference can be seen in the EACC (d). The MC had a change where only two 'hot spots' can now be seen (d). Concentrations in zooplankton were more evenly distributed in the MC (d), whereas the SEC (e) showed no 'hot spots'.

3.6.3. Manganese

Concentrations of Mn in zooplankton (Figure 3.16) showed interesting distribution patterns throughout the EACC (a, d), MC (b, e), and SEC (c, f). Throughout the southern part of the EACC (8°S to 10.5°S) relatively low Mn concentrations (20 mg/kg dm to 40 mg/kg dm) occurred. Sites situated close to the Rufiji River (7°S) had the highest Mn concentration in the EACC (a, d). Concentrations decreased towards 5°S, but concentrations in zooplankton were still higher than the southern part (a, d). Sites situated close to where the Pungani River (a, d) enters the Indian Ocean show elevated concentration. In the MC (b, e) a clear differentiation of Mn concentrations can be seen. Sites situated at 16°S had higher concentrations, with these concentrations steadily decreasing to 18°S (b, e). Between 18°S and 19°S, relatively high concentrations were found. Sites situated close to the Zambezi River had relatively low Mn concentrations (20 mg/kg dm to 40 mg/kg dm) (b, e). Concentrations found in the SEC (c) showed relatively low concentrations throughout the SEC (c, f). Only one sample site had a relatively high Mn concentration (c).

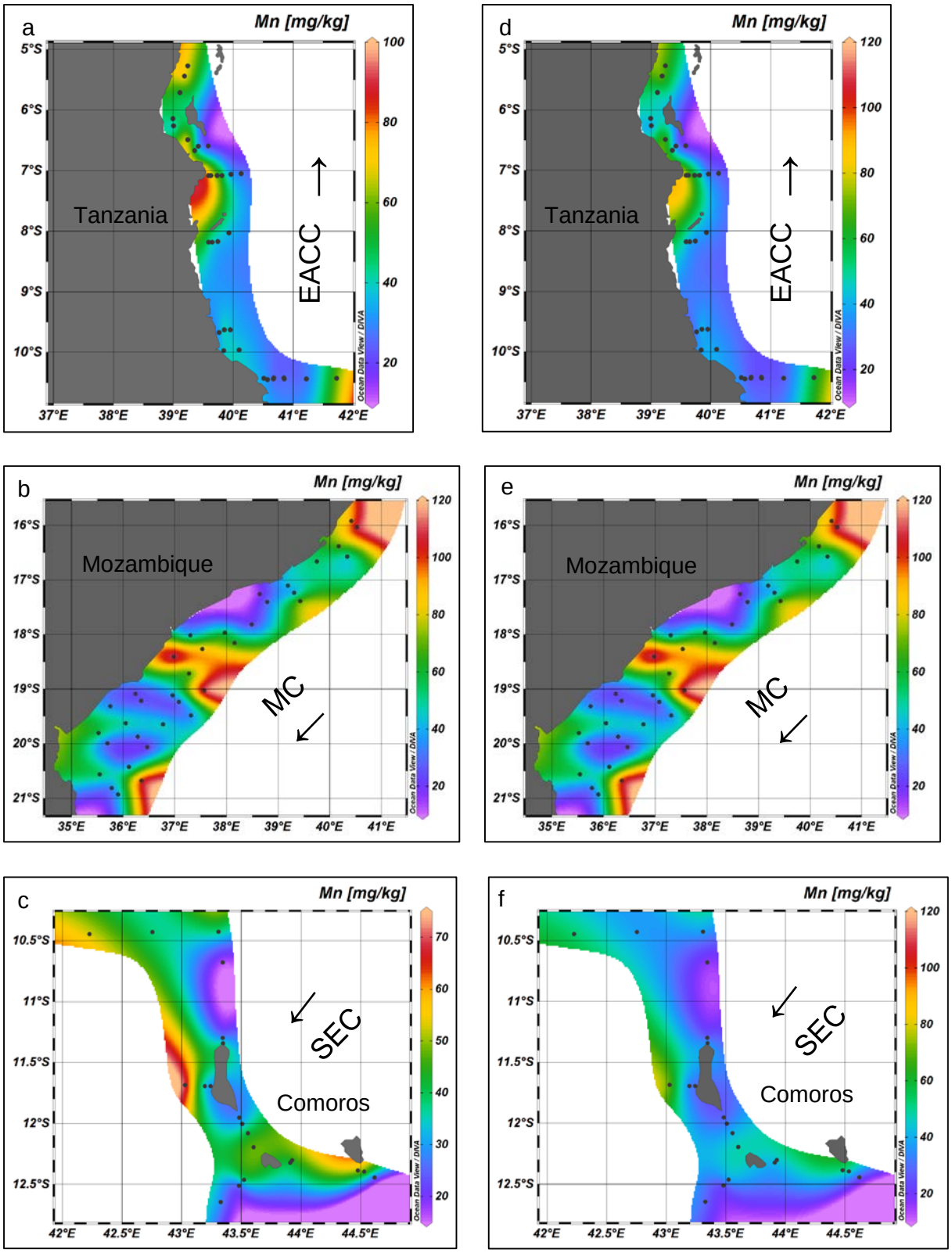

Figure 3.16: Distribution of manganese concentrations in zooplankton of the EACC (a), MC (b), and SEC (c) in mg/kg dm. Note difference in concentration scales (z-axes) between the two columns. The left-hand column is scaled for the maximum of each current, while the right-hand column (d, e, and f) has the same scale across each map. Concentrations are colour coded, with the highest concentrations in red, and the lowest in purple. The main current flow is indicated by an arrow.

3.6.4. Iron

In the EACC, the second highest concentration of Fe in zooplankton was 10 000 mg/kg dm (Figure 3.17 a). High concentrations occurred at sites situated close to river mouths. The southern half of the EACC (a) showed relatively lower concentrations compared with the northern part (a). The MC (b) had the highest concentration (17 500 mg/kg dm) of the three currents. Sites closer to the coastline had lower concentrations than those further away, except for sites situated close to harbours. The lowest concentration in the MC was found at sites close to the Zambezi River mouth (19°S, 36°E) (b). Relatively high Fe concentrations (b) occurred at a sampling site (19°S, 37.6°E) not situated close to any river mouths, major cities, or harbours (b). Concentrations found in the SEC showed large variations around the Islands of Comoros, with the highest concentrations found at (10.5°S, 42.2°E; 11.7°S, 43°E; and 12.4°S, 44.5°E).

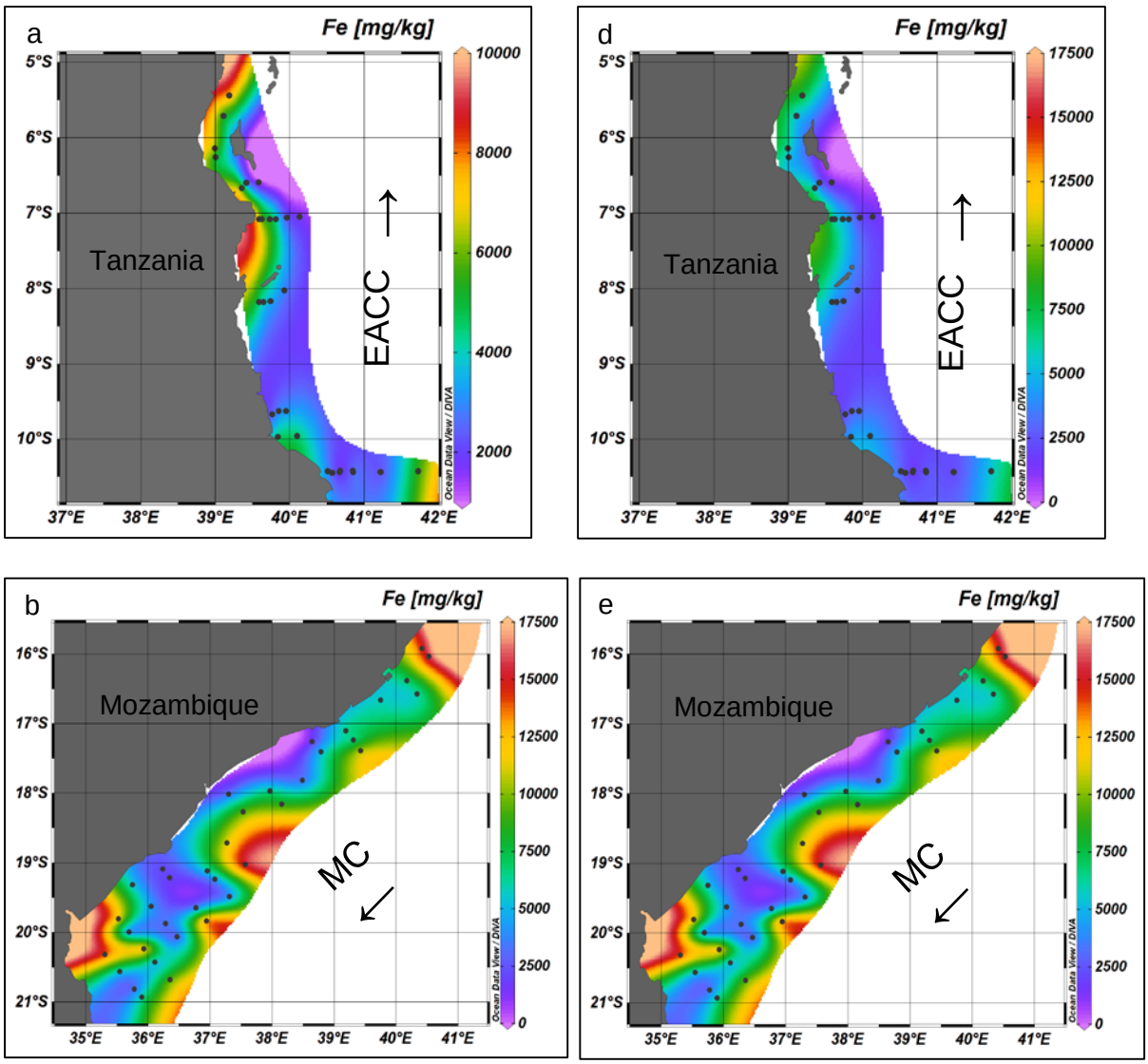

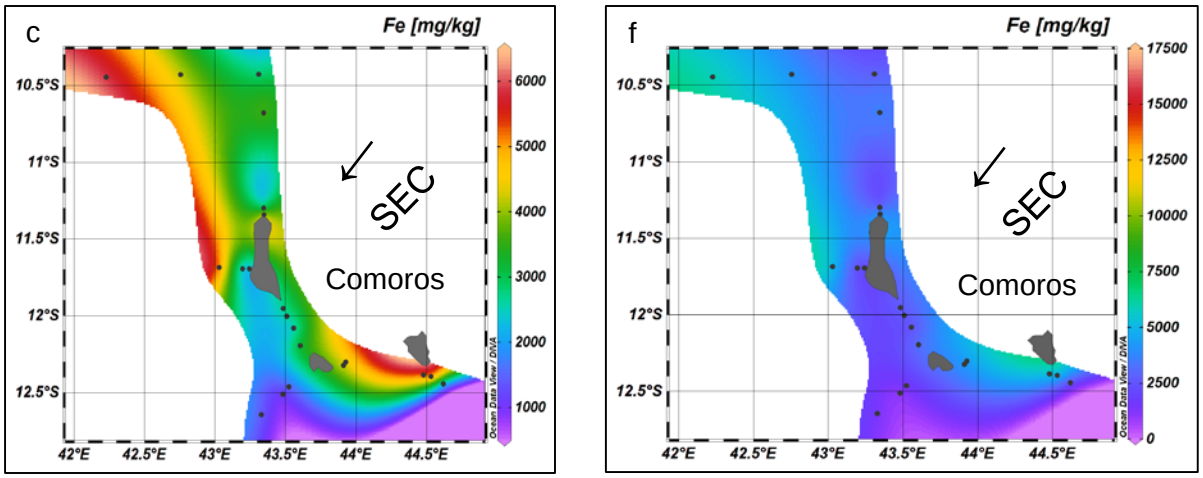

Figure 3.17: Interpolation of iron concentrations in zooplankton of the EACC (a), MC (b), and SEC (c) in mg/kg dm. Note difference in concentration scales (z-axes) between the two columns. The left-hand column is scaled for the maximum of each current, while the right-hand column (d, e, and f) has the same scale across each map. Concentrations are colour coded, with the highest concentrations in red, and the lowest in purple. The main current direction is indicated by an arrow.

Figure 3.17 (d) show relatively homogenous Fe concentrations in the EACC, with relatively higher concentrations (10000 mg/kg dm) close to river mouths (d). Concentrations in the MC (e) showed an even concentration pattern, whereas the SEC had high variations, indicating the lowest concentrations (f) in combination with evenly distributed concentrations (f), when compared with the other two currents (d, e).

3.6.5. Cobalt

Relatively low concentrations of Co in zooplankton occurred in the EACC (Figure 13.8 a) and the SEC (c), with the highest concentrations at 6.5 mg/kg dm (a) and 4.5 mg/kg dm (c), respectively. The EACC had higher concentrations at Dar es Salaam and around the Mafia islands along the coast of Tanzania (a). Relatively low Co concentrations occurred in the southern half of the EACC. The highest concentration was found in the MC (b, e), with relatively low concentrations of Co in zooplankton in the MC.

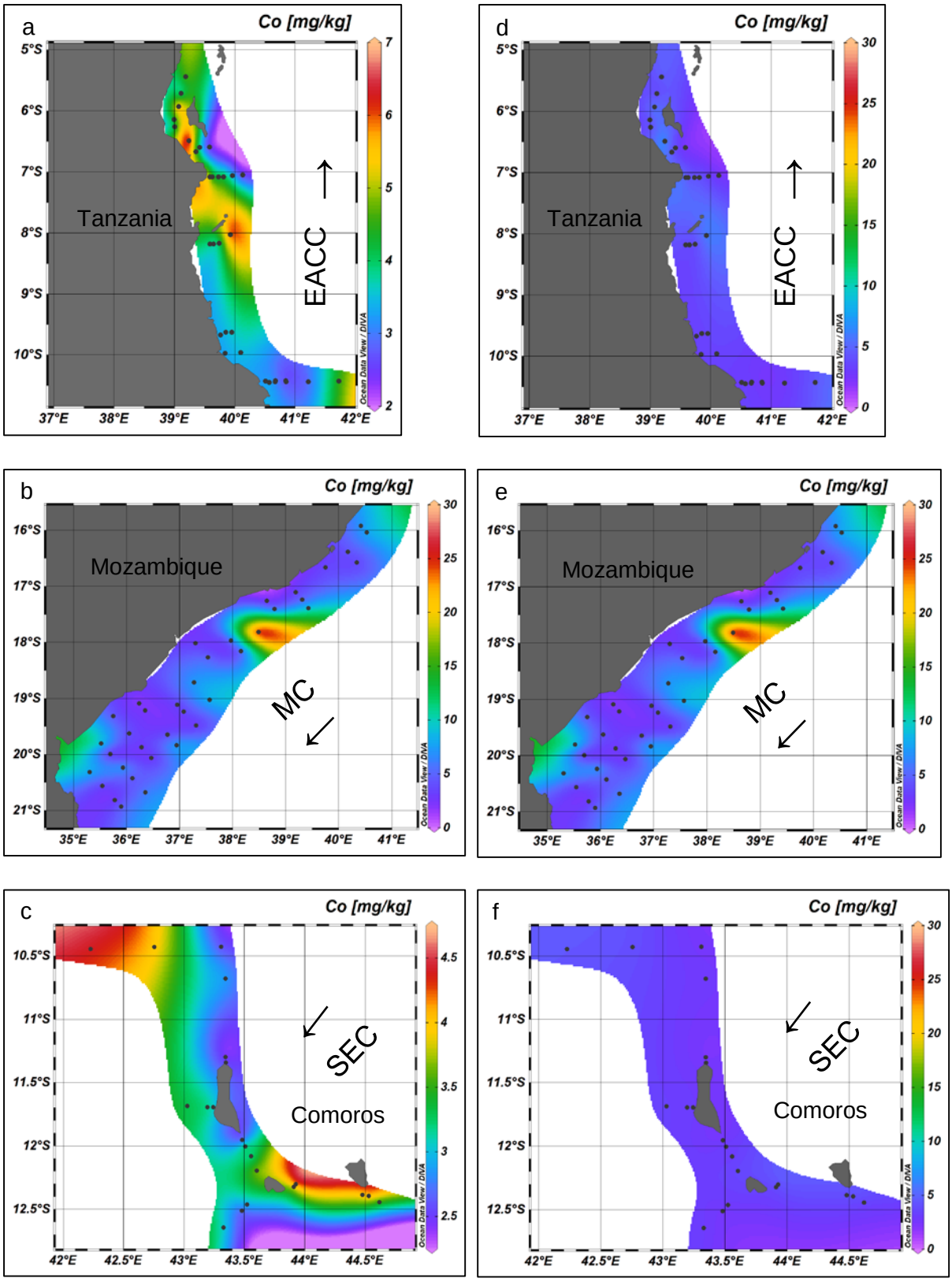

Figure 3.18: Distribution of cobalt concentrations in zooplankton of the EACC (a), MC (b), and SEC (c) in mg/kg dm. Note difference in concentration scales (z-axes) between the two columns. The left-hand column is scaled for the maximum of each current, while the right-hand column (d, e, and f) has the same scale across each map. Concentrations are

colour coded, with the highest concentrations in red, and the lowest in purple. The main current direction is indicated by an arrow.

Relatively high concentrations occurred close to two of the Comoran Islands in the SEC (c), with the lowest concentration in the SEC between 43°E and 43.5°E. Figures 13.8 d and f showed no notable 'hot spots' in the EACC and SEC, respectively.

3.6.6. Copper

Copper had relatively high concentrations in zooplankton in the EACC, with two distinct sites having high concentrations (Figure 13.9 a, d). Sites situated between 7°S and 10°S had moderately high concentrations (60 mg/kg dm) (a, d), with sites from the beginning of the EACC on the map having low Cu concentrations closer to the coast, gradually increasing as the EACC breaks off from the SEC (c). Sites situated close to Dar es Salaam also had elevated concentrations (75 mg/kg dm). Concentrations in the MC (b, e) showed no clear distribution patterns, but with three distinct 'hot spots' (b, e). Relatively low concentrations (20 mg/kg dm to 40 mg/kg dm) occurred at almost every site closest to the coastline (b, e) including sites situated between 20°S and 21°S. Concentrations between 16°S and 18°S vary between 80 mg/kg dm and 100 mg/kg dm at sites further away from the coast, respectively. Relatively high concentrations were between 11.4°S and 12.5°S in the SEC. The highest concentrations in the SEC were at 10.4°S, 42.2°E and 11.7°S, 43°E (c, f), with relatively low concentrations (40 mg/kg dm to 50 mg/kg dm) found at 12.5°S (c, f).

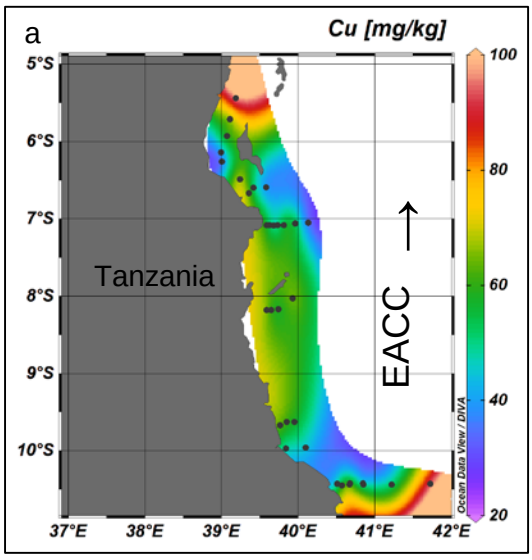

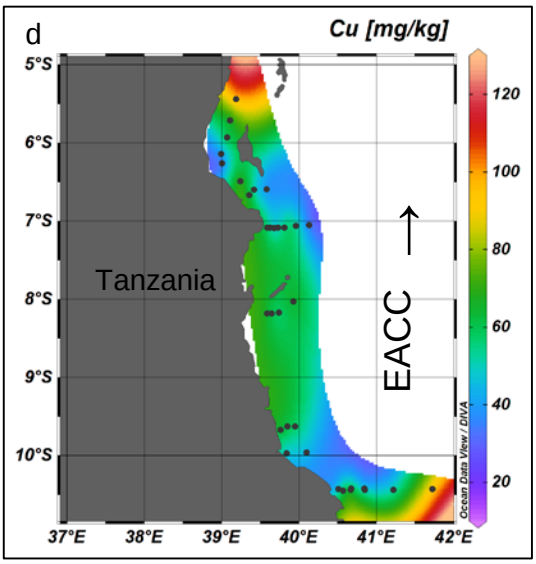

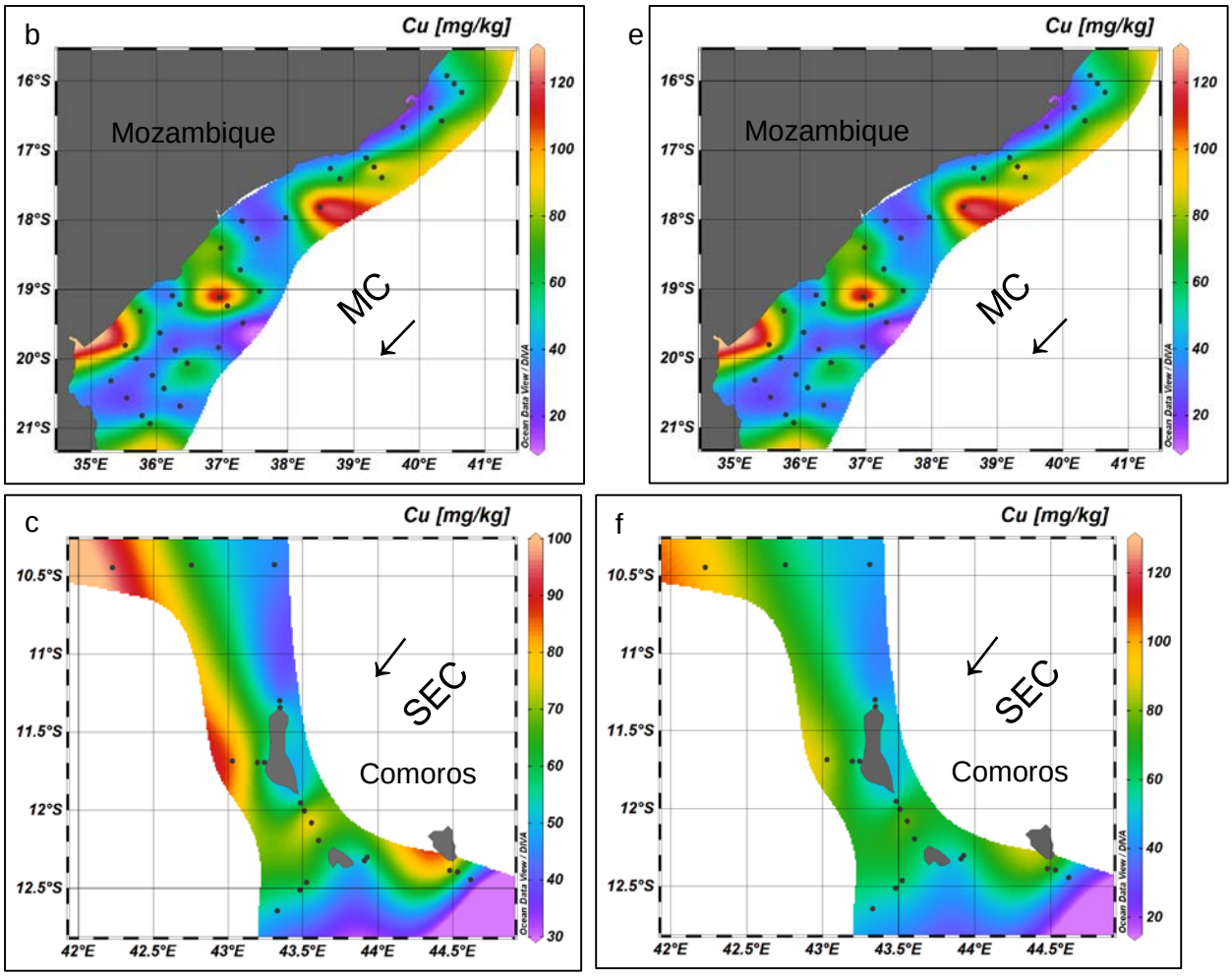

Figure 3.19: Distribution of copper concentrations in zooplankton of the EACC (a), MC (b), and SEC (c) in mg/kg dm. Note difference in concentration scales (z-axes) between the two columns. The left-hand column is scaled for the maximum of each current, while the right-hand column (d, e, and f) has the same scale across each map. Concentrations are colour coded, with the highest concentrations in red, and the lowest in purple. The main current direction is indicated by an arrow.

3.6.7. Zinc

Zinc concentrations in zooplankton (Figure 3.20 a) showed two distinct 'hot spots' in the EACC (a). Higher concentrations (1 250 mg/kg dm) occurred close to river mouths between 8°S and 10°S (a), while the concentrations increased between 5°S and 6°S, representing an additional source of contamination in the EACC. Concentrations found in the MC (b, e) were relatively evenly distributed throughout the entire study area, with only one distinct 'hot spot' between 18°S and 19°S (b, e). Slight concentration elevations can be seen near 16°S and 20°S in the MC. Of the three currents, the SEC (c, f) had the lowest maximum concentration (1400 mg/kg dm).

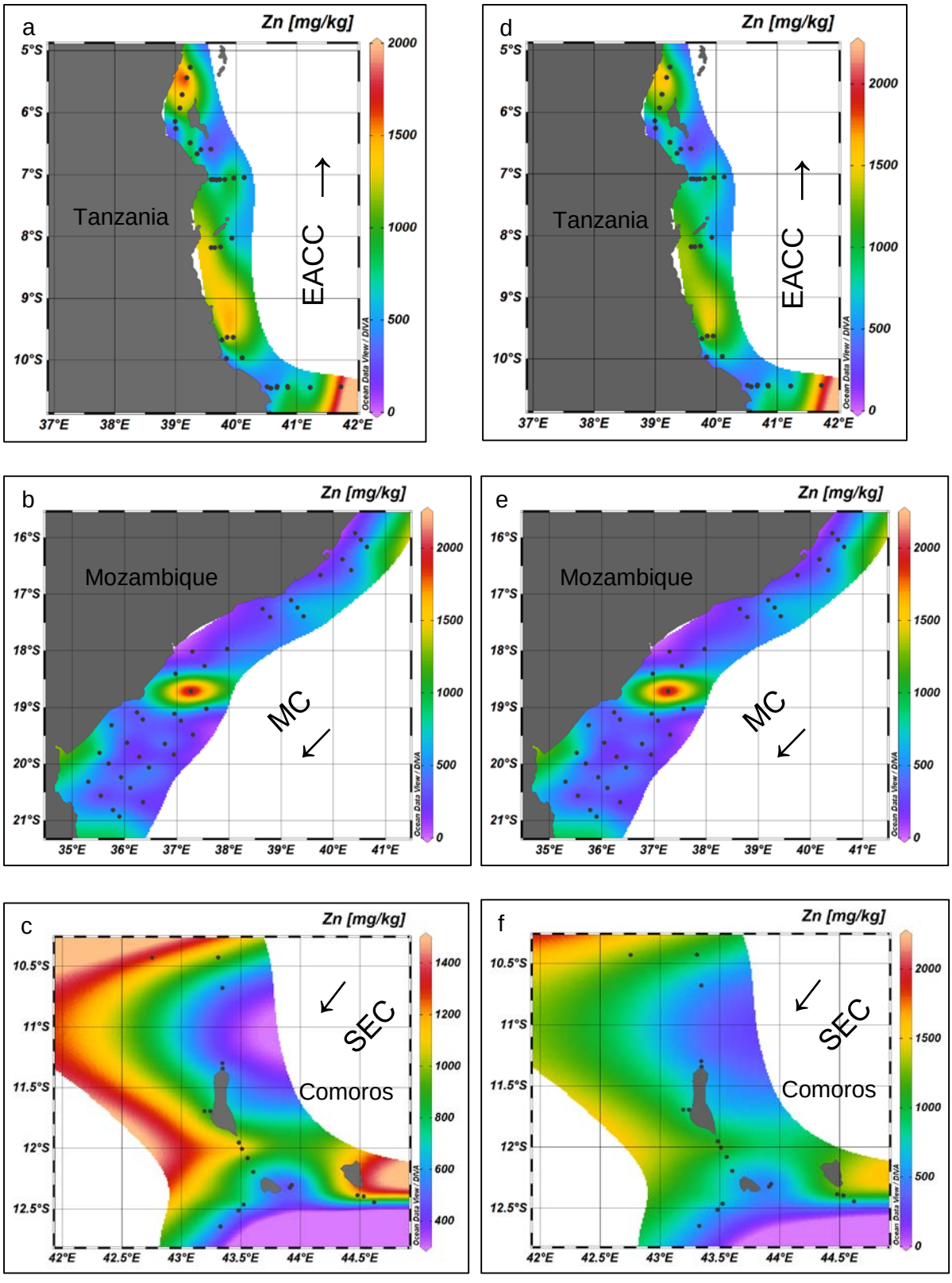

Figure 3.20: Interpolated distribution of zinc concentrations in zooplankton of the EACC (a), MC (b), and SEC (c) in mg/kg dm. Note difference in concentration scales (z-axes) between the two columns. The left-hand column is scaled for the maximum of each current, while the right-hand column (d, e, and f) has the same scale across each map. Concentrations are colour coded, with the highest concentrations in red, and the lowest in purple. The main current direction is indicated by an arrow.

Relatively high concentrations of Zn in zooplankton occurred near two of the three islands in the SEC (Figure3.20 c, f), while the lowest Zn concentration (500 mg/kg dm) around the islands were in zooplankton at 12.3°S and 43.9°E. The highest Zn concentration in the SEC (c) was at 10.5°S and 12.4°S (c, f).

3.6.8. Arsenic

Arsenic concentrations occurred at high concentrations (20 mg/kg dm) in zooplankton from the EACC (Figure 3.21 a, d). The highest concentrations occurred close to the Mafia islands, with concentrations gradually decreasing north and south of 8°S (a, d). The lowest observed concentration in the EACC was at 10°S, 40.05°E (a, d). Concentrations of As in zooplankton towards the SEC (c) at 10.5°S gradually increased with distance away from the coastline (a, d). The MC showed the lowest overall concentrations of AS between the three currents with a maximum of 8 mg/kg dm. Three 'hot spots' were evident (b). The lowest observed concentration was found close to the Zambezi River mouth (1.5 mg/kg dm).

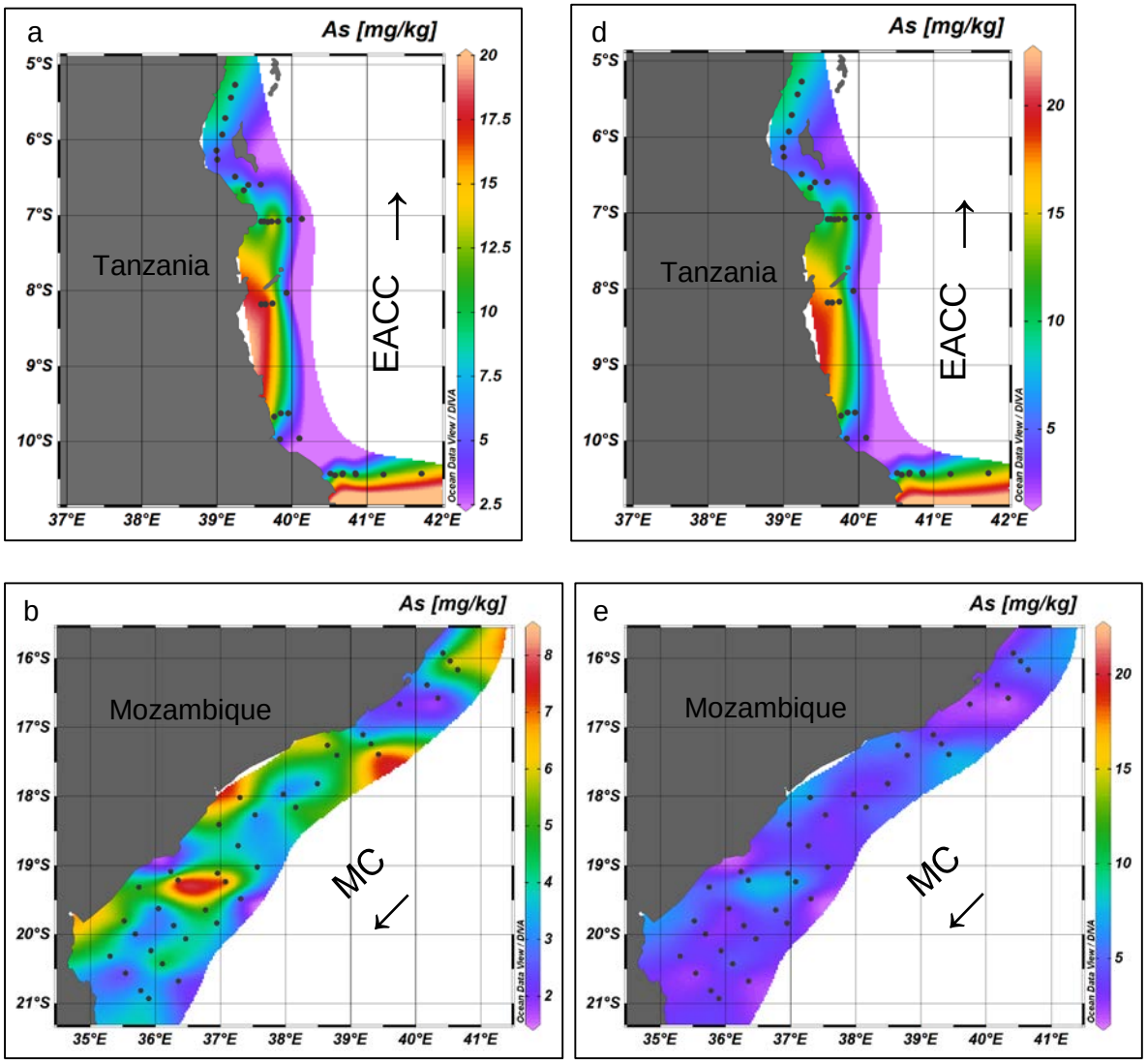

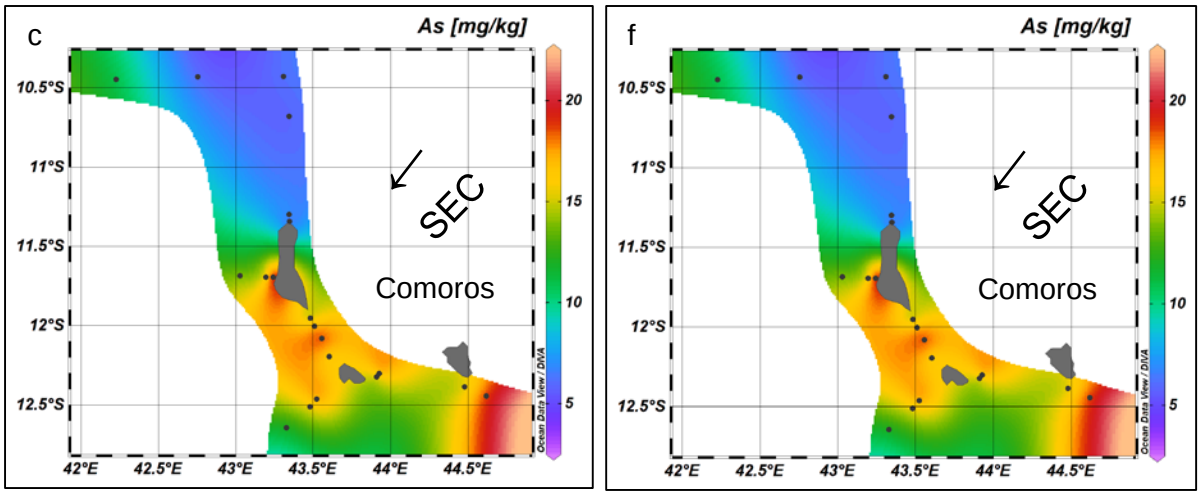

Figure 3.21: Distribution of arsenic concentrations in zooplankton of the EACC (a), MC (b), and SEC (c) in mg/kg dm. Note difference in concentration scales (z-axes) between the two columns. The left-hand column is scaled for the maximum of each current, while the right-hand column (d, e, and f) has the same scale across each map. Concentrations are colour coded, with the highest concentrations in red, and the lowest in purple. The main current direction is indicated by an arrow.

Relatively high As concentrations (5 mg/kg dm) in zooplankton occurred throughout the entire MC (Figure 3.21 b). Concentrations in zooplankton in the MC (e) compared with the EACC and SEC was low (e). The highest concentration of As (22.5 mg/kg dm) occurred in the SEC (c, f), possibly associated with the undersea volcano found in 2018. Concentrations became lower westwards towards the EACC (a). Elevated As concentrations (12.5 mg/kg dm to 17.5 mg/kg dm) occurred around the three islands of Comoros in the SEC (c, f).

3.6.9. Selenium

Selenium in zooplankton showed three specific regions of elevated concentrations (Figure 3.22 a, d) with the highest concentration (32 mg/kg dm) associated with river mouths. Relatively high concentrations occurred around Zanzibar with elevated concentrations close to the Pangani River mouth near the city of Tanga (a, d). Only one site in the MC (b, e) had high concentrations (30 mg/kg dm) of Se. Concentrations are relatively uniform in distribution with the lowest concentration found close to the Zambezi River mouth (b, e). Selenium concentrations in the SEC (c, f) showed two discrete concentration peaks, one near the city of Moroni, and the other in the SEC before it joins the EACC (a). A relatively uniform distribution occurred around the islands of Comoros with the lowest concentration found before the SEC enters the MC (c, f).

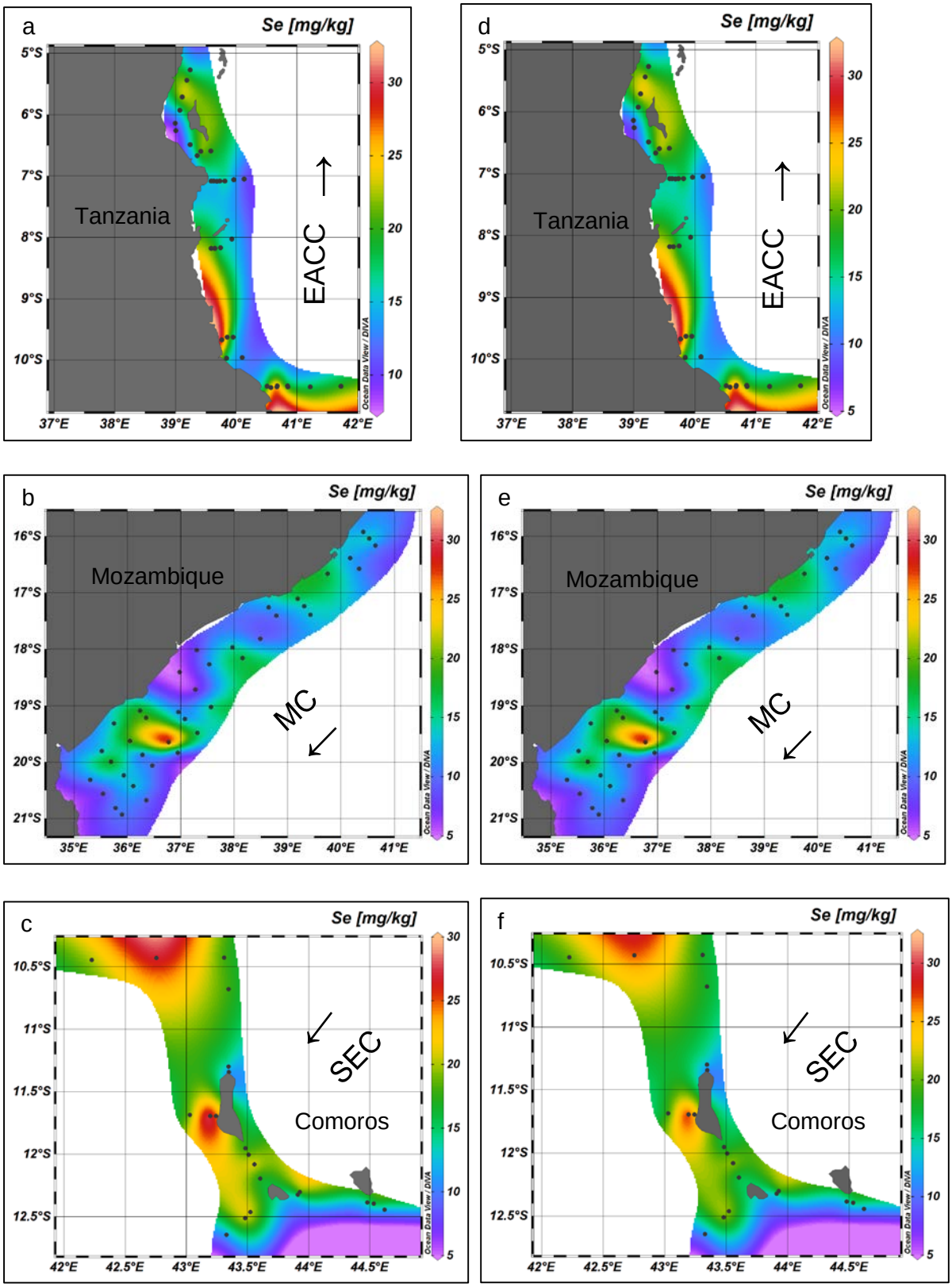

Figure 3.22: Distribution of selenium found in zooplankton of the EACC (a), MC (b), and SEC (c) in mg/kg dm. Note difference in concentration scales (z-axes) between the two columns. The left-hand column is scaled for the maximum of each current, while the right-hand column (d, e, and f) has the same scale across each map. Concentrations are colour

coded, with the highest concentrations in red, and the lowest in purple. The main current direction is indicated by an arrow.

3.6.10. Nickel

Higher concentrations of Ni in zooplankton in the EACC (Figure 3.23 a, d) showed two sites with elevated concentrations. The highest concentration was found close to the Pangani River mouth in the northern part of the EACC (a, d) whereas, relatively high concentrations occurred close to the Ruvuma river mouth (a, d). The MC (b) had the lowest concentrations found between the three currents, with the highest concentration (85 mg/kg dm) near the Zambezi River mouth (b). Relatively high concentrations occurred close to the harbour in Beira where the Buzi River, Pungwe River, and Sabi River discharge (b). Low Ni concentrations occurred in the SEC (c) with only one site showing elevated concentrations (200 mg/kg dm). Figures (e and f) shows an even distribution between concentrations.

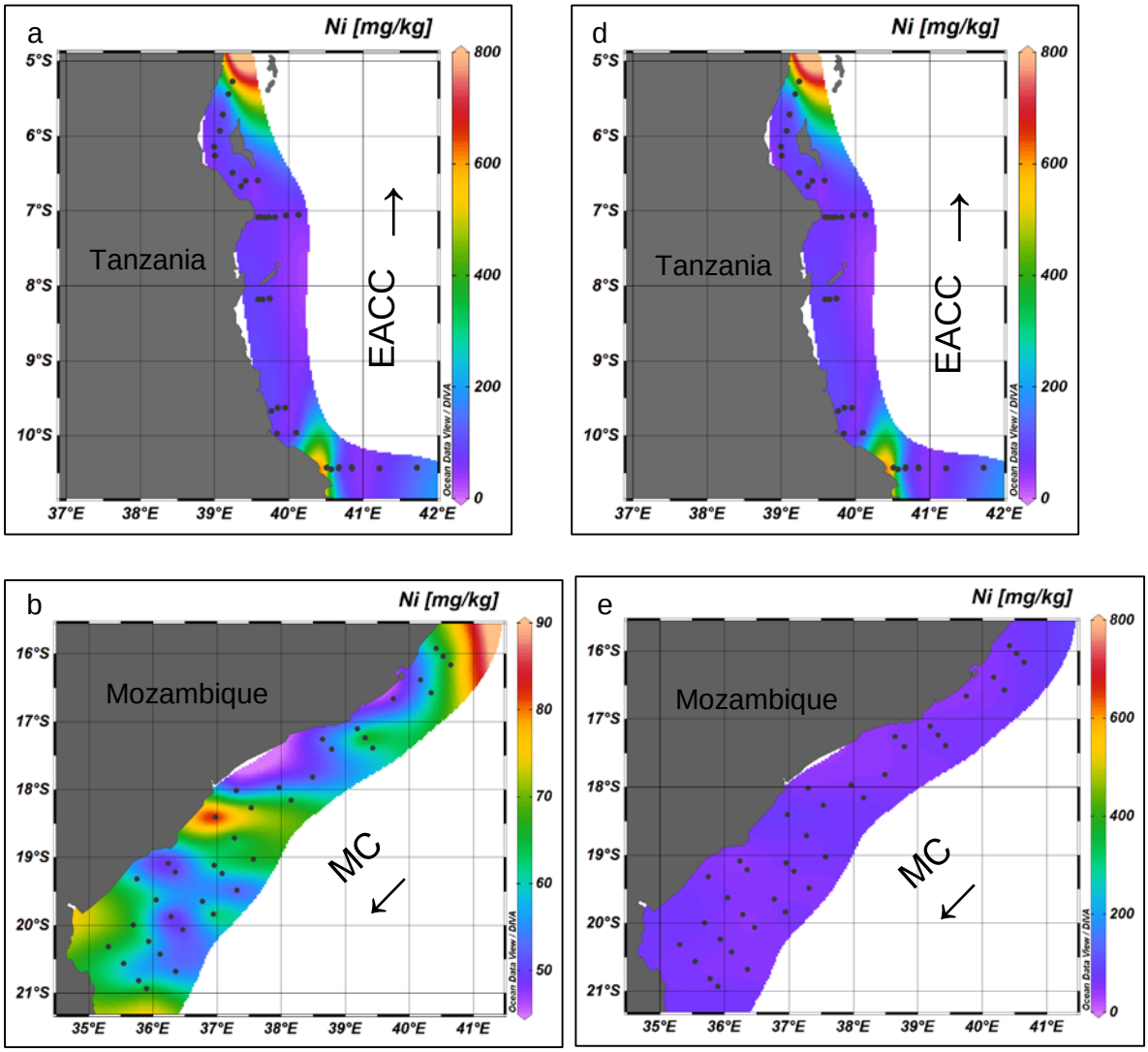

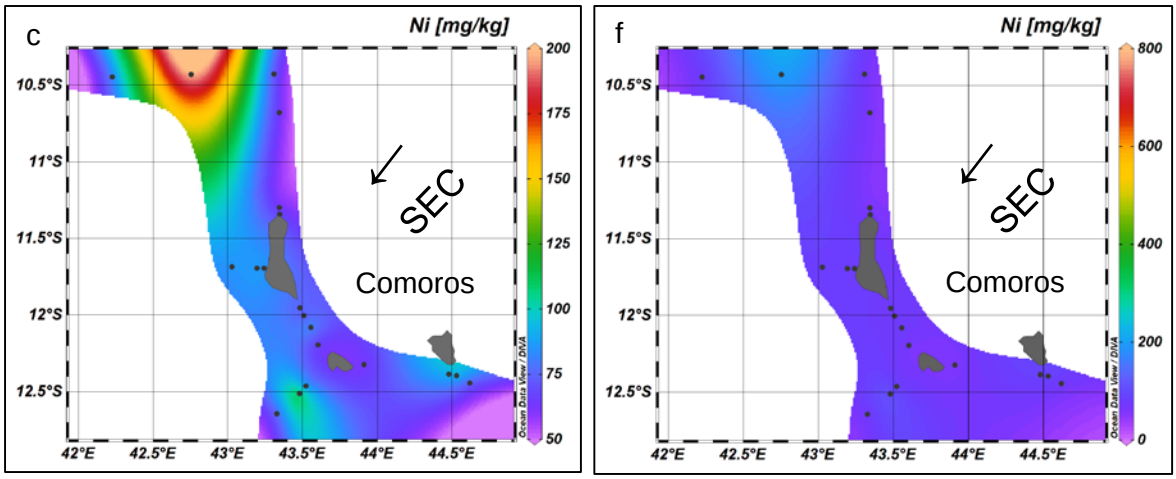

Figure 3.23: Horizontal distribution of nickel found within zooplankton, of the EACC (a), MC (b), and SEC (c) in mg/kg dm. Note difference in concentration scales (z-axis) between the two columns. The left-hand column is scaled for the maximum of each current, while the right-hand column (d, e, and f) has the same scale across each map. Concentrations are colour coded for better representation with the highest concentrations represented in red and the lowest in purple for each area. The main current direction is indicated by an arrow.

3.6.11. Cadmium

Throughout the entire EACC (Figure 3.24) concentrations of Cd are distributed relatively even (a, d). Lower concentrations occurred at sites nearer harbours than that of the Ruvuma and Pangai rivers (a, d). Elevated concentrations occurred close to Mafia (a, d) and gradually became lower towards 5°S and 10.5°S (a, d). The MC (b, e) shows distinct distributions of high, relatively high, and low concentrations. The highest concentrations occurred close the harbour of Beira (20°S) where concentrations decreased gradually up to 18°S. At 18°S, higher concentrations were seen. The lowest concentrations occurred between 16°S and 17°S, as well as close to the Zambezi and Sabi river mouths.

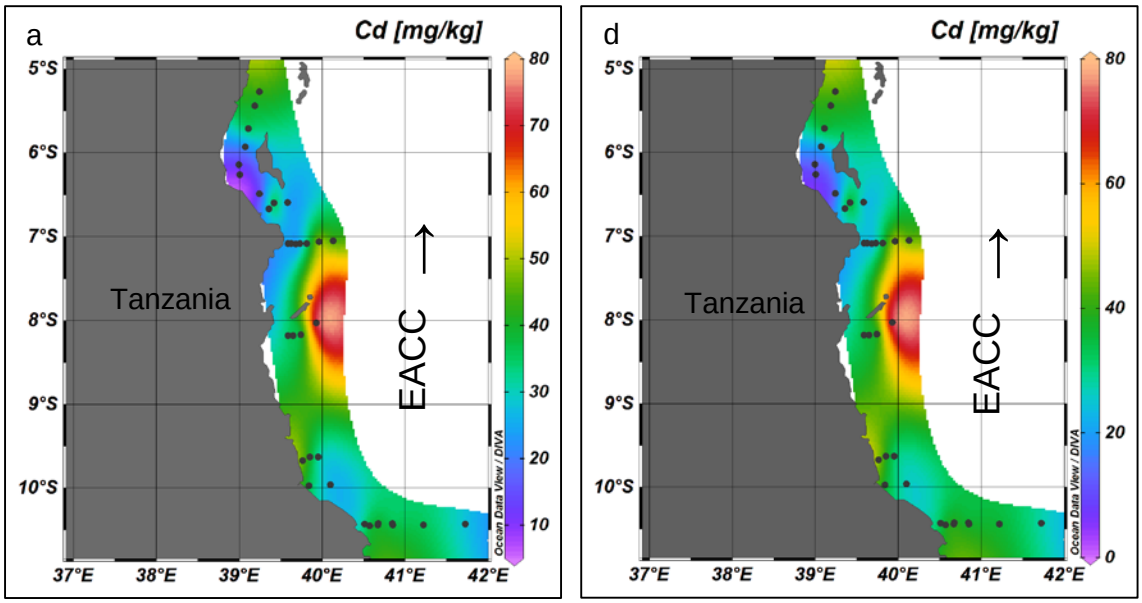

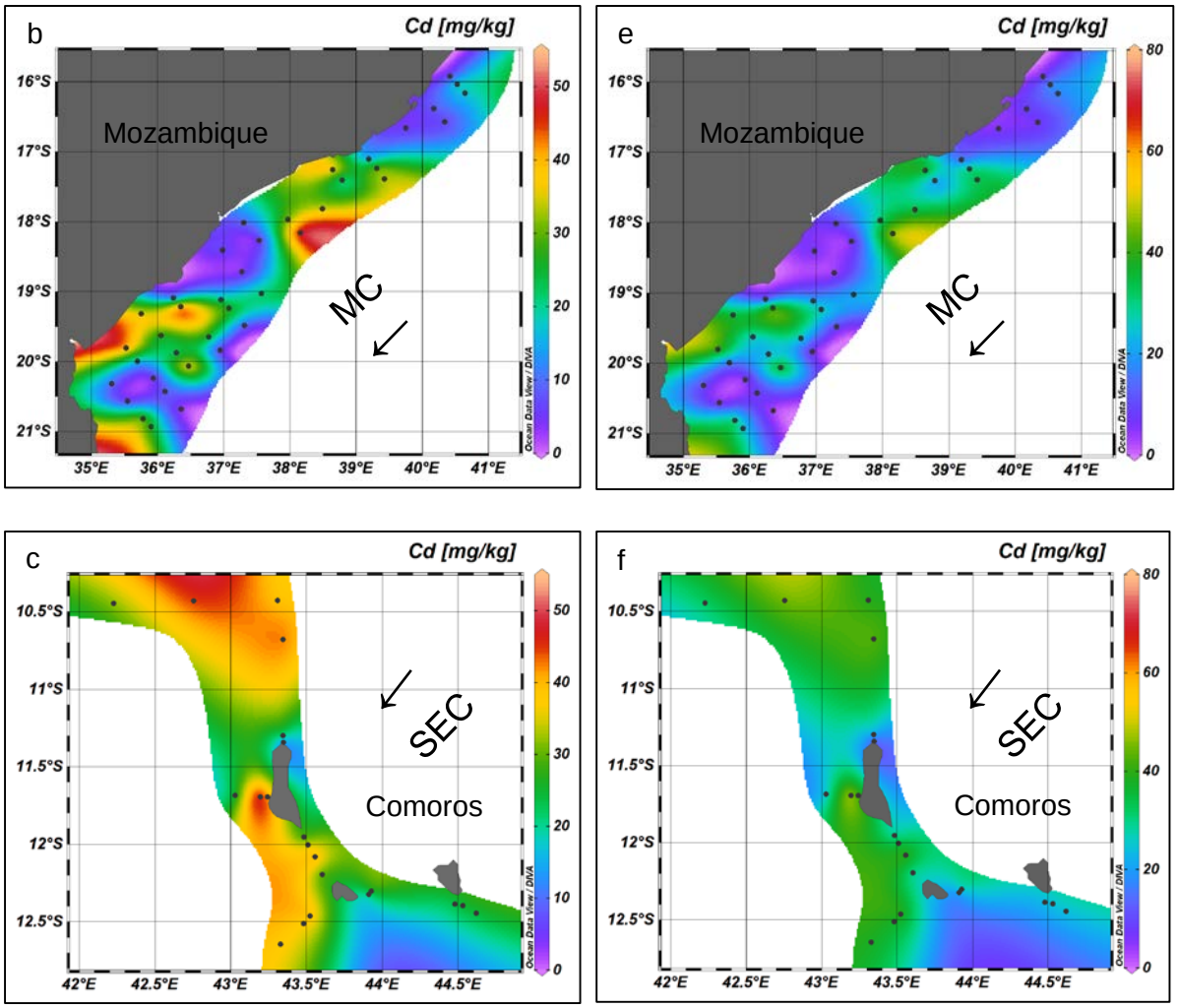

Figure 3.24: Distribution of cadmium found in zooplankton of the EACC (a), MC (b), and SEC (c) in mg/kg dm. Note difference in concentration scales (z-axes) between the two columns. The left-hand column is scaled for the maximum of each current, while the right-hand column (d, e, and f) has the same scale across each map. Concentrations are colour coded, with the highest concentrations in red, and the lowest in purple. The main current direction is indicated by an arrow.

In the SEC (Figure 3.24 c, d) two distinct 'hot spots' occurred with elevated concentrations around two of the three islands of Comoros in the SEC (c, f) and at sites close to 10.5°S (c, f).

3.6.12. Mercury

In general, relatively high concentrations of Hg in zooplankton occurred in all three currents (Figure 3.25) with the EACC (a) having the highest concentration (2.5 mg/kg dm). Relatively low Hg concentrations occurred scattered in the EACC (a, d) with only the sites close to the Pangani River, Ruvu River, and Mtwarra harbour having elevated concentrations (a, d). The MC (b) and SEC had the same maximum concentrations at 1.75 mg/kg dm. The MC (b) showed a more even distribution of lower Hg concentrations than that of the SEC, with the highest concentrations (1.75 mg/kg dm) occurring in the most northern part of the MC (b) and close to the harbour in Beira (b).

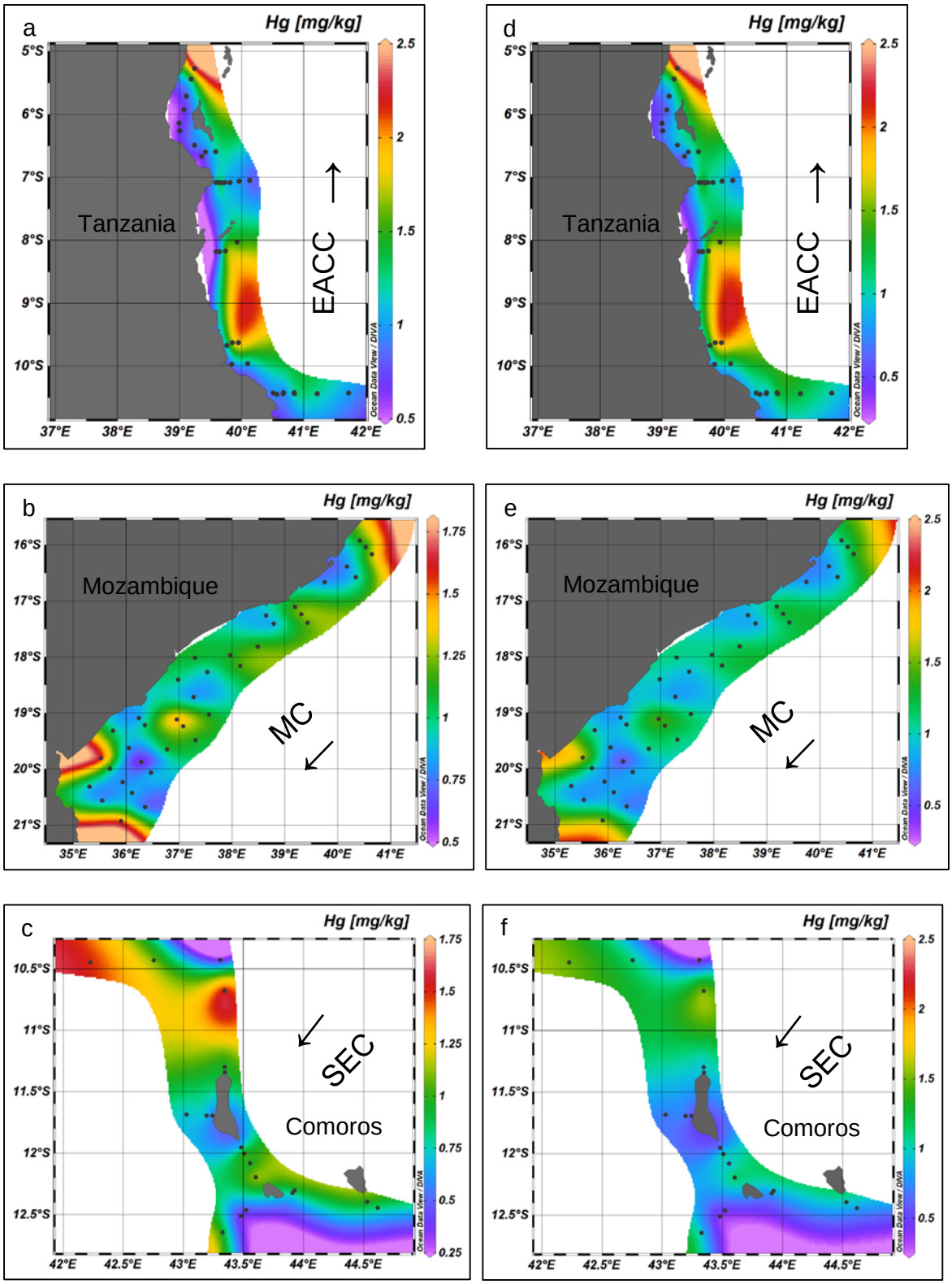

Figure 3.25: Distribution of mercury found in zooplankton of the EACC (a), MC (b), and SEC (c) in mg/kg dm. Note difference in concentration scales (z-axes) between the two columns. The left-hand column is scaled for the maximum of each current, while the right-hand column (d, e, and f) has the same scale across each map. Concentrations are colour coded, with the highest concentrations in red, and the lowest in purple. The main current direction is indicated by an arrow.

Elevated Hg concentrations (1.5 mg/kg dm) in zooplankton occurred between 10.4°S and 11°S in the SEC (c, f) with relatively low concentrations (0.75 m/kg dm) between 11.5°S and 12°S (c, f).

3.6.13. Lead

Distribution patterns of lead concentrations in zooplankton differed between all three currents (Figure 3.26 a-f). The highest lead concentration was found in the MC (b) followed by the SEC (c) and finally the EACC (a) with the lowest maximum concentration. Concentrations in the EACC had higher concentrations close to the coastline than the sites situated further away. Elevated concentrations (15 mg/kg dm to 20 mg/kg dm) occurred close to the Pangani River, Rufiji River, and Ruvu River mouths, with relatively low concentrations (5 mg/kg dm) at the Ruvuma River mouth (a, d). Elevated Pb concentrations (30 mg/kg dm) occurred close to the Zambezi River mouth as well as close to the Beira harbour (b, e).

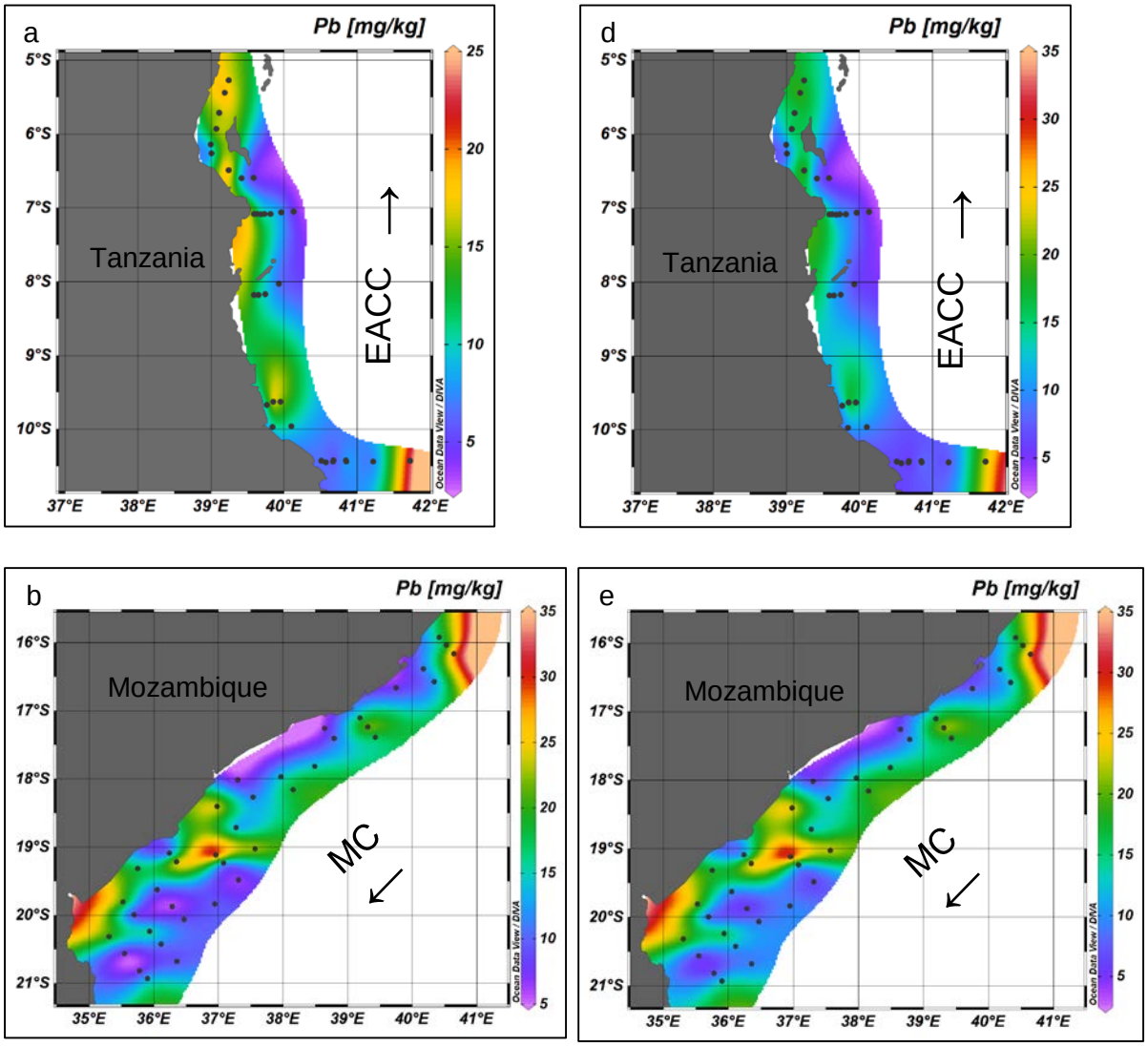

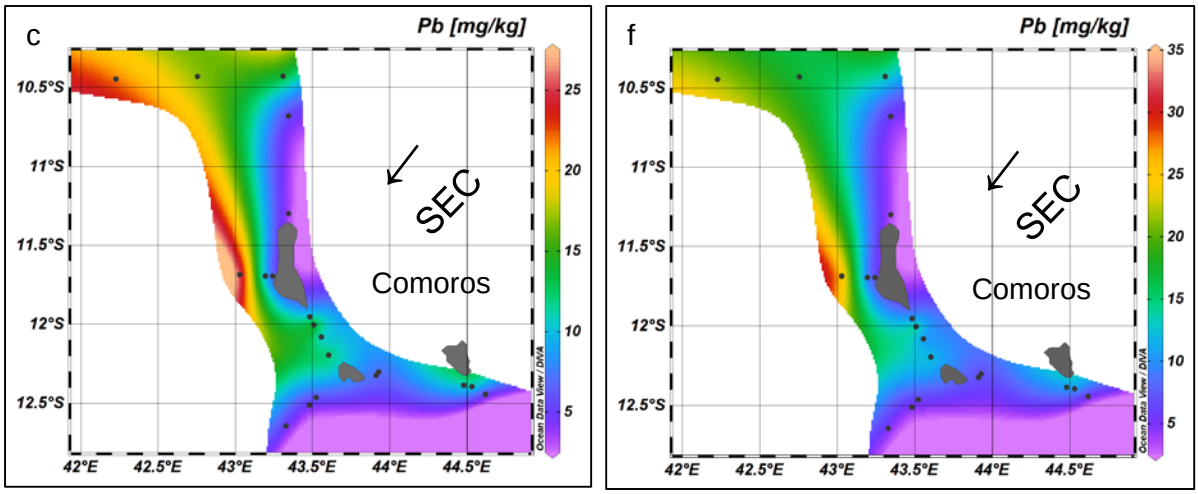

Figure 3.26: Distribution of lead found in zooplankton of the EACC (a), MC (b), and SEC (c) in mg/kg dm. Note difference in concentration scales (z-axes) between the two columns. The left-hand column is scaled for the maximum of each current, while the right-hand column (d, e, and f) has the same scale across each map. Concentrations are colour coded, with the highest concentrations in red, and the lowest in purple. The main current direction is indicated by an arrow.

Relatively low Pb concentrations (5 mg/kg dm) in zooplankton occurred scattered throughout the MC (Figure 3.26 b, e). Lead concentrations in the SEC was found at low concentrations (5 mg/kg dm) near the three islands of Comoros (c, f), with high concentrations between 11.5°S and 12°S (c, f).

3.6.14. Uranium

Between the three currents, U had a high concentration in zooplankton in the SEC (Figure 3.27 c), while the EACC (a) and the MC (b) had the same maximum concentrations. Elevated concentrations occurred along the coastline of Tanzania in the EACC with concentrations decreasing into the open ocean (a).

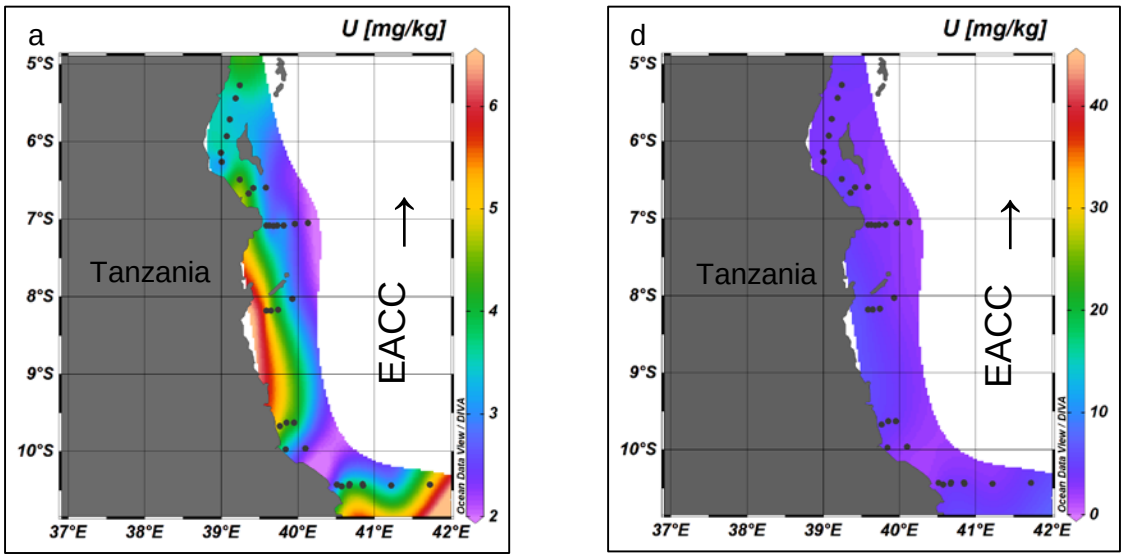

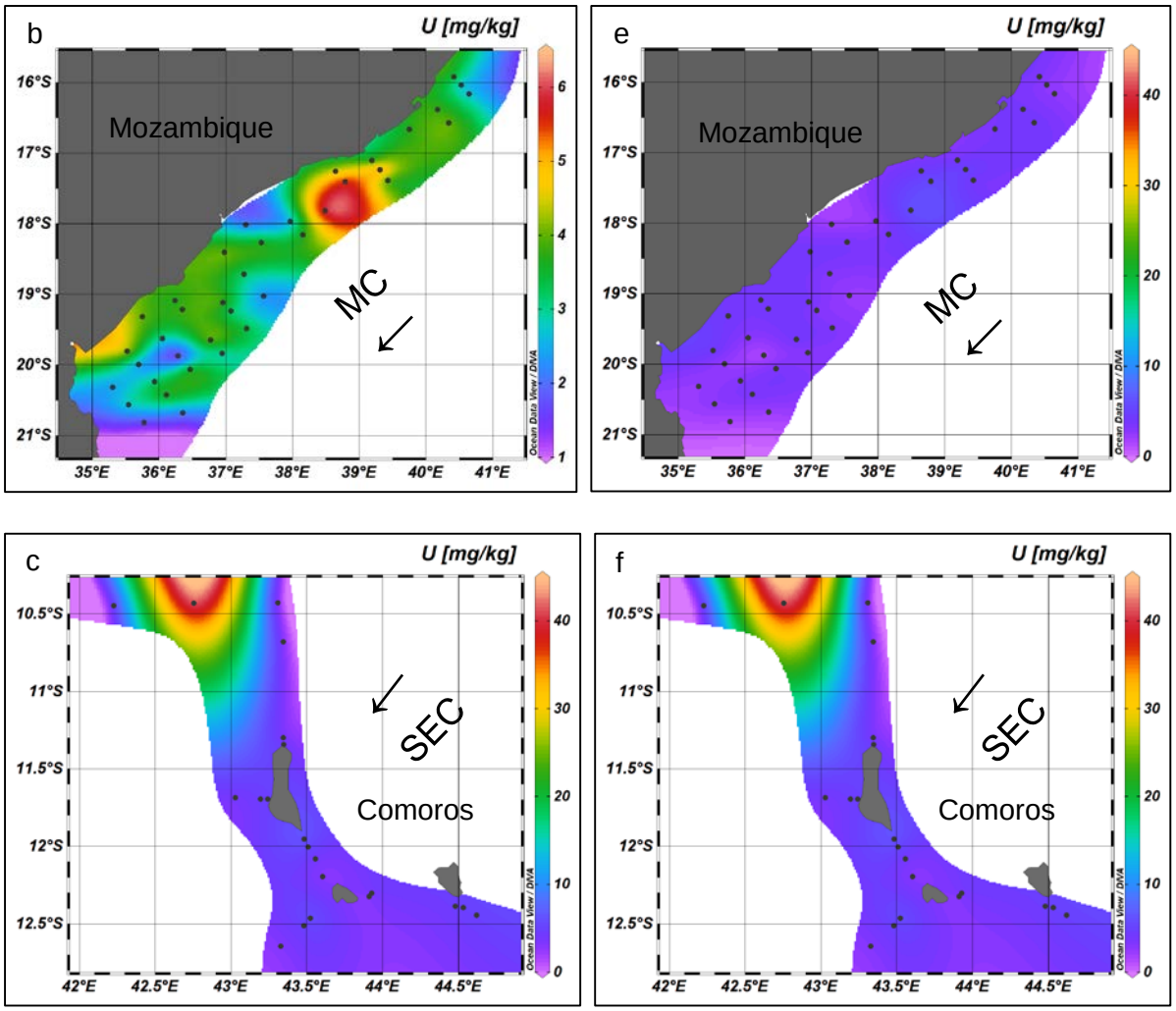

Figure 3.27: Distribution of uranium found in zooplankton of the EACC (a), MC (b), and SEC (c) in mg/kg dm. Note difference in concentration scales (z-axes) between the two columns. The left-hand column is scaled for the maximum of each current, while the right-hand column (d, e, and f) has the same scale across each map. Concentrations are colour coded, with the highest concentrations in red, and the lowest in purple. The main current direction is indicated by an arrow.

Zooplankton from sites close to the Ruvuma River mouth had lower U concentrations (3 mg/kg dm), increasing further away from the coast into the open ocean (a). A slight elevation can be seen at Dar es Salaam (a). Concentrations of Pb in the MC (b) showed relatively high concentrations (3.5 mg/kg dm) spread throughout the MC, with only two sites representing possible 'hot spots' (b). The highest concentration found of U was in the SEC (c, f). Relatively low concentrations (5 mg/kg dm) occurred throughout the SEC with only one site showing high U concentrations (40 mg/kg dm).

3.7. Summary of 'hot spots' associated with potential pollution sources

The information in the previous section was collated regarding potential terrestrial pollution sources from two of the three currents (Table 3.22). Four potential sources were identified from the MC, while the EACC had six potential pollution sources.

Table 3.22: Significance of 14 metallic elements compared with potential terrestrial pollution sources from the EACC and MC with sums of significant interactions across sources and elements.

Element	Beira Harbour	Dar es Salaam Harbour	Zambezi River	Ruvuma River	Ruvu River	Rufiji River	Pangani River	Macuze River	Angoche	Mafia island	
V	x					x	x		x		4
Cr	x	x		x	X	x	x		x	x	8
Mn			x			x	x	x	x		5
Fe	x					x	x	x	x		5
Co								x			1
Cu	x		x		X		x	x		x	6
Zn	x		x		X		x				4
As					X					x	2
Se			x	x	X		x				4
Ni				x			x				2
Cd	x							x		x	3
Hg	x				X		x		x		4
Pb	x	x	x			x	x		x		6
U											0
	8	2	5	3	6	5	10	5	6	4	

MC =Mozambique Channel, EACC = East African Coastal Current

Of the 14 elements in zooplankton, Cr, Cu, and Pb stood out consistently associated with the 11 potential sources identified. Beira harbour is prominent for eight of the 14 elements. The Pangani River was associated with ten of the 14 elements. Finally, the Ruvu River and Angoche was associated with six metallic 'hot spots'.

Table 23 represents a total of 104 “hot spots” of 14 metals were found throughout the EACC, MC, and SEC. The MC had the highest number of “hot spots” followed by the EACC, and lastly the SEC.

Table 3.23: Summary of geographical elemental hotspots from the MC, EACC, and SEC.

Element	MC	EACC	SEC	
V	5	2	3	10
Cr	4	3	4	11
Mn	4	2	2	8
Fe	4	3	3	10
Co	1	2	2	5
Cu	3	2	4	9
Zn	1	3	3	7
As	5	2	3	10
Se	1	2	2	5
Ni	3	2	1	6
Cd	5	1	2	8
Hg	4	2	2	8
Pb	3	1	1	5
U	2	2	1	5
	42	29	33	

MC =Mozambique Channel, EACC = East African Coastal Current,

SEC, South Equatorial Current

Chapter 4: Discussion and conclusion

Pollution is one of the greatest threats to the environment. With the human population increasing globally, especially within coastal areas, regulations to control the use and spread of pollution are necessary to ensure environmental health (Rouchon, 2015; Goswami *et al.,* 2014). Pollutants such as metallic elements are of major concern within coastal areas and within the open ocean (Goswami *et al.,* 2014). Upon entering the marine environment, metals enter the food web and accumulate within organisms. Metallic elements have been of concern for many decades with a growing number of elements being added to this list (Substance Priority List | ATSDR, 2020). The interactions of metallic elements within the marine environment are influenced by many environmental parameters. Temperature, pH, salinity, turbidity, oxygen, and depth all have an impact on the mobility, ionisation, binding and uptake of metallic elements by biota (Gissi *et al.,* 2013). Temperature is known to influence the metabolic activity of organisms and therefore influences the accumulation rate of metals by organisms (Gissi *et al.,* 2013).

Even though extensive research has been done on interactions of metallic elements in combination with environmental factors (Rieuwerts *et al.,* 1998; Tchounwou *et al.,* 2012; Zhong *et al.,* 2020), many elements still lack toxicological data for many species and ecological effects (Rouchon, 2015) especially for organisms such as marine zooplankton (Rejomon *et al.,* 2009). Goswami *et al.,* (2014) stated that zooplankton forms a crucial part of the marine food web since high concentrations of metallic elements have been found in fish tissue, essentially because they obtain the metallic elements from zooplankton. Since marine zooplankton forms a large proportion of the marine primary consumers, it is clear to say that they would be susceptible to environmental pollution with prolonged exposures and increased environmental concentrations (Goswami *et al.,* 2013).

In this dissertation, the concentrations and geographical patterns of 14 metallic elements (V, Cr, Mn, Fe, Co, Cu, Zn, As, Se, Ni, Cd, Hg, Pb, and U) were investigated in marine zooplankton from three distinct currents of the WIO (Table 3.21; Figure 3.14-3.27).

Elemental comparative studies with possible toxicological effects

4.1. Essential elements

Certain metallic elements are essential for physiological and metabolic regulation. This regulation maintains the homeostasis and general health of an organism (Squadron *et al.,* 2016; Tchounwou *et al.,* 2012). Below, I discuss the distribution patterns of eight priority substances that are also essential to life (Substance Priority List | ATSDR, 2020) V, Cr, Mn, Fe, Co, Cu, Zn, As, and Se in the three currents, their natural occurrence, possible anthropogenic sources, physiological roles and toxicities, and the implications.

Of the eight essential elements, higher concentrations were generally associated with the EACC and the MC. The distribution throughout the EACC and MC as well as the occurrence of “hot spots” in isolated areas such as at Tanga, Rufiji River, Ruvu River, and Mtwarra in the EACC, and Angoche, Macarau river, Caucau River, Zambesi River,

and Beira are all impacted by anthropogenic activities. These activities include shipping, natural gas extraction, mining, increased agriculture, energy production, atmospheric deposition, and leaching from underlying geology (ATSDR, 2003; Bjerregaard *et al*., 2015; Schiffer & Liber, 2017; Srichandan *et al*., 2016).

As mentioned in Section 3.7, there were four potential sources of pollution in the EACC and MC. Higher concentrations close to the Beira harbour, Mtwarra, and Tanga where the Pangani River mouth discharges were not unexpected, since Tanga has a rich gold concentration (Bosire *et al*., 2015) and the Pangani is used for mining, agriculture, and power generation. Mtwarra where the Rovuma River mouth enters the WIO are known for mining and natural gas extraction (Bosire *et al*., 2015; WIOMSA, 2009). At Beira, the biggest source of pollution is presumably from shipping and harbour-related activities introducing metals into the environment, either from the transportation of cargo, loading, spillage, natural gas, and from antifouling paints (Assem & Oskarsson, 2015; ATSDR, 2005b; Battuello *et al*., 2016; Bjerregaard *et al*., 2015; Klaassen & Watkins, 2015; Imtiaz *et al*.,2015; Schleshinger *et al*., 2017). It is not surprising that this area has been identified with numerous “hot spots” (Table 3.22).

Elements such as V, Cr, Mn, Fe, Zn, and As in zooplankton were most often associated with “hot spots” (Table 3.23) in the EACC and MC. Even though the MC is known for its mineral rich coastal zone (Wright, 2000), these elements at increased concentrations can have severe acute and sub-lethal chronic effects on zooplankton. These effects include, but are not limited to, developmental defects, decreased reproduction, and behavioural changes (Bjerregaard *et al*., 2015; Chung *et al*., 2014; Mazuka, 2008). With all of the essential elements found naturally in the environment, trace amounts will always be present in one way or another. Mining and upwelling events along the MC may also contribute to higher concentrations and “hot spots” of elements in zooplankton. Elevated concentrations observed in the SEC most likely can mostly be attributed to anthropogenic activities and natural leaching of elements from the volcanic islands of Grand Comoros, Moheli, and Anjouan (Bachelery *et al*., 2019; Lemoine *et al*., 2020). Open ocean “hot spots” are mainly found along 10.5°S, indicating a source of pollution in this area.

In general, it is also possible that the increased open ocean concentrations are due to zooplankton defecation and higher concentrations being depleted in the surface water due to high primary productivity. With high metal concentrations in all three currents, especially along the coast, upwelling and natural stratification can influence the distribution of metallic elements. Other factors such as depth, temperature, oxygen, density, and turbidity can also effect the concentration of metals found in these currents. Even though Figure 3.13 does not indicate interactions between environmental parameters and metals, the interactions could just be too small to observe with this modal used. Therefore, the increased concentrations of essential elements throughout the EACC, MC, and SEC can influence zooplankton abundance, growth and reproduction. Because of the prime importance of zooplankton in marine ecology, these essential elements should be monitored to warn of any increases that may affect productivity and local communities.

4.2. Non-essential elements

Non-essential metallic elements serves no proper biological function in the life of organisms, and can have severe toxicological effects, even at low concentrations (Squadron *et al.,* 2016). Below, I discuss the distribution patterns of five priority substances (Substance Priority List | ATSDR, 2020) Ni, Cd, Hg, Pb, and U in the three currents, their natural occurrence, possible anthropogenic sources associated with the currents, physiological roles and toxicities, and the implications.

For all the non-essential elements, the most number of "hot spots" were located in the MC, followed by the EACC and lastly the SEC (Table 3.23). Even though these non-essential elements occur in nature, any increase in concentration can be an indication of pollution from anthropogenic activities (Kamau *et al*., 2015). These elements usually enter the environment through mining, energy production, industrial effluent, and improper disposal of industrial waste (ATSDR, 2005[a]; ATSDR, 2012; Anandkumar *et al*., 2017; Bjerregaard *et al*., 2015; Srichandan *et al*., 2016). Increases in concentrations can have severe toxicological effects in zooplankton such as developmental, reproduction, growth, neurological and behavioural defects (Anandkumar *et al*., 2017; Goering et al., 1995; Lauer & Bianchini, 2010; Mohammed *et al*., 2010; Nordburg, 2009; Squadron *et al*., 2016). Even though Ni is known for its physiological role in enzyme activity, it is still considered a non-essential element. Nickel is also the only non-essential element that has a function in organisms. Concentrations of Cd, Hg, Pb, and U in zooplankton all suggest environmental pollution in "hot spots" in the three currents. Increased Ni concentrations around harbours can be attributed to shipping, since Ni is used as an antifouling agent in paint (Bjerregaard *et al*., 2015).

High Hg concentrations in zooplankton occurred throughout the EACC, MC, and SEC, likely due to mining and burning of fossil fuels (ATSDR, 2020; Anandkumar *et al*., 2017; Bjerregaard *et al*., 2015; Kojadinovic *et al*., 2007; Sydeman & Jarman., 1998). Hg concentrations zooplankton near Tanzania I surmise may be due to increased gold mining singe Tanzania is the second-biggest gold producing country in Africa next to South Africa (Bryceson *et al*., 2012). Uranium is an element known for its radioactivity, but natural uranium mostly enters the environment through leaching from rocks (Kaishwa *et al*., 2018; Rweyemamu & Kim, 2020). With 95% of mined U being used for energy production, trace releases are expected in the environment (Kimaro & Mdoe, 2018). However, increased concentrations may have severe effects on organisms. Lead, as mentioned in Section 3.7 (Table 3.22), is widely distributed throughout the EACC and MC. These increased concentrations of lead were mostly found close to river mouths suggesting that these higher concentrations were mainly anthropogenic in nature.

Even though it would seem that the EACC, MC and SEC would be experiencing environmental overload, most of the Ca ratios indicated that this was not the case. However, these three currents need to be monitored as decreases in primary and secondary productivity may follow increased releases and pollution, eventually influencing higher trophic levels and human health. Climate change might also have effects, the extent of which, in the marine environment, is difficult to predict.

Bibliography

Achary, M.S., Satpathy, K.K., Panigrahi, S., Mohanty, A.K., Padhi, R.K., Biswas, S., Prabhu, R.K., Vijayalakshmi, S., & Panigrahy, R.C. 2017. Concentration of heavy metals in the food chain components of the nearshore coastal waters of Kalpakkam, southeast coast of India. *Food control*. *Elsevier Ltd*. 72:232–243.

Agency for toxic substances and disease registry (ATSDR). 2020. *Substance priority list |ATSDR*. [online] available at: https://www.atsdr.cdc.gov/spl/index.html#2019spl [Accessed 12 August 2020].

Agency for toxic substances and disease registry (ATSDR). 2007. Toxicological profile for arsenic. Atlanta, GA: U.S. Department of health and human services, public health service.

Agency for toxic substances and disease registry (ATSDR). 2012. Toxicological profile for cadmium. Atlanta, GA: U.S. Department of health and human services, public health service.

Agency for toxic substances and disease registry (ATSDR). 2020. Toxicological profile for lead. Atlanta, GA: U.S. Department of health and human services, public health service.

Agency for toxic substances and disease registry (ATSDR). 1999. Toxicological profile for mercury. Atlanta, GA: U.S. Department of health and human services, public health service.

[a]Agency for toxic substances and disease registry (ATSDR). 2005. Toxicological profile for nickel. Atlanta, GA: U.S. Department of health and human services, public health service.

Agency for toxic substances and disease registry (ATSDR). 2003. Toxicological profile for selenium. Atlanta, GA: U.S. Department of health and human services, public health service.

Agency for toxic substances and disease registry (ATSDR). 2013. Toxicological profile for uranium. Atlanta, GA: U.S. Department of health and human services, public health service.

[b] Agency for toxic substances and disease registry (ATSDR). 2005. Toxicological profile for zinc. Atlanta, GA: U.S. Department of health and human services, public health service.

Al-Imarah, F.J., Khalaf, T.A., Ajeel, S.G., Khudhair, A.Y., & Saad, R., 2018. Accumulation of heavy metals in zooplanktons from Iraqi national waters. *International journal of marine science*, *8*.

Almutari, M.M., 2019. Improving crop quality: Investigations on soil selenium and zinc transfer and bioavailability (Doctoral dissertation, Kansas State University).

Amiel, A.J., Friedman, G.M., Miller, D.S., 1973. Distribution and nature of incorporation of trace elements in modern aragonitic corals. Sedimentology. 20: 47-64.

Anandkumar, A., Nagarajan, R., Prabakaran, K., & Rajaram, R., 2017. Trace metal dynamics and risk assessment in the commercially important marine shrimp species collected from the Miri coast, Sarawak, east Malaysia. *Regional studies in marine science*, 16:79-88.

Anderson, D.M., Glibert, P.M., & Burkholder, J.M., 2002. Harmful algal blooms and eutrophication: nutrient sources, composition, and consequences. *Estuaries*, 25(4):704-726.

Aparicio-González, A., Duarte, C.M., & Tovar-Sánchez, A. 2012. Trace metals in deep ocean waters: A review. *Journal of marine systems. Elsevier*, 100–101:26–33.

Aslam, S. & Yousafzai, A.M., 2017. Chromium toxicity in fish: A review article. *Journal of entomology and zoology studies*, *5*(3):1483-1488.

Assem, F.L. & Oskarsson, A., 2015. Chapter 60–vanadium. *Handbook on the toxicology of metals*, 1347-1367.

Bachelery, P., Di Muro, A., Gurioli, L., Besson, P., Burckel, P., & Nowak, S., 2019. Rapid response for on-land volcanic hazard assessment during the 2018-2019 submarine Mayotte volcano-tectonic crisis: Implications for volcanic risk quantification. *American geophysical union fall meeting*, 2019: V33A-02.

Balasubramanian, T., 2012. Heavy metal contamination and risk assessment in the marine environment of Arabian sea, along the southwest coast of India. *Journal of the american chemical society*, 2:191-208.

Barlow, R., Lamont, T., Morris, T., Sessions, H., & Van Den Berg, M. 2014. Adaptation of phytoplankton communities to mesoscale eddies in the Mozambique channel. *Deep sea research part II: Topical studies in oceanography*, 100:106- 118.

Barwick, M., & Maher, W., 2003. Biotransference and biomagnification of selenium copper, cadmium, zinc, arsenic and lead in a temperate seagrass ecosystem from lake macquarie estuary, NSW, Australia. *Marine environmental research*, 56(4):471-502.

Battuello, M., Brizio, P., Mussat Sartor, R., Nurra, N., Pessani, D., Abete, M.C., & Squadrone, S. 2016. Zooplankton from a north western mediterranean area as a model of metal transfer in a marine environment. *Ecological indicators. Elsevier Ltd*. 66:440–451.

Béhagle, N., du Buisson, L., Josse, E., Lebourges-Dhaussy, A., Roudaut, G., & Ménard, F., 2014. Mesoscale features and micronekton in the Mozambique channel: an acoustic approach. *Deep sea research part II: Topical studies in oceanography*, 100:164-173.

Bleise, A., Danesi, P.R., & Burkart, W., 2003. Properties, use and health effects of depleted uranium (DU): a general overview. *Journal of environmental radioactivity*, 64(2-3):93-112.

Boryło, A., Skwarzec, B., & Fabisiak, J., 2010. Bioaccumulation of uranium 234U and 238U in marine birds. *Journal of radioanalytical and nuclear chemistry*, *284*(1):165-172.

Bosire, J., Celliers, L., Groeneveld, J., Paula, J., & Schleyer, M.H., 2015. Regional state of the coast report-Western Indian Ocean. UNEP-Nairobi convention and WIOMSA.

Brown, P.B., Williams, C.D., Robinson, E.H., Akiyama, D.M., & Lawrence, A.L., 1986. Evaluation of methods for determining in vivo digestion coefficients for adult red swamp crayfish *Procambarus clarkii*. *Journal of the world aquaculture society*, 17(1-4):19-24.

Brugge, D., & Buchner, V., 2011. Health effects of uranium: new research findings. *Reviews on environmental health*, 26(4):231-249.

Bruland, K.W., & Lohan, M.C., 2006. Controls of trace metals in seawater. *The oceans and marine geochemistry*, 6:23-47.

Bryceson, D.F., Jønsson, J.B., Kinabo, C., & Shand, M., 2012. Unearthing treasure and trouble: mining as an impetus to urbanisation in Tanzania. *Journal of contemporary african studies*, 30(4):631-649.

Bjerregaard, P., Andersen, C.B., & Andersen, O., 2015. Ecotoxicology of metals—sources, transport, and effects on the ecosystem. In *handbook on the toxicology of metals,* 425-459. Academic Press.

Bungala, S.O., Machiwa, J.F., & Shilla, D.A., 2017. Concentration and biomagnification of heavy metals in biota of the coastal marine areas of Tanzania. *Journal of environmental science and engineering*, 6:406-424.

Burger, J., & Elbin, S., 2015. Metal levels in eggs of waterbirds in the New York harbor (USA): Trophic relationships and possible risk to human consumers. *Journal of toxicology and environmental health, Part A*, 78(2):78-91.

Chen, N., Peng, B., Hong, H., Turyaheebwa, N., Cui, S., & Mo, X., 2013. Nutrient enrichment and N: P ratio decline in a coastal bay–river system in southeast China: the need for a dual nutrient (N and P) management strategy. *Ocean & coastal management*, 81:7-13.

Chung, J.Y., Yu, S.D., & Hong, Y.S., 2014. Environmental source of arsenic exposure. *Journal of preventive medicine and public health*, 47(5):253.

Conceição, F., Catuane, F., Taímo, S., Carvalho, F.P., Oliveira, J.M., & Malta, M., 2018. Radiological assessment of heavy-mineral sand exploitation in Mozambique. In *naturally occurring radioactive material (NORM VIII). Proceedings of an international symposium*.

Crichton, R.R., 2008. -15--nickel and cobalt: Evolutionary relics. *Biological inorganic chemistry*, 257-269.

Dallas, H.F. & Day, J.A. 2004. The effect of water quality variables on aquatic ecosystems: a review. Republic of South Africa: University of Cape Town

DESA, U., 2019. United nations, Department of economic and social affairs, population division. World population prospects 2019: Highlights.

Dreschler, B., 2001. Small-scale mining and sustainable development within the SADC region. *Mining, minerals and sustainable development*, 84.

Durant, A.J., Bonadonna, C. and Horwell, C.J., 2010. Atmospheric and environmental impacts of volcanic particulates. *Elements*, 6(4):235-240.

Duvail, S., Hamerlynck, O., Paron, P., Herve, D., Nyingi, W.D., & Leone, M., 2017. The changing hydro-ecological dynamics of rivers and deltas of the Western Indian Ocean: Anthropogenic and environmental drivers, local adaptation and policy response. *Comptes rendus geoscience*, *349*(6-7):269-279.

DWAF, 1996. Department of water affairs and forestry, 1996. South African water quality guidelines, vol. 4. Agricultural use: Irrigation, water.

Echeveste, P., Galbán-Malagón, C., Dachs, J., Berrojalbiz, N., & Agustí, S. 2016. Toxicity of natural mixtures of organic pollutants in temperate and polar marine phytoplankton. *Science of the total environment. Elsevier B.V.* 571:34–41.

Everaert, G., De Laender, F., Goethals, P.L.M., & Janssen, C.R. 2015. Relative contribution of persistent organic pollutants to marine phytoplankton biomass dynamics in the North Sea and the kattegat. *Chemosphere*. *Elsevier Ltd*. 134:76–83.

Fernández-Severini, M.D., Hoffmeyer, M.S., & Marcovecchio, J.E., 2013. Heavy metals concentrations in zooplankton and suspended particulate matter in a southwestern Atlantic temperate estuary (Argentina). *Environmental monitoring and assessment*, *185*(2):1495-1513.

Filimonova, V., Goncalves, F., Marques, J.C., De Troch, M., & Goncalves, A.M., 2016. Biochemical and toxicological effects of organic (herbicide Primextra® Gold TZ) and inorganic (copper) compounds on zooplankton and phytoplankton species. *Aquatic toxicology*, 177:33-43.

Filippou, D., St-Germain, P. and Grammatikopoulos, T., 2007. Recovery of metal values from copper—arsenic minerals and other related resources. *Mineral processing and extractive metallurgy review*, 28(4):247-298.

Fisher, N.S. & Hook, S.E. 2002. Toxicology tests with aquatic animals need to consider the trophic transfer of metals. *Toxicology*. 181–182:531–536.

Flegal A.R., Settle, D.M., Patterson, C.C. 1986. Thallium in marine plankton. Marine biology. 90: 501-503.

Gál, J., Hursthouse, A., Tatner, P., Stewart, F., & Welton, R., 2008. Cobalt and secondary poisoning in the terrestrial food chain: data review and research gaps to support risk assessment. *Environment international*, 34(6):821-838.

García-Otero, N., Barciela-Alonso, M.C., Bermejo-Barrera, P., Moreda-Piñeiro, A., Jiménez, M.S., Gómez, M.T., & Castillo, J.R. 2013. Assessment of metals bound to marine plankton proteins and to dissolved proteins in seawater. *Analytica chimica acta*. 804:59–65.

Gault, N., Sandre, C., Poncy, J.L., Moulin, C., Lefaix, J.L., & Bresson, C., 2010. Cobalt toxicity: chemical and radiological combined effects on HaCaT keratinocyte cell line. *Toxicology in vitro*, 24(1):92-98.

George, R.M., 2005. Biogeochemistry of trace metals in the Indian EEZ of the Arabian sea and Bay of Bengal (Doctoral dissertation, National Institute of Oceanography).

George, M.D., & Kureishy, T.W., 1979. Trace metals in zooplankton from the Bay of Bengal.

Gissi, F., Binet, M.T., & Adams, M.S., 2013. Acute toxicity testing with the tropical marine copepod *Acartia sinjiensis*: Optimisation and application. *Ecotoxicology and environmental safety*, 97:86-93.

Goering, P.L., Waalkes, M.P., & Klaassen, C.D., 1995. Toxicology of cadmium. In *Toxicology of metals*, 189-214. Springer, Berlin, Heidelberg.

Goswami, P., Thirunavukkarasu, S., Godhantaraman, N., & Munuswamy, N., 2014. Monitoring of genotoxicity in marine zooplankton induced by toxic metals in Ennore estuary, Southeast coast of India. *Marine pollution bulletin*, 88(1-2):70-80.

Groeneveld, J.C., & Koranteng, K.A. 2017. *The RV Dr Fridtjof Nansen in the Western Indian Ocean: voyages of marine research and capacity development. [1975-2016]*. Food and agriculture organization of the united nations (FAO).

Habeck, M., 1992. Toxicological profile for manganese agency for toxic substances and disease registry. *United states public health service*.

Hagelstein, K., 2009. Globally sustainable manganese metal production and use. *Journal of environmental management*, 90(12):3736-3740.

Halo, I., Backeberg, B., Penven, P., Ansorge, I., Reason, C., & Ullgren, J.E., 2014. Eddy properties in the Mozambique Channel: A comparison between observations and two numerical ocean circulation models. *Deep sea research part II: Topical studies in oceanography*, 100:38-53.

Hashmi, M.Z., Abbasi, N.A., Tang, X., & Malik, R.N., 2015. Egg as a biomonitor of heavy metals in soil. In *heavy metal contamination of soils*, 127-143. Springer, Cham.

He, M., Wang, Z., & Tang, H. 1998. The chemical, toxicological and ecological studies in assessing the heavy metal pollution in Le An River, China. *Water research.* 32(2):510–518.

Henry, P.R., & Miles, R.D., 2001. Heavy metals–vanadium in poultry. *Ciência animal brasileira*, 2(1):11-26.

Hood, R.R., Bange, H.W., Beal, L., Beckley, L.E., Burkill, P., Cowie, G.L., D'Adamo, N., Ganssen, G., Hendon, H., Hermes, J., & Honda, M., 2015. The second international indian ocean expedition (IIOE-2): A basin-wide research program-science plan (2015-2020).

Howe, P., Malcolm, H., & Dobson, S., 2004. *Manganese and its compounds: environmental aspects*. World health organization.

Hipfner, J.M., Hobson, K.A., & Elliott, J.E. 2011. Ecological factors differentially affect mercury levels in two species of sympatric marine birds of the North Pacific. *Science of the total environment. Elsevier B.V.* 409(7):1328–1335.

Huggett, J.A. 2014. Mesoscale distribution and community composition of zooplankton

in the Mozambique channel. *Deep-sea research part II: Topical studies in oceanography. Elsevier*. 100:119–135.

Hung, C.C., Ko, F.C., Gong, G.C., Chen, K.S., Wu, J.M., Chiang, H.L., Peng, S.C., & Santschi, P.H., 2014. Increased zooplankton PAH concentrations across hydrographic fronts in the east China Sea. *Marine pollution bulletin*, 83(1):248-257.

Hutton, M., 1983. Sources of cadmium in the environment. *Ecotoxicology and environmental safety*, 7(1):9-24.

Imtiaz, M., Rizwan, M.S., Xiong, S., Li, H., Ashraf, M., Shahzad, S.M., Shahzad, M., Rizwan, M., & Tu, S., 2015. Vanadium, recent advancements and research prospects: a review. *Environment international*, 80:79-88.

Jose, Y.S., Aumont, O., Machu, E., Penven, P., Moloney, C.L., & Maury, O. 2014. Influence of mesoscale eddies on biological production in the Mozambique channel: Several contrasted examples from a coupled ocean-biogeochemistry model. *Deep-sea research part II: Topical studies in oceanography,* 100:79-93.

Kadam, S.S., & Tiwari, L.R., 2012. Zooplankton composition in dahanu creek-west coast of India. *Research journal of recent sciences*, 1(5):62-65.

Kai, E.T., & Marsac, F., 2010. Influence of mesoscale eddies on spatial structuring of top predators' communities in the Mozambique channel. *Progress in oceanography*, 86(1-2):214-223.

Kaishwa, S.J., Marwa, E.M., Msaky, J.J., & Mwakalasya, W.N., 2018. Uranium natural levels in soil, rock and water: assessment of the quality of drinking water in Singida urban district, Tanzania. *Journal of water and health*, 16(4):542-548.

Kaladharan, P., Prema, D., Valsala, K.K., Leelabhai, K.S., & Rajagopalan, M., 2005. Trends in heavy metal concentrations in sediment, finfishes and shellfishes in inshore waters of Cochin, southwest coast of India. *Journal of the marine biological association of India*, 47(1):1-7.

Kamau, J.N., Kuschk, P., Machiwa, J., Macia, A., Mothes, S., Mwangi, S., Munga, D., & Kappelmeyer, U., 2015. Investigating the distribution and fate of Al, Cd, Cr, Cu, Mn, Ni,

Pb and Zn in sewage-impacted mangrove-fringed creeks of Kenya, Tanzania and Mozambique. *Journal of soils and sediments*, 15(12):2453-2465.

Karthikeyan, P., Marigoudar, S.R., Nagarjuna, A., & Sharma, K.V., 2019. Toxicity assessment of cobalt and selenium on marine diatoms and copepods. *Environmental chemistry and ecotoxicology*, 1:36-42.

Kehrig, H.A., Palermo, E.F.A., Seixas, T.G., Branco, C.C., Moreira, I., & Malm, O., 2009. Trophic transfer of methylmercury and trace elements by tropical estuarine seston and plankton. *Estuarine, coastal and shelf science*, 85(1):36-44.

Khudhair, A.Y., Khalaf, T.A., Ajeel, S.G., & Saad, R., 2015. Estimation of heavy metals in zooplankton organisms of NW Arabian gulf.

Kimaro, E. & Mdoe, S., 2018. *Uranium mining in the united republic of tanzania: Current status, challenges and opportunities* (No. IAEA-CN--261).

Kojadinovic, J., Potier, M., Le Corre, M., Cosson, R.P., & Bustamante, P. 2007. Bioaccumulation of trace elements in pelagic fish from the Western Indian Ocean. *Environental pollution,* 146(2):548–566.

Kolasinski, J., Kaehler, S., & Jaquemet, S. 2012. Distribution and sources of particulate organic matter in a mesoscale eddy dipole in the Mozambique channel (south-western Indian Ocean): Insight from C and N stable isotopes. *Journal of marine systems. Elsevier B.V.* 96–97:122–131.

Kontas, A., 2008. Trace metals (cu, Mn, Ni, Zn, Fe) contamination in marine sediment and zooplankton samples from Izmir Bay.(Aegean Sea, Turkey). *Water, air, and soil pollution*, 188(1-4):323-333.

Lachassagne, P., Aunay, B., Frissant, N., Guilbert, M. and Malard, A., 2014. High-resolution conceptual hydrogeological model of complex basaltic volcanic islands: a Mayotte, Comoros, case study. *Terra nova*, 26(4):307-321.

Lagerström, M.E., Field, M.P., Séguret, M., Fischer, L., Hann, S., & Sherrell, R.M. 2013. Automated on-line flow-injection ICP-MS determination of trace metals (Mn, Fe, Co, Ni, Cu and Zn) in open ocean seawater: Application to the GEOTRACES program. *Marine chemistry, Elsevier B.V.* 155:71–80.

Lamont, T., Barlow, R.G., Morris, T., & Van Den Berg, M.A., 2014. Characterisation of mesoscale features and phytoplankton variability in the Mozambique channel. *Deep sea research part II: Topical studies in oceanography*, 100:94-105.

Lauer, M.M., & Bianchini, A., 2010. Chronic copper toxicity in the estuarine copepod *Acartia tonsa* at different salinities. *Environmental toxicology and chemistry*, 29(10):2297-2303.

Leal, M.C., Sá, C., Nordez, S., Brotas, V., & Paula, J., 2009. Distribution and vertical dynamics of planktonic communities at Sofala Bank, Mozambique. *Estuarine, Coastal and shelf science*, 84(4):605-616.

Lebourges-Dhaussy, A., Huggett, J., Ockhuis, S., Roudaut, G., Josse, E., & Verheye, H., 2014. Zooplankton size and distribution within mesoscale structures in the Mozambique channel: a comparative approach using the TAPS acoustic profiler, a multiple net sampler and ZooScan image analysis. *Deep sea research part II: Topical studies in oceanography*, 100:136-152.

Lemoine, A., Briole, P., Bertil, D., Roullé, A., Foumelis, M., Thinon, I., Raucoules, D., De Michele, M., Valty, P. and Colomer, R.H., 2020. The 2018–2019 seismo-volcanic crisis east of Mayotte, Comoros islands: seismicity and ground deformation markers of an exceptional submarine eruption. *Geophysical journal international*.

Llewellyn, L.E., English, S., & Barnwell, S., 2016. A roadmap to a sustainable Indian Ocean blue economy. *Journal of the indian ocean region*, 12(1):52-66.

Lutjeharms, J.R., & Bornman, T.G., 2010. The importance of the greater Agulhas current is increasingly being recognised. *South african journal of science*, 106(3-4):1-4.

Makarim, S., Sprintall, J., Liu, Z., Yu, W., Santoso, A., Yan, X.H., & Susanto, R.D. 2019. Previously unidentified indonesian throughflow pathways and freshening in the Indian Ocean during recent decades. *Scientific reports*, 9(1):7364.

Malauene, B.S., Shillington, F.A., Roberts, M.J., & Moloney, C.L., 2014. Cool, elevated chlorophyll-a waters off northern Mozambique. *Deep sea research part II: Topical studies in oceanography*, 100:68-78.

Marin, E., Vaccaro, C., Di Giuse, D., Procesi, M., Sciarra, A., & Zarlenga, F., 2016. Enrichment in heavy metal (HM) and rare earth element (REE) in fluvial placer deposits: Case study of zambesi river (Mozambique). *International journal of scientific research*, 5(163251).

Marsac, F., Barlow, R., Ternon, J.F., Ménard, F., & Roberts, M., 2014. Ecosystem functioning in the Mozambique Channel: Synthesis and future research. *Deep sea research part II: Topical studies in oceanography*, 100:212-220.

März, C., Hoffmann, J., Bleil, U., de Lange, G.J., & Kasten, S., 2008. Diagenetic changes of magnetic and geochemical signals by anaerobic methane oxidation in sediments of the Zambezi deep-sea fan (SW Indian Ocean). *Marine geology*, 255(3-4):118-130.

Masalu, D.C., 2002. Coastal erosion and its social and environmental aspects in Tanzania: a case study in illegal sand mining. *Coastal management*, 30(4):347-359.

Massarin, S., Alonzo, F., Garcia-Sanchez, L., Gilbin, R., Garnier-Laplace, J., & Poggiale, J.C., 2010. Effects of chronic uranium exposure on life history and physiology of *Daphnia magna* over three successive generations. *Aquatic toxicology*, 99(3):309-319.

Matthews, K.A., Grottoli, A.G., McDonough, W.F., & Palardy, J.E., 2008. Upwelling, species, and depth effects on coral skeletal cadmium-to-calcium ratios (Cd/Ca). *Geochimica et cosmochimica acta*, 72(18):4537-4550.

Mattio, L., Zubia, M., Maneveldt, G.W., Anderson, R.J., Bolton, J.J., de Gaillande, C., De Clerck, O., & Payri, C.E. 2016. Marine flora of the iles eparses (Scattered Islands): A longitudinal transect through the Mozambique channel. *Acta oecologica*. *Elsevier masson SAS*. 72:33–40.

McCune, B., Grace, J.B., & Urban, D.L., 2002. Analysis of ecological communities. MjM software design Gleneden beach, OR.

Meng, W., Qin, Y., Zheng, B., & Zhang, L. 2008. Heavy metal pollution in Tianjin Bohai Bay, China. *Journal of environmental sciences. (China)*. 20:814–819.

Metcheva, R., Yurukova, L., & Teodorova, S.E., 2011. Biogenic and toxic elements in feathers, eggs, and excreta of Gentoo Penguin (*Pygoscelis papua ellsworthii*) in the Antarctic. Environmental monitoring and assessment. 182, 571e585. https://doi.org/10.1007/s10661-011-1898-9.

Mohammed, E.H., Wang, G., & Jiang, J., 2010. The effects of nickel on the reproductive ability of three different marine copepods. *Ecotoxicology*, 19(5):911-916.

Morneau, J.P., 1997. Trace metal analysis of marine zooplankton from Conception Bay, Newfoundland, (Doctoral dissertation, Memorial University of Newfoundland).

Motulsky HM and Brown RE, Detecting outliers when fitting data with nonlinear regression – a new method based on robust nonlinear regression and the false discovery rate, BMC Bioinformatics 2006, 7:123.

Mubiana, V.K., Qadah, D., Meys, J., & Blust, R., 2005. Temporal and spatial trends in heavy metal concentrations in the marine mussel *Mytilus edulis* from the western scheldt estuary (The Netherlands). *Hydrobiologia*, 540(1-3):169-180.

Mukhopadhyay, S.K., Biswas, H.D.T.K., De, T.K. & Jana, T.K., 2006. Fluxes of nutrients from the tropical river hooghly at the land–ocean boundary of Sundarbans, NE Coast of Bay of Bengal, India. *Journal of marine systems*, 62(1-2):9-21.

Muscatello, J.R. & Liber, K., 2010. Uranium uptake and depuration in the aquatic invertebrate *Chironomus tentans*. *Environmental pollution*, 158(5):1696-1701.

Muzuka, A., 2008. Distribution of heavy metals in the coastal marine surficial sediments in the Msasani Bay-Dar es Salaam harbour area. *Western Indian Ocean journal of marine science*, 6(1).

Neff, J.M., 1997. Ecotoxicology of arsenic in the marine environment. *Environmental toxicology and chemistry: An international journal*, 16(5):917-927.

Nehama, F.P. & Reason, C.J., 2014. Morphology of the Zambezi river plume in the Sofala Bank, Mozambique. *Western Indian Ocean journal of marine science*, 13(1):1-10.

Nishioka, J., Obata, H., & Tsumune, D. 2013. Evidence of an extensive spread of

hydrothermal dissolved iron in the Indian Ocean. *Earth and planetary science letter. Elsevier*. 361:26–33.

Nordberg, G.F., 2009. Historical perspectives on cadmium toxicology. *Toxicology and applied pharmacology*, 238(3):192-200.

Nunez, C. 2019. Climate 101: Oceans. *Our oceans are under attack by climate change, overfishing*. Nationalgeographic.com. https://www.nationalgeographic.com/environment/habitats/ocean/. Date of access: 15 November, 2019.

Obura, D.O., Bandeira, S.O., Bodin, N., Burgener, V., Braulik, G., Chassot, E., Gullström, M., Kochzius, M., Nicoll, M., Osuka, K., & Ralison, H.O., 2019. The Northern Mozambique channel. In *world seas: an environmental evaluation*, 75-99. Academic press.

Pacheco, P.H., Spisso, A., Cerutti, S., Smichowski, P., & Martinez, L.D. 2010. Non-chromatographic screening method for the determination of mercury species. Application to the monitoring of mercury levels in Antarctic samples. *Talanta*. *Elsevier B.V.* 82(4):1505–1510.

Paul, J.T., Ramaiah, N. & Sardessai, S., 2008. Nutrient regimes and their effect on distribution of phytoplankton in the Bay of Bengal. *Marine environmental research*, 66(3):337-344.

Pease, R., 2019. Ship spies newborn underwater volcano.

Pechova, A. and Pavlata, L., 2007. Chromium as an essential nutrient: a review. *Veterinari medicina-praha-*, *52*(1):1.

Pamba, S., Shaghude, Y.W. and Muzuka, A.N., 2016. Hydrodynamic modelling on transport, dispersion and deposition of suspended particulate matter in pangani estuary, Tanzania. In *Estuaries: A lifeline of ecosystem services in the Western Indian Ocean*, 141-160. Springer, Cham.

Paterson, H., 2006. Microzooplankton from oligotrophic waters off south west western Australia: Biomass, diversity and impact on phytoplankton. University of Western Australia.

Paimpillil, J.S., Joseph, T., Rejomon, G., & Gerson, V.J., 2010. Metals in coastal zooplanktons-A coastal living resource hazard. Indian geological congress.

Pempkowiak, J., Walkusz-Miotk, J., Bełdowski, J., & Walkusz, W. 2006. Heavy metals in zooplankton from the southern Baltic. *Chemosphere*. 62(10):1697–1708.

Pitcher, T.J., Morato, T., Hart, P.J., Clark, M.R., Haggan, N., & Santos, R.S. eds., 2008. *Seamounts: ecology, fisheries and conservation*. John Wiley & Sons.

Potier, M., Bach, P., Ménard, F., & Marsac, F., 2014. Influence of mesoscale features on micronekton and large pelagic fish communities in the Mozambique channel. *Deep sea research part II: Topical studies in oceanography*, 100:184-199.

Pretorius, M., Huggett, J.A., & Gibbons, M.J., 2016. Summer and winter differences in zooplankton biomass, distribution and size composition in the KwaZulu-Natal bight, South Africa. *African journal of marine science*, 38(sup1): S155-S168.

Pripp, T., Gammelsrød, T., & Krakstad, J.O., 2014. Physical influence on biological production along the western shelf of Madagascar. *Deep sea research part II: Topical studies in oceanography*, 100:174-183.

Rauch, J.N., & Graedel, T.E., 2007. Earth's anthrobiogeochemical copper cycle. *Global biogeochemical cycles*, 21(2).

Rejomon, G., Balachandran, K.K., Nair, M., Joseph, T., Dinesh Kumar, P.K., Achuthankutty, C.T., Nair, K.K.C., & Pillai, N.G.K., 2008. Trace metal concentrations in zooplankton from the eastern Arabian sea and western Bay of Bengal. *Environmental forensics*, 9(1):22-32.

Rainbow, P.S. 2018. Trace metals in the environment and living organisms: The British Isles as a case study. Cambridge: Cambridge press.

Rejomon, G., Kumar, P.D., Nair, M., & Muraleedharan, K.R., 2010. Trace metal dynamics in zooplankton from the Bay of Bengal during summer monsoon. *Environmental toxicology*, 25(6):622-633.

Ritterhoff, J. & Zauke, G.P. 1997. Trace metals in field samples of zooplankton from the fram strait and the Greenland sea. *Science of the total environment.* 199(3):255–270.

Rieuwerts, J.S., Thornton, I., Farago, M.E., & Ashmore, M.R., 1998. Factors influencing metal bioavailability in soils: preliminary investigations for the development of a critical loads approach for metals. *Chemical speciation & bioavailability*, 10(2):61-75.

Robarts, R.D. and Zohary, T., 2018. Limnology and the future of African inland waters. *Inland waters*, 8(4):399-412.

Roe, A., 2016. *Tanzania: From mining to oil and gas* (No. 2016/79). Wider working paper.

Rouchon, A., 2015. Effects of metal toxicity on the early life stages of the sea urchin *Evechinus chloroticus*.

Rubio-Franchini, I., López-Hernández, M., Ramos-Espinosa, M.G., & Rico-Martínez, R., 2016. Bioaccumulation of metals arsenic, cadmium, and lead in zooplankton and fishes from the tula river Watershed, Mexico. *Water, air, & soil pollution*, 227(1):5.

Rumisha, C., Mdegela, R.H., Gwakisa, P.S., & Kochzius, M., 2018. Genetic diversity and gene flow among the giant mud crabs (*Scylla serrata*) in anthropogenic-polluted mangroves of mainland Tanzania: Implications for conservation. *Fisheries research*, 205:96-104.

Rweyemamu, M., & Kim, J., 2020. A study on health effects of uranium mining waste in Tanzania.

Salem, Z.B., & Ayadi, H., 2017. First investigation of trace metal distribution in surface seawater and copepods of the south coast of Sfax (Tunisia). *Environmental science and pollution research*, 24(24):9662-19670.

Scarlato, N.A., Marcovecchio, J.E., & Pucci, A.E., 1997. Heavy metal distribution in zooplankton from Buenos Aires coastal waters (Argentina). *Chemical speciation & bioavailability*, 9(1):21-26.

Schiffer, S., & Liber, K., 2017. Toxicity of aqueous vanadium to zooplankton and phytoplankton species of relevance to the athabasca oil sands region. *Ecotoxicology and environmental safety*, 137: 1-11.

Schlesinger, W.H., Klein, E.M., & Vengosh, A., 2017. Global biogeochemical cycle of vanadium. *Proceedings of the national academy of sciences*, 114(52): E11092-E11100.

Schultes, S., Sourisseau, M., Le Masson, E., Lunven, M., & Marié, L. 2013. Influence of physical forcing on mesozooplankton communities at the Ushant tidal front. *Journal of marine systems. Elsevier B.V.* 109–110(Sup): S191–S202.

Seixas, T.G., Moreira, I., & Kehrig, H.A., 2015. Mercury and selenium in seston, marine plankton and fish (*Sardinella brasiliensis*) as a tool for understanding a tropical food web. *Marine pollution bulletin*, 101(1):366-369.

Seixas, T.G., Moreira, I., Siciliano, S., Malm, O., & Kehrig, H.A., 2014. Mercury and selenium in tropical marine plankton and their trophic successors. *Chemosphere*, 111:32-39.

Semeniuk, D.M., Maldonado, M.T., & Jaccard, S.L., 2016. Chromium uptake and adsorption in marine phytoplankton–Implications for the marine chromium cycle. *Geochimica et cosmochimica acta*, 184:41-54.

Sen Gupta, R., & Singbal, S., 1988. Marine pollution in the Indian Ocean: problems, prospects and perspectives. *Journal of the indian fisheries association*, 18:333-356.

Shaghude, Y.W., 2016. Estuarine environmental and socio-economic impacts associated with upland agricultural irrigation and hydropower developments: the case of Rufiji and Pangani estuaries, Tanzania. In *Estuaries: a lifeline of ecosystem services in the Western Indian Ocean*, 169-182. Springer, Cham.

Sharaky, A.M., 2014. Mineral resources and exploration in Africa. *Department of natural resources, institute of African research and studies, Cairo University, Egypt*.

Shemdoe, R.S., 2010. Heavy metal concentrations in soils and leachetes of Mtoni dumpsite bordering the Indian Ocean in Dar es Salaam, Tanzania. *Scientific research and essays*, 5(16):2143-2147.

Sigman, D.M., & Hain, M.P., 2012. The biological productivity of the ocean. *Nature education knowledge*, 3(6):1-16.

Simonetti, P., Botté, S.E., & Marcovecchio, J.E., 2015. Exceptionally high Cd levels and

other trace elements in eggshells of American oystercatcher (*Haematopus palliatus*) from the Bahía Blanca estuary, Argentina. *Marine pollution bulletin*, 100(1):495-500.

Sletten, H.R., Gillikin, D.P., Halfa, J., Andrus, C.F.T., Guzmán., 2017. Skeletal growth controls on Mg/Ca and P/Ca ratios in tropical eastern Pacific rhodoliths (coralline red algae). Chemical geology. 465: 1-10.

Srichandan, S., Panigrahy, R.C., Baliarsingh, S.K., Rao B., S., Pati, P., Sahu, B.K., & Sahu, K.C. 2016. Distribution of trace metals in surface seawater and zooplankton of the Bay of Bengal, off rushikulya estuary, east coast of India. *Marine pollution bulletin. elsevier Ltd*. 111(1–2):468–475.

Srinivasan, M. and Swain, G.W., 2007. Managing the use of copper-based antifouling paints. *Environmental management*, 39(3):423-441.

Squadrone, S., Brizio, P., Stella, C., Prearo, M., Pastorino, P., Serracca, L., Ercolini, C., & Abete, M.C., 2016. Presence of trace metals in aquaculture marine ecosystems of the northwestern Mediterranean Sea (Italy). *Environmental pollution*, 215:77-83.

Summer, K., Reichelt-Brushett, A., & Howe, P., 2019. Toxicity of manganese to various life stages of selected marine cnidarian species. *Ecotoxicology and environmental safety*, 167:83-94.

Sydeman, W.J., & Jarman, W.M., 1998. Trace metals in seabirds, Steller sea lion, and forage fish and zooplankton from central California. *Marine pollution bulletin*, 36(10):828-832.

Tamele, I.J., & Loureiro, P.V., 2020. Lead, mercury and cadmium in fish and shellfish from the Indian Ocean and Red Sea (African Countries): Public health challenges. *Journal of marine science and engineering*, 8(5):344.

Tao, Y., Yuan, Z., Xiaona, H., & Wei, M., 2012. Distribution and bioaccumulation of heavy metals in aquatic organisms of different trophic levels and potential health risk assessment from Taihu lake, China. *Ecotoxicology and environmental safety*, 81:55-64.

Tchounwou, P.B., Yedjou, C.G., Patlolla, A.K., & Sutton, D.J., 2012. Heavy metal toxicity and the environment. In *Molecular, clinical and environmental toxicology,* 133-164. Springer, Basel.

Teichberg, M., Fox, S.E., Olsen, Y.S., Valiela, I., Martinetto, P., Iribarne, O., Muto, E.Y., Petti, M.A., Corbisier, T.N., Soto-Jimenez, M., & Páez-Osuna, F., 2010. Eutrophication and macroalgal blooms in temperate and tropical coastal waters: nutrient enrichment experiments with Ulva spp. *Global change biology*, 16(9):2624-2637.

[a]Ternon, J.F., Bach, P., Barlow, R., Huggett, J., Jaquemet, S., Marsac, F., Ménard, F., Penven, P., Potier, M., & Roberts, M.J. 2014. The Mozambique channel: from physics to upper trophic levels.

[b]Ternon, J.F., Roberts, M.J., Morris, T., Hancke, L., & Backeberg, B. 2014. In situ measured current structures of the eddy field in the Mozambique channel. *Deep sea research part II: Topical studies in oceanography*, 100:10-26.

Thirunavukkarasu, K., Soundarapandian, P., Varadharajan, D., & Gunalan, B., 2013. Phytoplankton composition and community structure of kottakudi and nari backwaters, south east of Tamil Nadu. *Journal of aquaculture research & development*, 5(211):2.

Thomassin, B.A., Garcia, F., Sarrazin, L., Schembri, T., Wafo, E., Lagadec, V., Risoul, V., & Wickel, J., 2010. Coastal seawater pollutants in the coral reef lagoon of a small tropical island in development: the Mayotte example (N Mozambique channel, SW Indian Ocean). In *Global change: mankind-marine environment interactions*, 401-407. Springer, Dordrecht.

Thuróczy, C.E., Boye, M., & Losno, R., 2010. Dissolution of cobalt and zinc from natural and anthropogenic dusts in seawater. *Biogeosciences*, 7(6):1927-1936.

Tu, N.P.C., Ha, N.N., Haruta, S., & Takeuchi, I. 2014. Trace element concentrations in barramundi (*Lates calcarifer*) collected along the coast of Vietnam. *Marine pollution bulletin. Elsevier Ltd*. 85(2):686–695.

Turner, A., 2010. Marine pollution from antifouling paint particles. *Marine pollution bulletin*, 60(2):159-171.

Twining, B.S., Baines, S.B., Bozard, J.B., Vogt, S., Walker, E.A., & Nelson, D.M. 2011. Metal quotas of plankton in the equatorial Pacific Ocean. *Deep sea research part II: Topical studies in oceanography, Elsevier*. 58(3–4):325–341.

United nations environment programme (UNEP) (2010) UNEP 2009 annual report. Technical report, united nations environment programme, ISBN No: 978-92-807-3071-5. [online] http://www.unep.org/publications/contents/pub_details_search.asp?ID=4105. Date of access: 23 September 2019.

van Aswegen, J.D., Nel, L., Strydom, N.A., Minnaar, K., Kylin, H., & Bouwman, H. 2019. Comparing the metallic elemental compositions of Kelp Gull *Larus dominicanus* eggs and eggshells from the Swartkops Estuary, Port Elizabeth, South Africa. *Chemosphere*, 221:533-542.

Van der Schyff, V., Yive, N.S.C.K., & Bouwman, H., 2020. Metal concentrations in corals from South Africa and the Mascarene Basin: A first assessment for the Western Indian Ocean. *Chemosphere*, 239:124784.

Velusamy, A., Satheesh Kumar, P., Ram, A., & Chinnadurai, S. 2014. Bioaccumulation of heavy metals in commercially important marine fishes from Mumbai Harbor, India. Marine pollution bulletin, *Elsevier Ltd*. 81(1):218–224.

Wang, H., McClean, J.L., Talley, L.D., & Yeager, S. 2018. Seasonal cycle and annual reversal of the Somali current in an eddy-resolving global ocean model. *Journal of geophysical research: Oceans*, 123(9):6562-6580.

Wei, M., Yanwen, Q., Zheng, B., & Zhang, L., 2008. Heavy metal pollution in Tianjin Bohai bay, China. *Journal of environmental sciences*, 20(7):814-819.

Willey, J.M., Sherwood, L., & Woolverton, C.J., 2011. Prescott's microbiology. 8th edit. ed.

Williams, M., Todd, G.D., Roney, N., Crawford, J., Coles, C., McClure, P.R., Garey, J.D., Zaccaria, K., & Citra, M., 2012. Toxicological profile for manganese (Atlanta, GA: Agency for toxic substances and disease registry (ATSDR) toxicological profiles).

(WIOMSA) Western Indian Ocean marine sciences association, 2009. Regional report on river-coast interactions in the Western Indian Ocean (WIO) region.

Windyty, S., n.d. *Windy As Forecasted*. [online] Windy.com/. Available at: <https://www.windy.com>. Date of access: 15 November 2019.

World Health Organization, 2004. Manganese in drinking-water (WHO): Background document for development of WHO. Guidelines for drinking-water quality (No. WHO/SDE/WSH/03.04/104). World health organization.

Wright, I., 2000. South African east coast heavy mineral mining and the development of Mozambique's heavy mineral industry. In *proceedings of workshops*.

WWF(World Wildlife Foundation). 2018. Assessing the threat of mining and oil & gas over coastal and marine protected areas (MPAs) and ecologically or biologically significant areas (EBSAs) in the southwest Indian Ocean (SWIO) region. Report, WWF Norway.

Yang, H., Rose, N.L., & Battarbee, R.W. 2002. Distribution of some trace metals in Lochnagar, a scottish mountain lake ecosystem and its catchment 1604. *Science of the total environment.* 285(1–3):197–208.

Yasin, J.A., Kroeze, C., & Mayorga, E., 2010. Nutrients export by rivers to the coastal waters of Africa: past and future trends. *Global biogeochemical cycles*, 24(4).

Zauke, G.P. & Schmalenbach, I. 2006. Heavy metals in zooplankton and decapod crustaceans from the Barents sea. *Science of the total environment,* 359(1–3):283–294.

Zhao, S., Feng, C., Quan, W., Chen, X., Niu, J., & Shen, Z., 2012. Role of living environments in the accumulation characteristics of heavy metals in fishes and crabs in the Yangtze river estuary, China. *Marine pollution bulletin*, 64(6):1163-1171.

Zhao, Y., Vance, D., Abouchami, W., & De Baar, H.J., 2014. Biogeochemical cycling of zinc and its isotopes in the southern Ocean. *Geochimica et cosmochimica acta*, 125:653-672.

Zhou, C., Vitiello, V., Casals, E., Puntes, V.F., Iamunno, F., Pellegrini, D., Changwen, W., Benvenuto, G., & Buttino, I., 2016. Toxicity of nickel in the marine calanoid copepod *Acartia tonsa*: nickel chloride versus nanoparticles. *Aquatic toxicology*, 170:1-12.

Zhong, X., Chen, Z., Li, Y., Ding, K., Liu, W., Liu, Y., Yuan, Y., Zhang, M., Baker, A.J., Yang, W., & Fei, Y., 2020. Factors influencing heavy metal availability and risk assessment of soils at typical metal mines in eastern China. *Journal of hazardous materials*, 123289.

Živkov Baloš, M., Ljubojević, D., & Jakšić, S., 2017. The role and importance of vanadium, chromium and nickel in poultry diet. *World's poultry science journal*, 73(1):5-16.

Ziyaadini, M., Mehdinia, A., Khaleghi, L., & Nassiri, M. 2016. Assessment of concentration, bioaccumulation and sources of polycyclic aromatic hydrocarbons in zooplankton of Chabahar Bay. *Marine pollution bulletin. Elsevier Ltd*. 107(1):408–412.